Doctoral theses at NTNU, 2022:251

Kasper Emil Thorvaldsen

# A Long-term Strategy Framework for Flexible Energy Operation of Residential Buildings

Doctoral thesis

NTNU
Norwegian University of Science and Technology
Thesis for the Degree of Philosophiae Doctor
Faculty of Information Technology and Electrical Engineering
Department of Electric Power Engineering

NTNU
Norwegian University of Science and Technology

Kasper Emil Thorvaldsen

# A Long-term Strategy Framework for Flexible Energy Operation of Residential Buildings

Thesis for the Degree of Philosophiae Doctor

Trondheim, November 2022

Norwegian University of Science and Technology
Faculty of Information Technology and Electrical Engineering
Department of Electric Power Engineering

NTNU
Norwegian University of
Science and Technology

**NTNU**
Norwegian University of Science and Technology

Thesis for the Degree of Philosophiae Doctor

Faculty of Information Technology and Electrical Engineering
Department of Electric Power Engineering



ISBN 978-82-326-6267-8 (printed ver.)
ISBN 978-82-326-5885-5 (electronic ver.)
ISSN 1503-8181 (printed ver.)
ISSN 2703-8084 (online ver.)

Doctoral theses at NTNU, 2022:251

Printed by NTNU Grafisk senter

*"Each man is the bard of his own existence"*

- Cormac McCarthy -

# Preface

The presented research was carried out at the Department of Electric Power Engineering, the Norwegian University of Science and Technology (NTNU). The research started in September 2018. My main supervisor has been Professor Hossein Farahmand from NTNU, with Professor Magnus Korpås from NTNU and Adjunct Associate Professor Karen Byskov Lindberg from SINTEF Community as co-supervisors.

This work has been part of a collaborative effort between the research centers Zero Emission Neighborhood (FME ZEN) and Centre for Intelligent Electricity Distribution (FME CINELDI). Both centres are financed by the Norwegian Research Council, with several partners from both industry and academia present.

# Acknowledgements

When looking back at the PhD period, I tend to forget the most impactful situations that I have encountered. However, it is safe to say that it has been a roller-coaster of an experience, to quote a shared opinion from many previous PhDs. There are times with doubt and stress, where uncertainty has influenced you and you start to reconsider if you are able to achieve this. But also times with excitement, achieving milestones solidifying your role and presence here. There is no lie saying that this has been tough, but at the same time, I am very happy that I was able to do this. I have managed to create something new in academic settings and gotten both praise and criticism along the way. The experience I have encountered throughout this PhD has been interesting, to say the least.

The academic quality of the work would have been difficult to achieve without a team to support me. Thanks to my supervisor Hossein for his support and assistance throughout the work, from day one and till submission. Without his valuable insight on my work and how to deal with my structuring weaknesses, I am certain the road would have been much more shaky and uncertain. My co-supervisor Magnus, who can be credited on pointing me toward this PhD-career, also deserves much praise for his help. His key attention to detail and finding a suitable paper topic after a five minute discussion, definitely helped me sort out my thoughts and get it down on paper. This includes his great feedback on my papers and thesis, where his witty comments makes feedback more enjoyable to handle. And thanks for the good off-topic discussions, whether it would be wind turbines, brewing, and so on! Thanks a lot to Karen for helping me when I got stuck and needed to see things from another point of view. The trip to you and your group at SINTEF Community in Oslo on January 2020 gave me a lot of good insights and ideas for my work! In all, thanks to all three for your support during the four years, I really appreciate it!

Thanks to all the good colleagues and other PhDs that have endured this trip together with me! It is fair to say that the good social atmosphere at work has been crucial for me to get through this, and the many fun and exciting events we have organized throughout the years have been valuable. Thanks for managing my many hallway wanders and quest for distractions. Had you all not let me do these things, it would not be easy for me to get the days going! The PhD group has changed a lot during my stay, so I try to give them all the mention they deserve. Thanks to the senior PhDs when I started, helping me learn the ropes and rules of this place and for great social interactions after completing your theses: Markus Löschenbrand, Erlend Engevik, Espen Flo Bødal, Sigurd Jakobsen, Hans Kristian Meyer and Salman Zaferanlouei. Thanks to our previous Post-Doc Venkatachalam Lakshmanan for his unlimited positivity and encouragement! Thanks to my office-mates that I have had over countless days and coffee-cups with: Christian Øyn Naversen, Sigurd Bjarghov, Linn Emelie

Schäffer, Ugur Halden, Emil Dimanchev, and Erik Bjørnerem. Thanks to the superb group located in the infamous forbidden corridor, for letting me stop by and distract them when needed, occasionally involving chocolate: Stine Fleischer Myhre, Marthe Fogstad Dynge, Runar Mellerud and Luke Whittington. Also, thanks a lot to the remaining colleagues in the EMESP group! Finally, I would give a big thanks to Adjunct Associate Professor Gro Klæboe, for her help and collaboration through the IDUN project. Your focus on psychological safeness as a mentor has been an important valve for me to express my feelings, both good and bad, when needed!

Getting through this challenge would not have been able without the external support available, to take my mind off work at the optimal times. Thanks to Martin and Vincent for their collaborative skills in the hunt for chicken dinners, refreshing my head for a new day at work! Thanks to my family for always being supportive, especially my mom and dad. Reading my stress level was probably very easy for them, indicated by the frequency of my calls, but, nonetheless, they always were available for a chat! We always start talking about my backup-plan as a baker when I doubt myself, luckily I have yet to buy a bakery!

Finally, I wanted to dedicate some mentions to my best friend/enemy; the impostor syndrome. Being with me from day one, you have surely made this experience more eventful than it needed to be. Troubling me for the first few years, you have challenged me to understand what is good enough, and what is expected of us as PhDs. With your help, I believed the level was way higher than it seemed to be, and thought my ideas were not good enough. Actually, I came up with the idea that became my thesis around 2-4 months into my PhD, but disregarded it as I found no academic sources working on the same idea. Thought to be a stupid idea, I stressed a lot with figuring out what was supposed to be my focus area, almost quitting as a result. Luckily, I came back with my original idea after 10-11 months into my PhD, when I realized that an empty Google search meant academic potential instead of stupid ideas! For that realization, I have to thank PhD Comics[1], with their way-too-relevant comic strips about PhD life, where many hit close to heart. In the end, the impostor syndrome is something I feel has been necessary to make me realize how important it is to stretch out for ambitious goals, but also realize how important it is to have your feet planted at the ground and understand the foundation around you.

[1] https://phdcomics.com

# Summary

Within the European power system, the electricity mix is experiencing more presence of variable power production due to the green shift. This shift causes increased need for flexibility measures to combat instability, which is achievable on both the generation and consumption side of the power system. Buildings, neighborhoods, and most end-users are able to assist with flexibility through demand side management, adjusting their consumption profile to react to the price signals given. This flexibility can be activated through the use of home energy management systems, which can control the flexible assets present in a given building. However, most of these applications only consider the short-term period of operation, up to a couple of days in the future when operating the flexible assets. Flexibility also has a value in operation beyond this period, and can assist in the long-term strategy of operation of the energy system in buildings, which could be many weeks or months into the future. This is important when accounting for long-term price signals or when operating seasonal flexible assets. Finding accurate and descriptive measures of representing the long-term value of flexibility use is needed to enable this.

The work presented in this thesis investigates the long-term value of flexibility in residential buildings at the end-user level, and how the value of flexibility can be represented for a short-term operational model. The work applies and describes a long-term strategy framework specifically aimed at generating cost curves representing the long-term value of flexibility. The cost curves describe the future consequence of operation based on the future price signals they include. The developed models enable price signals of different categories to be included in the strategy framework. These price signals could be grid tariffs, but also flexible assets themselves, for instance, seasonal storage. The strategy framework creates a coupling between short-term and long-term operation of buildings, to achieve better overall use of flexibility within buildings.

Overall, this thesis is made up of four scientific papers, where three are published and one is submitted for review at the present time. These publications comprise the contribution and discussion constituted in this thesis. A summary of the main results of this PhD is given below:

- A long-term strategy framework and toolbox for building operation has been created, to provide more information on the long-term value of flexibility for building operation. The toolbox **Long-term strategy framework for future building operation (LOSTFUTURE)** calculates the long-term value of flexibility, and represents this as future cost curves. The framework enables long-term price signals to be embedded into the strategy, such that the cost curves represent the consequence of operation on these

signals as well. Through the use of flexible assets, operation of the building can be controlled to react to the short-term and long-term consequences of operation.

- The LOSTFUTURE toolbox has been used in combination with several different long-term price signals, to analyze the long-term value of flexibility and strategic decisions during operation. For a monthly demand charge, penalizing peak-import of electricity, the strategy finds the cost-optimal peak-import level to aim for over the whole month, accounting for both the demand charge cost and value of operation from real-time price variation. For a price signal related to $CO_{2eq}$-inventory, motivating cost-optimal net zero-emission during yearly operation, the strategy captures the cost-optimal value of emission compensation and the optimal timing of performing this compensation. For long-term price signal as input to seasonal thermal energy storage operation, the strategy captures the value of using the seasonal storage unit to benefit from seasonal variation in operation.

- With the LOSTFUTURE toolbox, the flexible assets are controlled such that they are able to influence the short-term and long-term value of flexibility. The flexible assets in this work included a small-scale battery energy storage system, a controllable electric vehicle charger, and control of space heating to influence indoor temperature. For a case study surrounding a monthly demand charge price signal in a Norwegian building, each of these flexible assets individually provided means of flexibility use to react to the long-term price signal during operation. Despite only being able to perform flexibility within a day at the time, the flexible assets are able to react to the long-term price signals and cost-optimally balance cost of operation. While the battery and electric vehicle charger saw cost-reduction primarily in the demand charge price signal, space heating found a cost-optimal peak-import level that balanced savings from real-time prices. This showed that each flexible asset reacts to the price signals differently based on their characteristics.

- Multi-period price signals coupled to other price signals have been investigated and applied to the LOSTFUTURE toolbox. This enables the framework to include multiple price signals at once, including price signals that are repeatedly activated and only valid for a limited period at a time. This coupling was performed on a case study surrounding a Norwegian building with seasonal thermal energy storage and monthly demand charge, to find the operational strategy over a whole year. The model managed to accurately couple each monthly demand charge with the strategy surrounding the seasonal storage unit, such that the long-term value of flexibility on both price signals were preserved. The results showed a strategy that captured the accurate peak-import level of the demand charge for each month, and also the cost-effective use of seasonal storage.

# Contents

**1 Introduction** **1**
1.1 Motivation . . . . . 1
1.2 PhD Project Scope . . . . . 3
1.3 Contributions . . . . . 3
1.4 List of Publications . . . . . 4
1.5 Thesis Outline . . . . . 5

**2 Research Context** **7**
2.1 End-user Flexibility in Building Operation . . . . . 7
2.2 $CO_{2eq}$-emission during Operation of a Zero Emission Building . . . 15
2.3 Seasonal Energy Storage . . . . . 18

**3 Framework for Long-term Strategy of Energy Building Operation** **21**
3.1 The LOSTFUTURE Toolbox . . . . . 21
3.2 Model Overview for LOSTFUTURE . . . . . 23
3.3 LOSTFUTURE Optimization Problem . . . . . 29

**4 Results and Discussion** **39**
4.1 Relation between Long-term and Short-term Value of Flexibility . 39
4.2 The Role of Flexible Assets in a Long-term Strategy Framework . 49
4.3 Technical Experiences of Representing Long-term Value of Flexibility 58

**5 Conclusion and Future Work** **63**
5.1 Main Results . . . . . 63
5.2 Conclusion . . . . . 65
5.3 Suggestions for Future Work . . . . . 67

**Bibliography** **69**

**Publications** **77**
Paper I . . . . . 81
Paper II . . . . . 91
Paper III . . . . . 103
Paper IV . . . . . 119

# Nomenclature

**Index sets**

$\mathcal{D}_n$ Set containing list of coupling auxiliary points for state variable $n$

$\mathcal{G}$ Set of stages within the period

$\mathcal{N}$ Set of state variables

$\mathcal{N}_P$ Set of discrete segments for all state variable combinations

$\mathcal{P}$ Set of index positions for weighting variable $\gamma$ in the expected future cost curve

$\mathcal{P}_i$ Set containing list of connecting weighting variables for auxiliary variable $\lambda$, index $i$

$\mathcal{S}_{\mathcal{S}_g}$ Set of scenarios for stochastic variables for decision stage $g$

$\mathcal{S}_g$ Set containing information for decision stage $g$

$\mathcal{T}$ Set of time steps within a decision stage

**Parameters**

$\beta_i^{init}$ Auxiliary parameter taking the initial value for state variable $i$ for a decomposed optimization problem [-]

$\dot{E}^{B,dch,max}, \dot{E}^{B,ch,max}$ Discharge/charge capacity for battery $[\frac{\text{kWh}}{\text{h}}]$

$\dot{E}^{Max}$ Maximum EV charging capacity $[\frac{\text{kWh}}{\text{h}}]$

$\dot{E}_t^{STES,in,max}$ Rated input capacity limit for the STES at time step t $[\frac{\text{kWh}}{\text{h}}]$

$\dot{E}_t^{STES,out,max}$ Rated output capacity limit for the STES at time step t $[\frac{\text{kWh}}{\text{h}}]$

$\dot{Q}^{sh}$ Rated capacity for space heating radiator $[\frac{\text{kWh}}{\text{h}}]$

$\eta_{dch}^B, \eta_{ch}^B$ Discharge/charge efficiency for battery [p.u]

$\eta_{ch}^{EV}$ EV charging efficiency [p.u]

$\eta^{PV}$ Total efficiency for PV system [p.u]

$\eta^{STES}$ Storage loss for the STES at each stage [p.u]

$\Gamma(g, s_g^s)$ List containing input data to all stochastic variables for a decomposed problem in stage $g$, scenario $s_g^s$

$\mathcal{C}^{grid}$ DSO volumetric cost for imported energy [$\frac{\text{EUR}}{\text{kWh}}$]

$\mathcal{C}_p^{future}$ Expected future cost for segment $p$ [EUR]

$A^{PV}$ PV system area [$\text{m}^2$]

$C_i, C_e$ Heat capacity for interior and building envelope [$\frac{\text{kWh}}{^\circ\text{C}}$]

$C_{init}^{n,g}$ List containing new marginal cost for price signal that is deactivated at stage $g$, for state variable $n$ [$\frac{EUR}{-}$]

$COP^{HP}$ Coefficient of performance for the heat pump [p.u]

$D^{EV}$ EV storage discharge when not connected to the building [kWh]

$E_{CO2eq}^0$ Initial value of accumulated $CO_{2eq}$-inventory at beginning of decision stage [$kgCO_{2eq}$]

$E^{B,min}, E^{B,max}$ Battery lower and upper SoC bounds [kWh]

$E_{Rated}^{STES}$ Rated storage capacity for the STES tank [kWh]

$E_0^{STES}$ Initial state of charge for STES at beginning of decision stage [kWh]

$E_t^{EV,min}, E_t^{EV,max}$ Time dependent EV SoC capacity boundary [kWh]

$P^{HP}$ Rated electrical capacity for the HP [$\frac{\text{kWh}}{\text{h}}$]

$P^{Stages}$ List containing information on stages where a new price signal is initiated

$P_g^{States}$ List containing state variables that have a new active price signal at stage $g$

$P_{i,n}^{SV}$ Discrete value of state variable $n$ for segment $i$ [-]

$P_0^{imp}$ Initial highest peak-import of electricity [$\frac{\text{kWh}}{\text{h}}$]

$P_{init}^{n,g}$ List containing initial value condition for price-signal being active from decision stage $g$, for state variable $n$ [-]

$R_{ie}, R_{eo}$ The thermal resistance between the interior-building envelope and building envelope-outdoor area [$\frac{^\circ\text{C}}{\text{kWh}}$]

$T_t^{in,min}, T_t^{in,max}$ Lower/upper interior temperature boundary [°C]

**Decision variables**

$\alpha_{g+1}^{future}$ Expected future cost of operation for future stage $g+1$ [EUR]

$\gamma_p$ Weighted variable for segment $p$

$\lambda_i$ Auxiliary variable for discrete segments of state variable $n$, for index $i$ of list $D_n$

$E_t^B$ State of charge for BESS for time step t [kWh]

$E_t^{EV}$ State of charge for EV for time step t [kWh]

$E_t^{STES}$ State of charge for STES at time step t [kWh]

$e_{CO_{2eq}}$ Accumulated $CO_{2eq}$-inventory at end of decision stage [kg$CO_{2eq}$]

$p^{imp}$ Highest single-hour import of electricity [$\frac{\text{kWh}}{\text{h}}$]

$q_t^{sh}$ Thermal energy for space heating at time step t [$\frac{\text{kWh}}{\text{h}}$]

$T_t^{in}, T_t^e$ Interior and building envelope temperature at time step t [°C]

$y_t^{B,ch}, y_t^{B,dch}$ Power to/from the BESS for time step t [$\frac{\text{kWh}}{\text{h}}$]

$y_t^{EV,ch}$ Input power to EV for time step t [$\frac{\text{kWh}}{\text{h}}$]

$y_t^{HP,out}$ Output thermal energy from HP at time step t [$\frac{\text{kWh}}{\text{h}}$]

$y_t^{HP}$ Input electric power to HP at time step t [$\frac{\text{kWh}}{\text{h}}$]

$y_t^{imp}, y_t^{exp}$ Energy imported/exported to household at time step t [$\frac{\text{kWh}}{\text{h}}$]

$y_t^{PV}$ Power produced from PV system at time step t [$\frac{\text{kWh}}{\text{h}}$]

$y_t^{STES,in}$ Thermal energy input for STES at time step t [$\frac{\text{kWh}}{\text{h}}$]

$y_t^{STES,out}$ Thermal energy output from STES at time step t [$\frac{\text{kWh}}{\text{h}}$]

**Stochastic variables**

$\delta_t^{EV}$ Parameter stating if the EV is available to the building $\{0, 1\}$

$\mathcal{C}_t^{spot}$ Electricity spot price in time step t [$\frac{\text{EUR}}{\text{kWh}}$]

$D_t^{El}$ Consumer-specific electric load in time step t [kWh]

$D_t^{WT}$ Consumer-specific thermal load in time step t [kWh]

$f_t^{CO_{2eq}}$ Hourly average $CO_{2eq}$-intensity on electricity mix from the grid at time step t[$\frac{kgCO_{2eq}}{kWh}$]

$I_t^{Irr}$ Solar irradiation at building in time step t[$\frac{\text{kWh}}{\text{m}^2}$]

$T_t^{out}$ Outdoor temperature in time step t [°C]

# 1 Introduction

## 1.1 Motivation

In 2019, the global average temperature increased by 1.1°C compared to industrial levels [1]. To combat climate change, the European Union (EU) has set a target to reduce 1990-level greenhouse gas (GHG) emissions by 55% by 2030. This goal covers multiple sectors, and an essential one is the energy sector, which is driving toward a green shift. In the EU, European households account for 25% of the final energy consumption [2]. Out of these 25%, 50% of the total final energy consumption is primarily used for heating and cooling. Thus, the building stock plays an important role in reaching a carbon-neutral community by 2050 [2].

The European power system is experiencing a considerable change in the electricity mix as a result of the green shift [3]. Renewable, variable electricity production is being installed at a rapid rate, leading to more variation and uncertainty within production. With this trend increasing over the years to meet the goals in 2030 and 2050, the power grid will need more flexibility sources to preserve the security of supply in the future [4]. Increased variability, uncertainty, and more location dependency can lead to more imbalance within the power system and decrease reliability, increasing the need for active measures that can reinforce the system [5]. Flexibility is an important measure to keep the power system in balance, and can be achieved on both the generation and consumption side of the power system, changing their pattern to cooperate with the immediate power system behavior. End-users can participate with flexibility to the power system through their home, where demand-side management (DSM) can play a role in the transition [6]. DSM can not only be an active counter-measure for variation in production, but also to avoid local grid congestion, and reduce peak-hour consumption when electricity demand is high.

End-users are able to perform DSM by adjusting their consumption profile, which can be a reaction to different price signals. Their consumption profile can be operated through home energy management systems (HEMS), which control certain loads or flexibility in their home or building [7]. Flexible assets are able to shift and influence the consumption profile, and can be controlled to optimize the value of flexibility. Within short-term operation, most work using HEMS normally consider the value of flexibility up to a couple of days in the future [8]. However, flexibility does not only influence short-term operation, but also provides valuable potential in the long-term strategy of operation, which could be many weeks or months into the future. This is especially true with the presence of long-term

price signals that demand response needs to react to. As such, models need to account for the long-term value of operation.

There is a need to find accurate and descriptive measures of representing the long-term value of flexibility. There exist demand response programs that account for longer periods than what is normally forecast in HEMS-formulations. For instance, the grid tariff monthly demand charge, present in some countries in Europe [9], sets a cost based on highest import of electricity over a whole month. Accounting for this grid tariff during operation of an HEMS would require sufficient information of the future to capture the long-term value of flexibility. In addition, seasonal flexibility and long-term storage require an operational strategy that accounts for the value of operation over the different seasons ahead. Including information on long-term value of flexibility into short-term operation of buildings can complicate the overall problem. As such, representing the long-term value of flexibility, without increasing the complexity of the overall problem too much, needs to be explored.

Accounting for the long-term value of flexibility during short-term operation would provide more information to improve short-term decisions. This could respond to reduction in operational costs, both by representing long-term cost-based price signals and enabling accurate operation of seasonal energy storage systems. In addition, other long-term price signals that promote operational goals outside of cost-based decisions could be incorporated and visualized, like $CO_{2eq}$-impact of operation. For buildings or energy systems that want to include $CO_{2eq}$-intensity and compensation into the operational planning, like Zero Emission Buildings (ZEBs) [10], a long-term operational strategy would showcase the value of flexibility toward compensation. This includes both here-and-now and the future value of compensation. Finding the long-term value of flexibility would promote cost-optimal use of flexibility to achieve the emission-based goals during operation. Thus, long-term value of flexibility incorporated to price signals of different characteristics would increase the level of detail during operational decisions.

This thesis investigates how to represent the long-term value of flexibility and incorporate long-term price signals into residential building operation. The work applies and describes a long-term strategy framework for residential building operation, generating cost curves representing the long-term value of flexibility. This strategy framework analyzes the long-term influence of operation, including long-term price signals in the overall analysis. These long-term price signals could, for instance, be grid tariffs, seasonal energy storage systems like heat or hydrogen, or others. The framework returns simplified cost curves that explain the future consequence of operation based on the long-term price signals, describing the future change in cost of operating the system. The strategy framework helps create a coupling between short-term and long-term operation of residential buildings, to achieve better overall use of flexibility within residential buildings, and ulti-

mately reduce operational costs. For further explanation, residential buildings are denoted as buildings, unless stated otherwise.

## 1.2 PhD Project Scope

The main aim of this thesis is to answer several key research questions linked to coupling long-term value of flexibility into building operation and incorporating long-term price signals into short-term operation. A main research question has been defined to address the research gap:

**Main Research Question:** How can the long-term impact of building energy system operation be represented to capture the long-term value of flexibility?

The main research question has been divided into several subcategories that supplement it, to more concretely specify the different goals within:

- **RQ1**: What is the relation between long-term and short-term value of flexibility for scheduling of the building energy system?
- **RQ2**: How do different flexible assets in scheduling of the building energy system impact long-term value of flexibility?
- **RQ3**: What is the long-term value of $CO_{2eq}$-emission savings for a zero emission building during the operational phase?
- **RQ4**: How can long-term, seasonal flexibility be represented for short-term operation of buildings?

The overall scope of this thesis can be divided into two main parts. The first part aim to present the application of a long-term strategy framework and the area of use for this framework. The second part focuses more on different long-term price signals, and how to extend the framework to increase accuracy.

## 1.3 Contributions

The contributions of this PhD thesis are listed as follows:

- A long-term strategy framework for calculating and representing the long-term value of flexibility for building operation has been performed.
- The influence flexible assets have on long-term price signals has been investigated. The role of flexible assets has been investigated individually, and cooperatively, with different case studies surrounding varying price signals.

- The long-term strategy framework for building operation has been investigated for several long-term price signals, that are difficult to represent directly for short-term operational models. These price signals include grid tariffs, seasonal flexible assets, and a way to account for the $CO_{2eq}$-emission inventory during operation.
- A framework for accounting for multiple long-term price signals of different length and pattern has been developed.
- This work has demonstrated the added value of operation and use of flexibility when accounting for long-term operation, and how this can be incorporated to short-term operation models to improve overall performance.

All the mentioned contributions are presented within the publications that are part of this PhD thesis. In addition, some additional results based on the published work are included in this work, that supplements the overall analysis.

## 1.4 List of Publications

Over the course of this PhD, multiple papers have been created and published as the foundation of this research. The papers that create this foundation are listed below, and can be found in full in the "Publications" section in this document. Currently, Paper IV is under review, and as such, is expected to undergo modifications in the future.

**Paper I** K. E. Thorvaldsen, S. Bjarghov, and H. Farahmand. "Representing Long-term Impact of Residential Building Energy Management using Stochastic Dynamic Programming", in *2020 International Conference on Probabilistic Methods Applied to Power Systems (PMAPS), IEEE*, Aug 2020.
DOI: https://doi.org/10.1109/PMAPS47429.2020.9183623

**Paper II** K. E. Thorvaldsen, M. Korpås, and H. Farahmand. "Long-term Value of Flexibility from Flexible Assets in Building Operation", *International Journal of Electrical Power & Energy Systems*, vol. 138, June 2022.
DOI: https://doi.org/10.1016/j.ijepes.2021.107811

**Paper III** K. E. Thorvaldsen, M. Korpås, K. B. Lindberg, and H. Farahmand. "A stochastic operational planning model for a zero emission building with emission compensation", *Applied Energy*, vol. 302, Nov 2021.
DOI: https://doi.org/10.1016/j.apenergy.2021.117415

**Paper IV** K. E. Thorvaldsen, and H. Farahmand. "Long-term strategy framework for residential building operation with seasonal storage and capacity-based grid tariffs", under review in *Elsevier: Applied Energy*, submitted March 2022.

An additional paper has been published during the timeline of the PhD, to which the contribution from the author has been limited. This paper is relevant in regards to the topic, as the operation of flexible commercial buildings with a long-term price signal was investigated. The publication is given here:

- I. E. Skoglund, M. Rostad, and K. E. Thorvaldsen, "Impact of shared battery energy storage system on total system costs and power peak reduction in commercial buildings", in *In Journal of Physics: Conference Series, IOP Publishing*, Vol. 2042, Nov 2021.
  DOI: https://doi.org/10.1088/1742-6596/2042/1/012108

## 1.5 Thesis Outline

This thesis presents an overview of the key research context necessary for the overall work in Chapter 2. In Chapter 3, the methodological approach created for the long-term strategy framework is presented in its entirety. Next, Chapter 4 showcases and discusses the main findings of this thesis, being a combination of published work and additional results answering the overall research questions. The findings are further discussed and a conclusion is presented in Chapter 5, with suggestions for future work to improve this important research field.

The four papers created during this thesis, with three published and one a work-in-progress, are presented in their entirety at the end of this thesis. When these papers are referred to in the thesis, the content is based on the attached versions with their corresponding paper number.

# 2 Research Context

This chapter aims to describe the research context behind each research question, providing necessary information about the motivation behind them. The description here will focus on residential building operation and flexibility within buildings. For each research question, some description on existing practices and relevant literature will be presented. Chapter 2.1 is related to RQ1 and RQ2, Chapter 2.2 explains the relevance of RQ3, while Chapter 2.3 describes the current status related to RQ4.

## 2.1 End-user Flexibility in Building Operation

### 2.1.1 End-user Flexibility

The role of the end-users has seen a shift in recent years. From being considered a passive consumer with inflexible demand, their characteristics and behavior are undergoing a transition in accordance with the changes happening in the power system. With the introduction of more power-intense applications, like EV chargers, induction ovens, etc., consumption becomes more power-consuming over a shorter duration. The high need for electricity by many at once strains the local distribution grid and makes it more prone to congestion. With the roll-out of smart meters, DSM is more accessible through automation and smart control, to react to price signals by adjusting their consumption profile [6]. As peak-consumption from end-users create potential bottlenecks that can strain the local distributional grid, most motivations behind enabling DSM lies with lowering peak-consumption and shifting the load to off-peak hours. Taking a daily consumption profile as the basis, DSM comprises six common categories to flatten consumption [11], shown by Fig. 2.1. The focus in this work makes most use of the peak shaving, valley filling, and load shifting categories.

A similar description within DSM is demand response (DR). DR programs are price signals that aim to induce change in consumption profiles [12]. There are multiple DR programs formulated, and these are typically divided between price-based and incentive-based programs. Price-based programs give price signals about cost of electricity consumption, with Time-of-use (ToU), Real-time pricing (RTP), and critical peak pricing (CPP) all in this category. By giving cost-based signals on using electricity at certain periods, these programs will motivate the user to shift consumption to reduce cost. RTP is a common practice in Norway, enabled by the presence of smart meters [13]. Incentive-based programs aim to

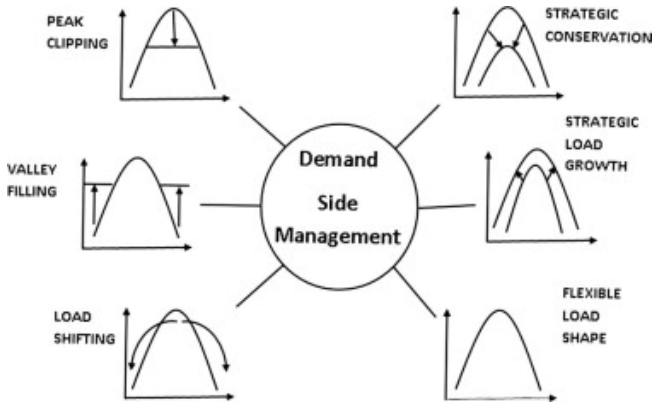


Figure 2.1: Different demand side management categories [11].

encourage flexibility by benefiting the end-users. Some examples include capacity market programs and ancillary service markets, where the end-user can be paid by providing flexibility. To be able to participate in the different DR programs or to enable DSM, it is necessary to have flexibility within the building and appropriate flexible measures that limit discomfort for the residents.

### 2.1.2 Flexible Assets in Buildings

Within a building, several flexible mechanisms could be activated to enable DSM. In theory, all load is flexible, but some is based on the users' preference and willingness to change. Based on the components available in the building, the flexibility potential differs. A study on different flexibility types was conducted in [14], characterizing the flexibility within a building. Within this study, the distribution of different flexibility types based on scope was performed, where buildings were one of these scopes. Buildings have components with high flexibility potential on load-shifting, and some potential on shedding and generation. The focus in this work will mostly explain some of the flexible assets in the load-shifting category.

#### Battery Energy Storage System

A Battery Energy Storage Systems (BESS) is a flexible asset that is used for storing and discharging electricity to the energy system at cost-optimal times. A BESS contains a stationary battery unit connected to inverters that converts the electricity to appropriate current types between the battery and the external connection. The storage medium can vary, and there exists a wide variety of storage mediums suited for a BESS, as showcased in reference [15], but lithium-

ion is by far the most common medium. The BESS can be charged and discharged with electricity when needed, and thus can contribute to peak-shaving and valley-filling flexibility [16]. Note that this flexible asset is not a load in a building system, and would not change the consumption pattern for demand, but would influence interaction with the electricity grid by reducing or increasing need of electricity to the building. It could also be used strategically to store excess local production from, for instance, a Photovoltaic (PV) system, to increase self-consumption, which was carried out in [17]. The influence from the BESS is based on the installed capacity, and by the inverter capacity, whereas each limit storage capacity and power input/output, respectively. Based on the ratio between these two components, known as the C-rate [18], the goal of the BESS can go from short-term, high-power influence, to long-term, low-power influence.

### Electric Vehicles

EVs are becoming more present at homes, and charging these can also be seen as a flexible asset. The primary goal when charging EVs is to have sufficient state of charge (SoC) at departure to ensure sufficient driving range for the upcoming trip. Standard EV chargers have no automatic activated control system, which means that, in a passive manner, the EV is being charged when plugged into the charger. As the EV is also dependent on user-behavior, the EV is typically plugged in during the evening after the user returns from work, as was shown in reference [19] when analyzing EV flexibility. With a passive charging strategy, this would increase the expected electricity demand from a building during the evening, which also is a period with possible bottlenecks and higher demand from other sources. The EV charger can be flexible by shifting the charging period toward the night and during off-peak hours, to flatten the demand curve. This option is becoming more accessible currently, with most EVs allowing pre-specified charging periods, and some companies offering EV chargers, like Easee [20], that enable smart control of charging based on RTP-prices in the spot market. In addition, bi-directional flow of electricity from EVs, enables more characteristics from a BESS to be inherited to the EV. Peak-shaving is an increased flexibility option with bi-directional flow, as was explored in [21].

### Space Heating

Space heating (SH) is another important asset that could be considered a flexible asset. Indoor heating or cooling to maintain a stable and comfortable temperature is a load with substantial consumption of electricity over the course of a year, depending on the seasons. In Norway, heating demand is normally covered through electricity and heat pumps, while gas and oil is more common in European countries [22]. However, this trend is changing and electric heating is

expected to be more prevalent in the future as a decarbonization strategy [23]. As mentioned earlier, energy consumption for heating and cooling of the building stock in EU amounts to a substantial portion of energy use [24], meaning energy savings obtained by more strategically operating these assets have a high value. Flexibility within SH is tied to the timing of heating or cooling the building, where pre-heating and pre-cooling is an important DSM measure, as proposed with regards to thermal flexibility in [25]. If there is flexibility within indoor temperature, where the temperature can deviate within a given boundary, this provides more opportunities to shift the consumption and still be within appreciated limits. Comfortable temperature boundaries are important for SH and making use of this to shift heating or cooling could improve operation while not affecting the user comfort. A study in [26] showed how comfortable temperature ranges depend on the room and time of year, highlighting the worth of temperature flexibility for optimal control. With smart control of space heating, accurate temperatures can be maintained, and this also enables strategic pre-heating of the areas when optimal.

#### Other Flexible Assets

There are multiple other flexible assets that are available in a building than the ones previously mentioned. The work in this thesis primarily considers at the aforementioned assets, but there exists other assets that could provide flexibility. For instance, water heaters supplying domestic hot water could be modeled and controlled by a HEMS. These water heaters could provide flexibility to the system on different levels, as was carried out in [27]. This work analyzed the flexibility potential of an electric water heater, and discussed the flexibility potential toward flexibility markets such as frequency containment reserve and frequency restoration reserve. Other electrical appliances include clothes washer, clothes dryer, dishwasher, refrigerator, etc., as was listed in [28]. This work investigated the demand response opportunity these appliances could provide, and their coupling to user comfort. As such, multiple flexible assets exist in a building and can provide flexibility, but it is important that controlling them limits the influence on user comfort.

### 2.1.3 Building Operation

To activate and make use of the available flexibility within residential buildings, it is necessary to have control systems and means of operating flexible assets. To control the flexibility, HEMSs have been developed as a means to adjust energy input and output from the flexible assets, based on the measures that the HEMS accounts for during operation of the building. These measures can be internal information such as indoor temperature, but also external factors such as RTP

and cost of operation. Such controllable measures for a HEMS can differ, and the logical process behind the decisions depends on the overall goal of the system.

The review in [8] provided an overview of literature addressing HEMS, focusing on modeling approaches and their corresponding impact on operation. Models are used to simplify the operational process, and are typically divided into three approaches: Mathematical optimization, meta-heuristic, and heuristic methods. A mathematical optimization approach makes use of input data to obtain an optimal solution to the overall problem defined. The complexity of such mathematical formulations are based on the structure of the problem, and the level of detail included. As such, their computational effort can be significant. Meta-heuristic algorithms searches over a large set of feasible solutions, to converge toward an acceptable solution. This approach requires less computational effort and can also be applied to optimization problems. Heuristic methods use determined rules to find an approximate solution. The accuracy of the rules applied to the heuristic method influences the results. All the mentioned methods describe and use the the system differently, aiming to accurately capture the main goal and objective of the HEMS.

Use of optimization problems for operating flexible assets within HEMSs has been carried out in many studies. In [29], a mixed integer linear problem was formulated within a HEMS, to operate a system with PV, BESS, and a bi-directional EV charger. Their goal was to operate under dynamic pricing and limitations on peak power consumption over 24 hours, reaching a 35% cost reduction compared to a base case without PV or BESS. A model-predictive control (MPC) formulation was applied in [30], controlling a heat pump, with thermal storage alongside a BESS. The MPC model was used to control the different flexible assets in a problem including uncertainty, achieving a 11.6% cost reduction and improved performance compared to a reference case. A rolling horizon strategy was applied to an optimization model in [31], which operated a microgrid with PV, wind turbines, a diesel generator, BESS, and DSM options. These are some of the many published works that have examined different techniques for operating a HEMS. A different review of recent works on HEMSs was done in [16], where optimization problems in HEMS and MPC formulations had a substantial taxonomy of previous work especially included. For a further overview of the existing work in these fields, refer to [16].

When creating optimization problems that aim to control a HEMS, the scheduling horizon of the problem can differ. The length of the horizon is important to capture the longer effects of using the flexible assets, for instance, accounting for price signals with longer periods, or preparing for future use of flexibility. In addition, the time resolution also determines in how much detail the system is described and the influence on use of flexibility during operation. The literature review in [8] also included an overview of the coupling between time resolution and scheduling horizon. A majority of the references used hourly time resolu-

tion with a 24-hour scheduling horizon. The scheduling horizon is important in accordance to what kind of data format is used to portray the future, and if uncertainty is included during operation. By representing the future uncertainty with forecasting, which is commonly done in MPC-models [8], the accuracy of the forecasts decrease with longer horizons due to the increasing span of error in the forecast. Another approach to deal with uncertainty is to include scenarios into the optimization problem, formulated as scenario trees. However, this would grow exponentially with an increasing horizon, creating more complexity that would increase computation time. As such, limitations on scheduling horizons are connected to the accuracy of the future and the uncertainty within it, while at the same time making the optimization problem efficient to solve without too much complexity within.

### 2.1.4 Long-term Price Signals for Building Operation

Optimization models that operate a HEMS for buildings limit the long-term horizon that is considered. Based on the method use for representing future uncertain demand and input data, this is to decrease computational time and inaccuracy of the long-term data [8]. During operation of buildings, the flexible assets within try to react to price signals to reduce the overall cost of operation. DR-programs use price signals as a means to promote flexibility. Most of these price signals, like RTPs, have a relatively short-term time-frame and influence on operation, since they are realized on a daily basis. However, by having a short-term scheduling horizon during operation, the long-term value of flexibility beyond the horizon is simplified, or left out of the operational decision. This limits the performance of the flexible assets. In addition, this ignores any long-term price signals or considerations that would influence operation of the flexible assets in the short-term time-frame.

A long-term price signal within building operation is a type of demand response signal aimed to influence operational strategy over a prolonged period. The duration of these signals can vary depending on motivation and type of signal, and the signal itself is not required to be cost-based or to induce a cost. These signals could be used as guidance for cost-optimal control of seasonal flexibility, so that seasonal and long-term storage represent the future value of operation. Signals like these exist and are used for operation today, for instance within hydropower scheduling. Water values, which are long-/medium-term price signals for reservoir levels in hydropower scheduling, offer information on the future value of storing water for producing electricity [32]. The price signal is only meant as a means to put a price on the current water available, comparing the long-term value of storing water versus the here-and-now benefits of using the water.

There exist cost-based long-term price signals that depend on the operational performance of a building over longer periods. Within grid tariffs, long-term

price signals could be incorporated to motivate predictable and stable consumption profiles, and avoid unnecessary peaks of import. These would normally be given by distribution system operators (DSOs). An example of this is a grid tariff called a monthly demand charge. The demand charge puts a cost on the consumer based on the highest single-hour import-quantity over the duration of a month. This is a type of price-based DR that aims to flatten the consumption profile of the consumers, where the user is penalized for unnecessary peaks of import. The grid tariff has been investigated prior for buildings to reduce peak consumption, as discussed initially in [33]. This grid tariff was set to be implemented for residential users in Norway in 2022 but was delayed before being replaced with a new grid tariff [34]. For commercial buildings and large energy-consuming residential users in Norway, it has existed for several years as part of their grid tariff structure [35]. Within Europe, this grid tariff is present in some countries [9]. Another grid tariff that includes a long-term horizon is the subscribed capacity grid tariff, where the user is penalized for using more electricity than their subscribed limit. In Norwegian settings, this grid tariff has been investigated for yearly subscription periods [36], but other studies have also decreased the period down to weekly subscriptions [37]. The mentioned capacity-based grid tariffs show that accounting for longer periods of operation could become more common for end-users.

### 2.1.5 Coupling Short- and Long-term Value of Flexibility

HEMSs aim to operate the flexible assets to take full advantage of the value of flexibility. With the existing short-term operational models, the short-term value of flexibility is utilized explicitly. However, the long-term value of flexibility is not captured in the existing models, and is left out of the decision process. With long-term price signals as part of demand response programs, like the monthly demand charge, the need to couple the short-term and long-term operation is important to make overall optimal decisions. The flexible assets used in the short-term could also provide valuable flexibility on the long-term goal. To enable this long-term consideration, accurate and representative signals that gives information on the long-term value is needed. This could be given as input to a short-term model, that includes operational impact beyond the short-term scheduling horizon.

The monthly demand charge has been investigated and looked into in the existing literature for residential buildings. The goal of these works has been to find a way to identify an optimal peak-import level to balance demand charge cost and RTP-savings from increasing peak capacity. In [38], an adaptive optimal monthly peak demand limiting strategy for buildings with monthly demand charge cost was established. Their work used an optimal threshold resetting scheme to capture the future cost-savings of demand-limiting control, which sets an appropriate peak-import level during operation based on expectations. This study was extended in [39], where they tried to capture the tradeoff between load predictions and

actual power usage. Three different tradeoff schemes, which all consider different inputs of predicted and known data, are used here to find the optimal threshold for peak-import. The demand charge cost was investigated under a different approach in [40], where a metaheuristic approach was used. The approach aimed to balance cost-savings from RTP versus the demand charge cost, where a user-defined weighting constant put a cost on the grid tariff cost in the future.

In the aforementioned articles, the goal has been to give information to the short-term model on the potential long-term consequences of operation here-and-now. It offers additional information to existing models for HEMS operation, without complicating the problem further, to a certain extent. However, these approaches are limited in terms of representing general long-term price signals, since they are specifically made for the monthly demand charge. Based on the existing literature, there exists no general formulation or approach for representing long-term price signals into short-term operational models on the building side, or other end-users such as industry. Since the nature of these price signals can be quite different, this complicates the establishment of a general framework to deal with many variations of the signals. In addition, having multiple signals at once could also be required, which also raises the need for a general framework.

Within hydropower scheduling, splitting the operation of hydropower into short-, medium-, and long-term phases enables the long-term value of flexibility to be captured. The medium- and long-term phases analyze the long-term price signals, like reservoir level, environmental constraints, price and inflow data, and the outputs of the analysis are cost curves. These cost curves contain the long-term value of altering the short-term strategy, which can be fed into a short-term operational model. This is illustrated in [41]. For the medium- and long-term horizon, decomposition techniques such as Stochastic Dynamic Programming (SDP) and Stochastic Dual-Dynamic Programming (SDDP) have been frequently used to calculate the long-term value of flexibility. These techniques are general and enable different long-term price signals to be included. Dividing the operational decision into multiple phases enables the global, long-term value of flexibility to be captured during real-time operation of the HEMS, to improve the value of operation while also representing long-term price signals.

The use of SDP and SDDP as decomposition techniques has been investigated within the end-user side of the energy system recently. In [42], the authors used SDP on a multi-stage stochastic electricity market model with grid constraints, batteries, and intermittent renewable energy sources. Similar work was done in [43] using SDDP, but where both a short- and long-term model were coupled together to capture and showcase the long-term value of flexibility. The same main author has studied battery degradation using SDDP for a microgrid in [44] and how long-term planning can increase battery lifetime with degradation in [45]. The presence of these works together with the work related to this thesis, show that the long-term value of flexibility on the consumer side is becoming more

relevant and a more prominent topic of study.

## 2.2 $CO_{2eq}$-emission during Operation of a Zero Emission Building

### 2.2.1 Zero Emission Buildings

In 2010, the EU's Energy Performance of Buildings Directive (EPBD) launched the concept of Zero Energy Buildings [46], with the aim of promoting research on how buildings can assist in reducing emissions and bolstering security of supply. In recent years, the topic has expanded, with Zero Emission Buildings (ZEBs) [47] and Zero Emission Neighborhoods (ZENs) [48] being researched to determine how buildings can achieve net zero emission during their lifetime. Within these areas, all phases of the lifetime are taken into account, but the operational phase is deemed critical due to its role in reducing emissions through smart operation [49].

Reference [50] found that for a ZEB, the operational phase is influenced by building location, electricity mix in the grid, local on-site production, and how the building is designed and constructed. When it comes to emission compensation for ZEBs, the $CO_{2eq}$-intensity of the electricity grid is used as the indicator, and compensation is based on the electricity mix in the grid. A Norwegian standard definition states that emission compensation for buildings can be linked to export of electricity to the electricity grid, where the emission factor can be based on the local time-dependent electricity mix in the grid [51]. The value of emission compensation is then linked with import and export of electricity for the ZEB during operation.

Some literature looking at design of ZEBs, where the operational phase is included, has used annual average $CO_{2eq}$-intensity. This was done in [52] for a near-ZEB in Norway, where four PV technologies were investigated for different yearly average $CO_{2eq}$-intensities, seeing that PV increases compensation contribution with higher $CO_{2eq}$-intensity in the electricity mix. The emission factors used were taken from [53], where yearly average and marginal emission were calculated for different zones in Europe, based on several future scenarios on electricity mix. Yearly average $CO_{2eq}$-intensity was also used in [54] for electricity use, where optimal design of a school building was analyzed. For other technologies that did not use electricity, primal energy indicators presented their influence on emissions. The findings showed how the $CO_{2eq}$-intensity impacted installation of energy carriers, especially based on how strict the net zero-emission target should be. With a stronger net zero-emission target, investment in local PV production was prioritized, using the electricity grid as a virtual seasonal storage unit. During summer, excess electricity is exported, which is brought back during winter.

Given the use of yearly average $CO_{2eq}$-intensity, the net balance between import and export to the grid is emphasized, while the timing is not accounted for.

Some works have estimated hourly average $CO_{2eq}$-intensity values for the electricity system in Europe. A methodology to calculate these values for all hours, for different bidding zones in Europe, was presented in [55]. This was done by tracing the origin of electricity back to where it was generated. A similar approach was also taken in [56]. These approaches motivate more analysis on emission compensation for ZEBs on an hourly basis during operation. The work analyzed in [54] was extended in [57], where they compared hourly average $CO_{2eq}$-intensity and yearly average when designing a ZEN in Norway. They did not find that much changes to the design when comparing the two alternatives.

The two different ways of measuring $CO_{2eq}$-intensity on electricity from the grid have different consequences in terms of operational decisions for the energy system. With a yearly average, the overall goal lies in the net exchange of electricity over the year, where timing and seasonal variation is neglected. This limits the value flexible assets in a building can have on emission compensation, since load shifting does not influence the net import or export noticeably. This promotes more planning regarding the overall quantity of production and consumption over the year. With hourly $CO_{2eq}$-intensity, timing of interaction with the grid has more influence on emission compensation. As with RTP, $CO_{2eq}$-intensity varies from hour to hour, which creates an opportunity to use available flexibility to shift consumption and strategically interact when the $CO_{2eq}$-intensity is favorable. With high intensity, export of electricity is favored, while lower intensity promotes import of electricity. The finer resolution on the $CO_{2eq}$-intensity enables more possibilities to work on emission compensation in the continuous operation of the building over a year.

Another timing-dependent $CO_{2eq}$-intensity value that has been investigated is the hourly marginal $CO_{2eq}$-intensity value. This marginal factor is linked to the change in emissions from electricity when the load is increased or decreased. The emission savings or increase is linked to the marginal unit that would change production as a result of change in demand. Marginal values were included in the analysis of a ZEN in [57], and lead to lower cost of the energy system compared to only using average values. For the work in this thesis, the use of timing-dependent $CO_{2eq}$-intensity is limited to hourly average values.

### 2.2.2 Operation of Zero Emission Buildings

Operation of a ZEB would focus on managing the demand in the energy system, while accounting for emissions to achieve net zero-emission. As buildings have estimated lifetimes of approximately 60 years [58], analyzing for a representative operational year is a way to simplify the contribution on emissions for

the operational phase. As yearly operation enables the seasonal variations in the energy system to be captured, during operation of the energy system in the building, both cost of operation over the year and accumulated $CO_{2eq}$-inventory should be considered. This makes the goal of operating look at both economic and emission-based considerations. Emission-based consideration is not directly economic; it can either be included as a constraint, as was done in [54], or it can be converted by a conversion factor into an economic influence. The latter was done in [57] for a ZEN, where they used external compensation price options as the conversion factor, making emissions part of the economic objective function. This makes the overall objective function of operation multi-objective.

Little work has been conducted on optimal operation of ZEBs or ZENs, with a focus on net zero-emission. Such buildings and neighborhoods have been designed, where the operational phase has been included as part of the decision leading to the optimal design. Examples of these were presented in the previous subchapter. These works presented a whole year during the operational phase, to include the seasonal variation in operation. However, the operational phase was simplified since the overall goal laid on the design. An exception to this is [59], which investigated clustering methods, with the aim of designing the energy system of a ZEN. The clustering methods would simplify the operational phase to only include parts of the year, decreasing the complexity of the overall problem. The output in the model gave the optimal design of a ZEN. This method provides a way to account for the future operation in a simplified manner, to have some idea of the long-term consequence of operation.

The operational strategy for a ZEB including emission compensation is dependent on the seasonal variations. During winter, high thermal demand would promote flexibility use to shift consumption to hours with lower $CO_{2eq}$-intensity. The summer period would have high local production from PV systems, which with flexibility can either cover the user's own consumption or be exported to the grid when the $CO_{2eq}$-intensity is high. However, there is also a need to capture the necessary flexibility use to achieve the net zero-emission goal over the year. The performance of operation during winter and summer is coupled, as the strategic decision in each season influence each other. With a cost-effective strategy, sufficient compensation should be done without unnecessary use of flexibility that would increase cost of operation. The accumulated $CO_{2eq}$-inventory affects the strategic decision at different periods of the year, making the strategy of emission compensation coupled in time. In addition, the role of uncertainty during operation affects the importance of compensation and the possibility to perform cost-effective decisions. When strategically trying to operate a ZEB cost-optimally, having information on the future value of emission compensation would provide a means to take accurate actions during the year.

## 2.3 Seasonal Energy Storage

The role of flexible assets is ultimately to assist in the energy system by providing system service and better utilization of resources and infrastructure. The flexibility aims to adjust the consumption profile for the building to fit the price signals and cost-effective goals of operation. Some flexible assets have a shorter available time period in which their flexibility is effective. However, there also exist long-term flexible assets. These flexible assets aim to take advantage of long-term change in the energy system, for instance, seasonal variations.

Seasonal energy storage systems are able to take advantage of the seasonal variation in the energy system. These kinds of flexible assets have been investigated in some works. A literature review investigated the role of storage in the energy system [60], where long-term storage was examined. The need for electricity storage was found to be dependent on the percentage of renewables in the power system. Multiple seasonal storage medium options are listed, for instance, underground hydrogen storage and heating. Underground hydrogen storage was investigated in [61] to provide long-term storage. Both design and operation were considered regarding how the hydrogen storage could assist in emission reduction. Heating as seasonal storage is very beneficial on the consumer side, as heating demand covers a large portion of the energy demand [2].

A report in [62] lists seasonal thermal energy storage (STES) as a suitable long-term flexible asset within ZEN. The key objective for the STES is to store surplus heat generated during the summer and deliver this to the system during winter. The STES can store heating within different mediums, like hot water tank storage, water-gravel pit storage, and aquifer thermal energy storage, to name a few [63]. The STES is able to increase the self-sufficiency with renewable sources, which was investigated in [64], where the STES stored excess local solar production. These properties are important for the goal of more effective use of local production and to decrease the need from the electricity grid. Some drawbacks with STES are related to overall storage efficiency. A review from the techno-economic perspective of STES was conducted in [65], where different STES mediums and their performance were evaluated. For storage volumes around 10000 $m^3$, storage efficiency could fluctuate between 20-80%, depending on the medium. As such, the use of STES comes with potential losses, motivating efficient and accurate use of the STES during operation.

### 2.3.1 Operation of Seasonal Thermal Energy Storage

Operation of an STES would focus on either storing or releasing heat, based on the seasonal period and storage quantity. STES, as part of the energy systems, has been investigated in some studies. In [66], the STES was coupled with a

combined heat and power (CHP) plant, providing flexibility during operation to increase efficiency on the CHP. The work in [67] looked at a sector-coupled energy system model of Europe, to find the optimal investment and operation of the system. The STES was part of the investment option, assisting with the variation of demand and renewables in the long-term setting.

There is limited work that exclusively investigates the operational strategy for use of long-term flexible assets as STES. In studies where STES has been part of the analysis, the main goal has primarily been focused on design phases. However, the work in [68] investigated how the STES could assist in a district heating network to lower total system cost. The aim of the study was primarily targeting toward the operational side, where uncertainty in terms of demand for each month over a year would influence the strategic storage amount during the different seasons. A drawback of the work was the computational complexity, as the multi-stage multi-scenario problem took about eight to nine hours to solve. Also, each month was simplified as a representative day, and with three scenarios each for eight of the twelve months, the scenario tree included 6,561 different combinations. This shows that the operational setting includes much complexity and that it is beneficial to deal with this using decomposition techniques. The work managed to show how the strategic planning of the STES could provide long-term benefits for the system in an operational setting. Since the STES primarily deals with seasonal variation, having information on the consequence of operation between the seasons is vital to capture the benefit of long-term storage. As such, there is great potential in capturing the long-term value of flexibility for a storage system like an STES during operation.

# 3 Framework for Long-term Strategy of Energy Building Operation

This chapter presents the **Long-term Strategy Framework for Future Building Operation (LOSTFUTURE)** toolbox. The LOSTFUTURE toolbox is used to create a long-term strategy framework for operation of the energy system in buildings, finding the long-term value of flexibility. The toolbox can account for long-term price signals that are valid for longer periods during operation and account for the value of flexibility for multiple variables at once. The outputs of this toolbox are cost curves for the whole period, containing information on the long-term value of flexibility for the chosen variables, denoted as expected future cost curves (EFCCs). This chapter details the methodology of the toolbox, including the optimization problem defined for the building and the decomposition methodology for calculating the EFCCs. The analysis of results from using the LOSTFUTURE tool will be presented in Chapter 4.

## 3.1 The LOSTFUTURE Toolbox

During the PhD-period, investigating the long-term strategy framework has been the basis off all published work, and the formulated research questions. This has led to the creation of the LOSTFUTURE toolbox, which is a general formulation of the strategy framework. This formulation makes use of an optimization problem describing the energy system of a building, to generate expected future cost curves, representing the long-term value of flexibility beyond the current decision stage.

This toolbox searches for the long-term value of flexibility and global cost-optimal operation of a building with several flexible assets present. The long-term value of flexibility includes the short-term benefits of controlling the flexible assets and their influence on the long-term price signals. The outputs are several EFCCs, for each decision stage the overall period is decomposed into. The EFCC describes the long-term influence on variable values within a discrete state space. Thus, the EFCCs provide updated relevant future information based on the current stage and circumstances surrounding the use of flexible assets.

The overall framework can be integrated into various formulations of the energy system in buildings. This work has formulated a simplified building energy system, with most attention on the electrical system. This includes flexible and non-flexible loads, flexible assets of different types, and local PV-production.

The thermal system has been formulated to cover SH. In **Paper IV**, the thermal system was expanded with the presence of STES. The flexible assets are all considered behind-the-meter of the building, influencing the interaction with the electricity grid where electricity is purchased or sold.

The long-term price signals that are investigated in the overall problem have different goals, which changes the operational strategy. By incorporating these into the EFCCs, they are able to be represented and accounted for in a short-term setting, giving additional information to short-term operation models. An illustration of the LOSTFUTURE toolbox and the coupling to short-term operation models is shown in Fig. 3.1. As illustrated, the LOSTFUTURE toolbox analyzes input data, uses decomposition techniques to analyze the long-term period, and outputs several EFCCs for different decision stages during the overall period. The output then represents the future value of flexibility beyond a specified point in time.

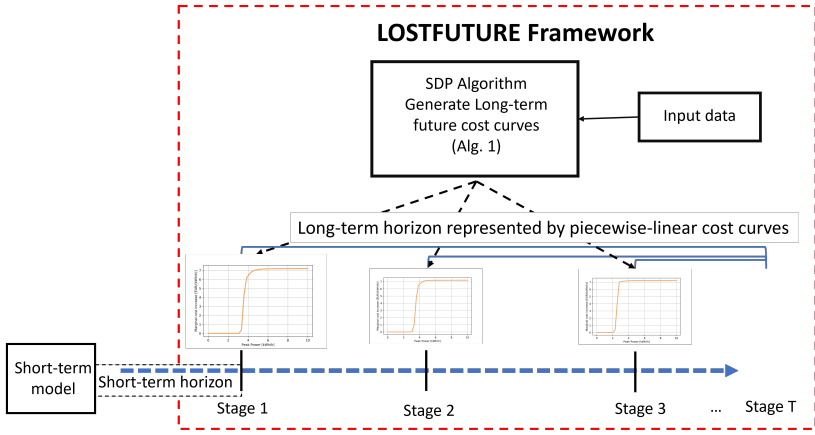


Figure 3.1: Illustration showcasing the purpose of the LOSTFUTURE Framework. The framework generates future cost curves that act as future price signals for a short-term operational model.

The toolbox is divided into two parts. The first part describes the formulation and structure of the strategy framework, including decomposition of the problem. This specific work has used SDP as the decomposition technique. The second part is the mathematical formulation making up the energy system of the building, including the different price signals and flexible assets present. The formulation of the overall problem and decomposition technique used will be presented in Chapter 3.2. The mathematical formulation of the energy system used can be found in Chapter 3.3.

## 3.2 Model Overview for LOSTFUTURE

The overall goal of the LOSTFUTURE toolbox is to provide a long-term strategy framework for building operation. Over a longer period and planning horizon, the toolbox generates operating strategies for several decision stages, representing the future cost of operation as EFCCs. The overall objective is to minimize the cost of operation for the energy system. The cost of operation include purchase of electricity from the local distributional grid, grid tariffs, and other price-based signals the end-user considers.

Over the course of the long-term period, the flexible assets within the building are intended to minimize the cost of operation. Their interaction is based on the here-and-now value of operation for a given decision stage, and according to the long-term implications by their operational decisions, denoted as the long-term value of flexibility. With the presence of long-term price signals that are valid for periods longer than a given decision stage, which are captured within the EFCCs, the variables making up the EFCC are coupled in time. For a specified short-term period, the operational decision and the actions taken here-and-now are influenced by the initial conditions, and by the future consequences of operation. With the presence of uncertainty, the overall operational decision is made up of multiple possible directions that could occur. This coupling between the long-term period gives the overall problem a dynamic nature, and the problem can be formulated as a multi-stage, multi-scenario optimization problem.

A multi-stage, multi-scenario optimization problem can be very large and time-consuming to solve. This depends mainly on the size of the problem, and the level of detail and scenarios present. For instance, the work in [68] formulated a multi-stage, multi-scenario optimization problem when analyzing the role of an STES in a neighborhood, where simplifications in decision stages were made to make the problem solve quicker. To simplify the problem, and to make it easier to solve and analyze the future value of operation, decomposition techniques can be applied. As mentioned within hydropower scheduling in Chapter 2.1.5, common techniques for decomposing similar problems are SDP and SDDP [41].

For the LOSTFUTURE toolbox, the original problem is decomposed into smaller decision stages. Each decision stage is decoupled from the others, only connected through the EFCC, and the state variables making up this cost curve. The solution procedure coupling the decision stages uses SDP as the foundation. Here, the state variables are discretized, and we analyze the operational performance for all the discrete values of the state variables and for all scenarios, in each decomposed decision stage. The analysis is done in a backward procedure, starting at the end of the long-term period and analyzing toward the first decision stage. More detail on the solution procedure is found in Section 3.2.3.

SDP was chosen as decomposition technique due to the origin of the problem. With SDP, the whole period can be analyzed without high computational effort by solving several smaller decomposed optimization problems. The influence of the discrete state space enable us to see how initial conditions of these variables affect operation. Another advantage is that SDP allows for non-convexity problems to be formulated and solved, which a standard SDDP technique is not capable of doing without modifications. The EFCCs within LOSTFUTURE can be piece-wise linear in nature and thus enables the non-convex value of flexibility to be represented. A drawback with SDP is that the computational effort increases with a larger system being analyzed. The number of decision stages, number of scenarios, and number of discretized state variable values all influence the total number of decomposed problems to analyze. Especially with both an increasing number of state variables and discrete values, the problem grows exponentially, known as the "curse of dimensionality". The accuracy of the cost curves acquired by the solution procedure depends on the step size of the discrete state variable points, which then poses an accuracy versus computation time issue.

### 3.2.1 Coupling between Decision Stages

When the overall problem is decomposed into several smaller, decomposed decision stages, the coupling between stages needs to be formulated. The set $\mathcal{S}_g$ contains information that is relevant for the decision stage $g$, including information that is carried over between the stages. This set is made up of two separate subsets; $\mathcal{S}_{\mathcal{S}_g}$ includes all scenarios and corresponding stochastic variables that are dependent on the decision stage $g$, while $\mathcal{N}_P$ contains the discrete state variables values that will be investigated and are part of the EFCC. Together, a decomposed decision problem is for a specific scenario and state variable initial condition defined as $s_g^s, n_p \in \mathcal{S}_g$. Thus, for each decision stage $g$, we investigate all combinations of scenarios and state variable initial conditions, which will be the foundation of calculating the EFCCs for each stage.

The coupling between stages and information carried over is directly linked to the EFCC. The EFCC contains the variables that we allow to couple the stages, and their relationship is captured by the cost change within the EFCC. Other information that is not part of the EFCC cannot be coupled between stages in a dynamic pattern. As such, this type of data must be simplified, such that a feasible transition between stages is possible. For instance, if a BESS SoC is not part of the EFCC, the start and end SoC condition must satisfy the other stages initial and ending values. The setup in LOSTFUTURE assumes a fixed start/end condition for short-term storage levels and flexible assets not part of the EFCC. This fixed parameter value can be determined by the user.

### 3.2.2 Stochastic Scenarios

The stochastic scenarios that are embedded in the long-term strategy framework increase the complexity of the overall problem. With a long-term price signal present, which for some could be decided at the end of the period, accounting for the future consequences are vital, and as such, this motivates a backward procedure in the decomposition technique. However, uncertainty and their dependencies can cause problems with the backward procedure. Some uncertainty, like for instance weather, has a serial correlation, as history defines the current scenarios. This is an issue that must be addressed for the SDP decomposition technique to be applicable backward. This is accounted for by treating the scenarios and assumptions for all stochastic variables as Markov Decision processes (MDP), and representing each scenario as a discrete occurrence [69]. MDP assumes memoryless scenarios, removing the dependencies on the historical coupling [70]. With MDP, we disregard how we got here, and only consider what scenarios can occur in the future, with their corresponding probability weights. This enables the backward procedure within SDP to be applied. The scenario coupling between stages is showcased in the lower half of Fig. 3.2.

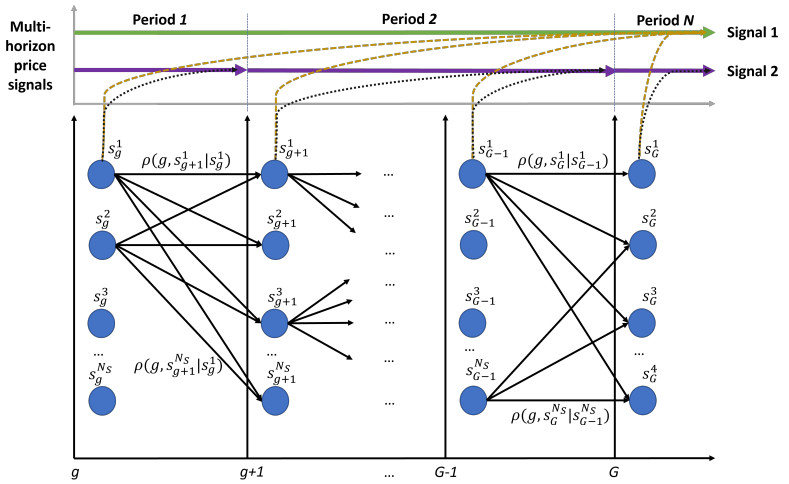


Figure 3.2: Illustration of scenario coupling between stage transition, and the correlation between stages and multiple price signals. Figure taken from **Paper IV**.

The different scenarios in the problem, as shown in Fig. 3.2, have an MDP behavior. There is no scenario tree expansion, since the dependencies have been removed by the assumed MDP behavior. Each decision stage has a finite number of scenarios $s_g^s \in \mathcal{S}_{\mathcal{S}_g}$ that could occur, with different parameter values for the stochastic variables. The transition probability $\rho(g, s_g^s | s_{g-1}^s)$ is the probability

of going from a specific scenario node to another when advancing the decision stage $g-1$ to $g$. Within a specific scenario, the stochastic variables in the overall optimization problem are given as parameter data. This makes each decomposed problem for a given stochastic scenario deterministic. Within LOSTFUTURE, most of the input data can be stochastic, depending on the use case and nature of the analysis. For instance, the list below mentions some possible stochastic parameters that could be set within LOSTFUTURE:

- Power system values: Spot price, $CO_{2eq}$-intensity values
- Weather-dependent parameters: Solar irradiation, outdoor temperature
- User-dependent parameters: Non-flexible electric demand, DHW demand, EV availability
- Seasonal parameters: Intake/outtake limitation for flow of heat to/from the STES

### 3.2.3 Solution Procedure: The SDP-algorithm

The solution procedure within LOSTFUTURE follows an SDP-algorithm layout. The SDP-algorithm is given in Alg. 1. For every decision stage $g \in \mathcal{G}$, for every scenario $s_g^s \in \mathcal{S}_{\mathcal{S}_g}$, and for every discrete point combination of all state variables $n_p \in \mathcal{N}_P$, the optimization problem presented in Chapter 3.3 is executed. The economic results from the optimization problem make up new EFCCs for every decision stage. The solution procedure operates backward, where we start in the last stage and move toward the first decision stage. This makes the generated EFCCs provide information on the future value of flexibility from that stage and beyond, based on the state variables. The algorithm follows a description of SDP, but an extension to the algorithm is given at lines 11-12, initiating an algorithm extension that is part of the work in this thesis. These lines are described in detail in Chapter 3.2.4.

Here, the algorithm will be explained in more detail. The SDP-algorithm initiates multiple for-loops at the start, one for stages and one for all discrete state variable initial values, in lines 1 and 2, respectively. Line 3 sets the state variable initial conditions for the applicable variables. $\beta$ is an auxiliary parameter representing the initial condition for each state variable. The formulation enables multiple state variables to be defined, and as such the index $n_p$ includes initial values for all state variables. Further on, the for-loop for every scenario is executed in Line 4, and the stochastic variables are defined in Line 5. The realized stochastic variables are specified from $\Gamma$, based on the current scenario and decision stage. The EFCC for this specific stage and scenario is set in Line 6, portraying the future value of flexibility. For the initial case $g = \mathcal{G}$, the EFCC could be specified

**Algorithm 1:** The SDP algorithm

1 **for** $g = \mathcal{G}, \mathcal{G}-1, .., 1$ **do**
2  **for** $n_p \in \mathcal{N}_P$ **do**
3  $\beta_i^{init} \leftarrow P_{i,\mathcal{N}_i}^{SV}$ for $i \in n_p$
4  **for** $s_g^s \in \mathcal{S}_{\mathcal{S}_g}$ **do**
5  $\{\mathcal{C}_t^{spot}, D_t^{El}, f_t^{CO_{2eq}}, D_t^{WT}, \delta_t^{EV}, I_t^{Irr}, T_t^{out}\} \leftarrow \Gamma(g, s_g^s)$
6  $\mathcal{C}_p^{future} \leftarrow \Phi(p, s_g^s, g+1)$ for $p = 1..\mathcal{N}_P$
7  $\mathcal{C}_{s_g^s, n_p} \leftarrow Optimize(3.1) - (3.9)$
8  **for** $s_{g-1}^s \in \mathcal{S}_{\mathcal{S}_g}$ **do**
9  $\Phi(n_p, s_{g-1}^s, g) = \sum_{s_g^s=1}^{\mathcal{S}_{\mathcal{S}_g}} \mathcal{C}_{s_g^s, n_p} \cdot \rho(g, s_g^s | s_{g-1}^s)$
10  **if** $g \in P^{Stages}$ **then**
11  $\Phi(...) \leftarrow UpdateEFCC(g, n, \Phi(...)) \quad \forall n \in P_g^{States}$

as end-values for the corresponding state variables at the end of the period, defined by the user. Line 7 solves the deterministic decomposed optimization problem, where the objective function result is stored in the $\mathcal{C}_{s_g^s, n_p}$ variable. The economic results are used to define the new EFCC for this stage in Lines 8-9. This for-loop is based on the scenarios that occur in the next stage $g-1$, which is the observation point for which the EFCCs will be valid. An EFCC is generated for each scenario combination, based on the weighted probability $\rho(g, s_g^s | s_{g-1}^s)$ during stage transition. The EFCC is the weighted sum of the objective function for each discrete variable value. The output then portrays an EFCC, where each discrete point captures the future value of flexibility given uncertainty and change in state variable values. When the EFCC has been completed for this stage $g$, the loop continues for the next stage until an EFCC has been generated for each stage over the period.

### 3.2.4 Extension to SDP-algorithm: Solution Strategy for Multi-period Price Signals

**Paper IV** describes an extension to the SDP-algorithm, where multiple long-term price signals of different characteristics and lengths where investigated. A specific case study involved having two price signals with different lengths, and where one would reoccur multiple times during the overall period. This multi-period price signal needs to be coupled to the EFCCs, so that only the period currently active is captured directly. This was intertwined in Alg 1 by lines 10-11, checking if the current stage provokes a new price signal period in $P^{Stages}$. If so, it performs this update for all state variables with a new price signal $\forall n \in P_g^{States}$.

The motivation behind this extension lies in situations with different long-term price signals being part of the EFCC, where one is repeating multiple times during the overall planning period. For instance, an STES considers a year to capture the seasonal variations of operating the flexible asset, while a monthly demand charge would consider a month at a time. Over a year, the monthly demand charge price signal would occur 12 instances during the planning period of the STES. For shorter but repeatable price signals, the EFCC needs to be updated during price signal transition, but still contain some level of information on their influence on price signals that are still active. During a transition, state variables need to keep coupling with each other correctly, so their information gives an accurate description of the future and their influence on each other. A new price signal contains no historical coupling with an existing price signal, but the existing price signal has historical influence on the old price signal. An illustration of the coupling between stages and situations with different periods are shown in the top part of Fig. 3.2.

The two signals used in Fig. 3.2 show how each stage always considers both price signals, while one of the price signals is having shorter, repeatable periods. Signal 2 has multiple periods being active or renewed, while Signal 1 considers the whole planning period. The EFCCs generated by this formulation should only consider the future cost of operation for the active price signals. As such, Signal 2 should only consider the period currently active, and not consider any information on future or historical periods. During transition of price signal periods, the EFCCs need to be updated to remove any direct cost association with the deactivated price signal, and must include the cost for the now present price signal in Signal 2. For Signal 1, it should still consider the whole future period. That includes periods when Signal 2 has different price signal periods active, and as such, some indirect influence on operation from these future periods of Signal 2 can be embedded within Signal 1. This coupling between price signals with different periods and lengths leads to the formulation of the extension within the SDP-algorithm, which is presented below in Alg. 2. Note that this formulation uses two state variables, but the formulation could be generalized.

Line 2 defines the new marginal cost for the long-term price signal that is being introduced. In Line 3, the initial state variable value for the price signal removed is stated. Line 4 initiate the for-loop for all scenarios, since the EFCC exists for all scenarios $s_g^s \in \mathcal{S}_{\mathcal{S}_g}$. Line 5 sets the EFCC cost for the (0,0) point, acting as the starting point of the EFCC matrix. The for-loop in Line 6 is for all discrete points of the state variable with the new price signal. At first, the marginal cost change for this state variable dimension is recalculated in Line 7, based on the new marginal cost $C_{init}^{val}$. This removes any information on the future value of flexibility from the removed price signal, and replaces it with the end-cost for the new price signal.

Lines 8-9 couple the new price signal with the other still-active price signals,

**Algorithm 2:** Function UpdateEFCC(...)

1 **Input:** $g, n, \Phi(...)$
2 $C_{init}^{val} \leftarrow C_{init}^{n,g}$
3 $n_{init} \leftarrow P_{init}^{n,g}$
4 **for** $s_g^s \in \mathcal{S}_{\mathcal{S}_g}$ **do**
5 $\quad \alpha(0,0) \leftarrow \Phi(0,0,s_{g-1}^s, g)$
6 $\quad$ **for** $n_0 \in \mathcal{N}_P^n$ **do**
7 $\quad\quad \alpha(n_0,0) \leftarrow \alpha(n_0-1,0)) + (P_{n_0,n}^{SV} - P_{n_0-1,n}^{SV}) \cdot C_{init}^{val}$
8 $\quad\quad$ **for** $n_1 \in \mathcal{N}_P^{\neq n} \backslash n_1 \neq 0$ **do**
9 $\quad\quad\quad \alpha(n_0,n_1) \leftarrow$
$\quad\quad\quad\quad \alpha(n_0,n_1-1) + \Phi(n_{init}, n_1, s_{g-1}^s, g) - \Phi(n_{init}, n_1-1, s_{g-1}^s, g)$
10 $\quad \Phi_{new}(n_0,n_1,s_{g-1}^s,g) \leftarrow \alpha(n_0,n_1)\ \forall n_0,n_1 \in \mathcal{N}_P^0, \mathcal{N}_P^1$
11 **Output:** $\Phi_{new}(...)$

generating a new EFCC. In these lines, the marginal cost changes for all other state variables are acquired from the existing EFCC, $\Phi$. An important part of this line is that the marginal cost we take from $\Phi$ is for the specific initial condition value of the removed price signal, as set in Line 3, $n_{init}$. This is done to deal with the existing coupling between the different price signals that is apparent in $\Phi$. For the new price signal, it has no dependencies to the other price signals. However, the old price signal has some coupling to the other, and the initial condition of this old price signal will be the basis when we arrive at this stage. By using $n_{init}$, the other price signals include information under the situation that at stage $g$, the future price signal will have an initial condition value $n_{init}$. We then get the marginal cost change in the new EFCC for a starting condition $n_{init}$. After the new EFCC has been formulated for all scenarios, the EFCC is returned to the SDP-algorithm in Alg. 1, and the general strategy framework calculation can continue. The new EFCC then includes a new price signal, no dependencies between that price signal and the others, but still information on the future price signals and their influence on operation.

## 3.3 LOSTFUTURE Optimization Problem

This section presents the general mathematical formulation of the optimization problem used within the LOSTFUTURE toolbox. The optimization problem describes the energy system within a single-family house. Within the energy system, different flexible assets are included, being controllable by the optimization problem. External and internal signals are included within the problem, such as grid tariffs and cost of electricity from the local distributional grid. The different papers have some deviations on the overall optimization problem, depending on

the system analyzed. This will be highlighted where applicable.

An illustration of the energy system within the building can be found in Fig. 3.3. The building contains several flexible assets that are controllable using the optimization problem, giving opportunity for DSM. The energy system considers mostly the electrical side, but the thermal system is also present in a simplified manner, in the form of SH flexibility.

The optimization problem is coupled to the solution procedure in that it describes a decomposed decision problem. For a specific stage, specific scenario, and for a specific initial conditions on the state variables, the optimization problem is formulated and solved, as formulated in lines 3-7 in the solution procedure in Alg. 1. The stochastic variables are realized within the problem as input data, making the problem deterministic within the decomposed formulation.

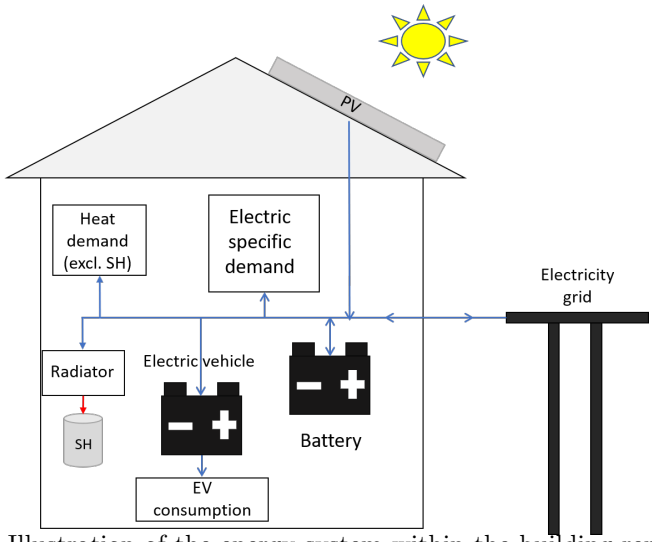


Figure 3.3: Illustration of the energy system within the building represented by the optimization problem, used in **Paper II**.

### 3.3.1 Objective Function

The overall objective function is to minimize the total cost of operation for the building, relative to the energy system and electricity usage. The objective function is divided into two different cost-considerations. The first is the cost associated with electricity purchase and sale with the local distributional grid, where RTP and volumetric grid tariff costs are accounted for. The second part is the expected future cost of operation, $\alpha_{g+1}^{future}$, which is portraying the long-term value of flexibility. This is based on the EFCCs generated, which for a specific

future stage $g+1$ is given as input for this optimization problem. With this formulation, the objective function accounts for the short-term cost of operation and the long-term value of flexibility. The costs that the EFCC considers are described in more detail in Chapter 3.3.7.

$$min\{\sum_{t\in\mathcal{T}}[\mathcal{C}_t^{spot}\cdot(y_t^{imp}-y_t^{exp})+\mathcal{C}^{grid}\cdot y_t^{imp}]+\alpha_{g+1}^{future}\} \tag{3.1}$$

### 3.3.2 Electrical Energy Balance

The electrical energy balance is described in Eq. (3.2). This covers interaction with the electricity grid, PV production, BESS, SH, EV, and electricity demand. This work has considered specific electricity usage from residents as non-flexible demand. The hot water tank included can be part of the electrical or thermal energy balance, and was placed in the thermal system in **Paper IV**. The thermal system is connected to the electrical side, so all heat is produced through electricity, from either a heat pump or radiator. This, however, is dependent on the case study and the thermal system used.

$$y_t^{imp}-y_t^{exp}+y_t^{B,dch}+y_t^{PV}=D_t^{El}+D_t^{WT}+y_t^{EV,ch}+y_t^{HP}+y_t^{B,ch}\quad\forall t \tag{3.2}$$

### 3.3.3 Electric Vehicle

The electric vehicle (EV) model is formulated in Eqs. (3.3a)-(3.3c). This work presents an EV modeled as a uni-directional battery, with continuous charging rate. The EV is only chargeable when connected to the building, set by the stochastic variable $\delta_t^{EV}$, and is discharged with a constant load discharge when away to simulate driving consumption. The EV has a time-dependent SoC range on the battery, which can be adjusted when, for instance, the EV is about to travel.

$$E_t^{EV}-E_{t-1}^{EV}=y_t^{EV,ch}\eta_{ch}^{EV}\delta_t^{EV}-D^{EV}(1-\delta_t^{EV})\qquad\forall t \tag{3.3a}$$

$$0\le y_t^{EV,ch}\le\dot{E}^{Max}\quad\forall t \tag{3.3b}$$

$$E_t^{EV,min}\le E_t^{EV}\le E_t^{EV,max}\quad\forall t \tag{3.3c}$$

### 3.3.4 Battery Energy Storage System

The building has a bi-directional BESS connected to the electrical system, with the characteristics as explained in Eqs. (3.4a)-(3.4d). The battery can be discharged and charged at a continuous rate, limited by power capacity and storage capacity. Battery degradation is left out of this formulation.

$$E_t^B - E_{t-1}^B = y_t^{B,ch}\eta_{ch}^B - \frac{y_t^{B,dch}}{\eta_{dch}^B} \quad \forall t \tag{3.4a}$$

$$0 \leq y_t^{B,ch}\eta_{ch}^B \leq \dot{E}^{B,ch,max} \quad \forall t \in \mathcal{T} \tag{3.4b}$$

$$0 \leq y_t^{B,dch} \leq \dot{E}^{B,dch,max} \quad \forall t \in \mathcal{T} \tag{3.4c}$$

$$E^{B,min} \leq E_t^B \leq E^{B,max} \quad \forall t \tag{3.4d}$$

### 3.3.5 Photovoltaic System

A PV system is roof-mounted at the building and provides local electricity to the building. The system, connected through the HEMS, can alter the power output up to the maximum time-dependent irradiation-dependent production.

$$0 \leq y_t^{PV} \leq A^{PV} \cdot \eta^{PV} \cdot I_t^{Irr} \quad \forall t \in \mathcal{T} \tag{3.5}$$

### 3.3.6 Thermal System

The thermal system involves all thermal energy needs for the building. In the first works, the thermal system only made up the SH section for indoor temperature control, but a larger system has been explored specifically in **Paper IV**, where an STES unit was included. Thermal energy delivery is only available from the electrical side of the energy system of the building. The explanation below is based on the formulation in **Paper IV**, for the extended thermal system with STES.

#### Heat Pump

The thermal system is connected to a heat pump (HP) that produce heat from electricity. The coefficient of performance (COP) is assumed to be constant at

all times. The production is continuous up to the rated capacity.

$$y_t^{HP,out} = COP^{HP} \cdot y_t^{HP}, \forall t \tag{3.6a}$$
$$0 \leq y_t^{HP} \leq P^{HP}, \forall t \tag{3.6b}$$
$$\tag{3.6c}$$

### Thermal Energy Balance

The thermal energy balance is captured through Eq. (3.7a). Heat can be provided by both the HP and STES discharge, which is used to cover SH-demand, hot water tank demand (if applicable and not present on the electrical side), or to be stored in the STES.

$$y_t^{HP,out} + y_t^{STES,out} = D_t^{WT} + q_t^{sh} + y_t^{STES,in} \quad \forall t \tag{3.7a}$$
$$\tag{3.7b}$$

### Seasonal Thermal Energy Storage

The STES is coupled to the thermal system, and can either provide or store heat based on the optimal decision. Eqs. (3.8a)-(3.8e) explain the characteristics of the STES. The STES has time-dependent limitation on flow of heat, giving options to seasonal limitation on flow if represented as stochastic variables. The STES can store heat up to the rated capacity of the storage unit. Efficiency losses of the system are captured through a constant efficiency loss factor, initiated at the start of operation for each decision stage. As the STES considers seasonal storage, being a long-term flexible asset, there is a need to couple the STES SoC

with the EFCC to be able to store heat between decision stages.

$$E_t^{STES} - E_0^{STES} \cdot (1 - \eta^{STES}) = y_t^{STES,in} - y_t^{STES,out}, t = 1 \tag{3.8a}$$

$$E_t^{STES} - E_{t-1}^{STES} = y_t^{STES,in} - y_t^{STES,out}, \forall t \tag{3.8b}$$

$$0 \leq E_t^{STES} \leq E_{Rated}^{STES}, \forall t \tag{3.8c}$$

$$0 \leq y_t^{STES,in} \leq \dot{E}_t^{STES,in,max}, \forall t \tag{3.8d}$$

$$0 \leq y_t^{STES,out} \leq \dot{E}_t^{STES,out,max}, \forall t \tag{3.8e}$$

### Space Heating

The indoor SH system covers the heating demand to keep the indoor temperature at comfortable levels. The system itself has been assumed to behave as a grey-box model, formulated as a linear state-space model [71, 72]. Using an RC-network model, the SH system and the dynamics between heaters, outdoor temperatures, and such can be coupled together. This work has used an 2R2C model in the optimization problem, formulated in Eqs. (3.9a)-(3.9d). With this 2R2C formulation, the SH system is divided into three zones: the indoor, the envelope acting as the walls around the building, and the outdoor area. All of these zones have their respective temperature, with the outdoor temperature being given as input. The indoor temperature is adjustable through the radiator providing heat, with temperature ranges given as input to specify the levels deemed comfortable for the residents.

$$0 \leq q_t^{sh} \leq \dot{Q}^{sh} \quad \forall t \tag{3.9a}$$

$$T_t^{in,min} \leq T_t^{in} \leq T_t^{in,max} \quad \forall t \tag{3.9b}$$

$$T_t^{in} - T_{t-1}^{in} = \frac{1}{R_{ie}C_i}[T_{t-1}^{e} - T_{t-1}^{in}] + \frac{1}{C_i}q_t^{sh} \quad \forall t \tag{3.9c}$$

$$T_t^{e} - T_{t-1}^{e} = \frac{1}{R_{ie}C_e}[T_{t-1}^{in} - T_{t-1}^{e}] + \frac{1}{R_{eo}C_i}(T_{t-1}^{out} - T_{t-1}^{e}) \quad \forall t \tag{3.9d}$$

### 3.3.7 Expected Future Cost Curve

The EFCCs are formulated within the optimization problem to describe the future cost change for the building, based on the state variable values. This expression allows the optimization problem to consider the consequences of operation beyond the detailed horizon in the decision stage. The EFCCs are generated as part of the solution procedure, explained in Chapter 3.2.3.

The formulation of the EFCC in a general manner is demonstrated in Eqs. (3.10a)-(3.10g). The formulation enables up to $\mathcal{N}$ number of state variables being coupled to the EFCC. The EFCC is based on discrete points of the state variables, where the weighting variable $\gamma_p$ defines all discrete points within the curve, in up to $\mathcal{N}$-dimensions. The sum of the weighting variable must be equal to 1 in Eq. (3.10a). Based on the weighted variables, the future cost is defined in Eq. (3.10b), where the future cost for each discrete point $\mathcal{C}_p^{future}$ is multiplied by their weighted variables. This future cost is coupled to the objective function.

$$\sum_{p}^{\mathcal{P}} \gamma_p = 1 \tag{3.10a}$$

$$\alpha_{g+1}^{future} = \sum_{p}^{\mathcal{P}} \gamma_p \cdot C_p^{future} \tag{3.10b}$$

$$\sum_{i}^{\mathcal{D}_n} \lambda_i = 1, \quad \forall n \in \mathcal{N} \tag{3.10c}$$

$$\lambda_i = \sum_{p}^{\mathcal{P}_i} \gamma_p, \quad \forall i \in \mathcal{D}_n, \forall n \in \mathcal{N} \tag{3.10d}$$

$$0 \leq \gamma_p \leq 1, \quad \forall p \in \mathcal{P} \tag{3.10e}$$

$$0 \leq \lambda_i \leq 1, \quad SOS2 \quad \forall i \in \mathcal{D}_n, \forall n \in \mathcal{N} \tag{3.10f}$$

$$SV_n = \sum_{i}^{\mathcal{D}_n} P_{i,n}^{SV} \cdot \lambda_i, \quad \forall n \in \mathcal{N} \tag{3.10g}$$

The state variables are connected to the EFCCs through the auxiliary variable $\lambda_i$. $\lambda_i$ makes up discrete representation of the state variables, where a specified number of indices $i \in \mathcal{D}_n$ are connected to each state variable $n$, as given in Eq. (3.10c). The coupling of the auxiliary variables and the weighting variables $\gamma$ are done in Eq. (3.10d), tying the EFCC to the state variables. To illustrate this modeling approach, Fig. 3.4 shows how the auxiliary and weighted variables are connected, for a system with two state variables ($\mathcal{N} = 2$). Each state variable is made up of several discrete points, where each auxiliary variable point is con-

nected to several weighting variables $\gamma_p$. For instance, auxiliary variable point $\lambda_0$ would in Eq. (3.10d) sum up every weighting variable $\gamma_p$ for $[(0,0),(0,1),(0,2)]$ in that dimension, which is repeated for all discrete points and for all state variables in the matrix. With this, the state variables are connected to the EFCC through the weighting variables. The auxiliary variable points $\lambda_i$ are coupled to their corresponding state variable in Eq. (3.10g), where $SV$ is a generalized formulation for the chosen decision variables making up the EFCC.

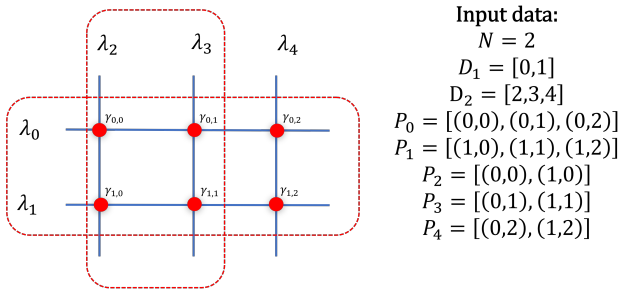


Figure 3.4: Illustration of an EFCC with 2 state variables, and example input data to showcase the coupling of state variables and weighting variables. The dotted red lines overlapping show how the formulation represents a piecewise-linear plane for 2 state variables.

The state variables can have continuous value, meaning the discrete weighted points in the EFCC can be made up of several weighted points. For linear and convex optimization problems, piecewise-linear weighting between adjacent points would occur naturally as part of the problem formulation. For instances where non-linear problems exist, this can be handled by coupling the discrete state variables points $\lambda_i$, $\forall i \in \mathcal{D}_n$ together with an special ordered set of type 2 (SOS2)-nature for all $n$. SOS2-nature means that for a set of variables, up to two of them can be non-zero, and additionally they must be adjacent to each other in the set [73]. Eqs. (3.10e) and (3.10f) describe the value range for the weighting variable and state variable points, respectively, whereas the latter can include an SOS2-formulation.

### 3.3.8 Long-term Price Signals

The different works in this thesis have implemented several long-term price signals as part of the EFCC. These all have a unique formulation that ties them to the EFCC-constraints, and that makes up the state variables in $\lambda$. For a given state variable $n$, the mathematical coupling to the EFCC would be as formulated in Eq. (3.10g).

Each of the long-term price signals analyzed in this work are given here, in their mathematical formulation. Note that this list is exclusively related to the published work in this thesis, but this does not prelude other decision variables or price signals from being formulated with this layout. In fact, this is encouraged to improve the framework and possible strategies to be formulated.

### Monthly Demand Charge

**Papers I, II, and IV** investigate a monthly demand charge as long-term price signal. This grid tariff puts a cost on the highest single-hour import quantity over the entire month. The mathematical formulation of this grid tariff is presented in Eqs. (3.11a) and (3.11b) for a specific decision stage. The state variable $p^{imp}$ sets the highest peak import level achieved, which can be based on the historically highest peak import value in Eq. (3.11a), or based on the operational decision on import of electricity during this stage in Eq. (3.11b).

$$p^{imp} \geq P_0^{imp} \tag{3.11a}$$

$$p^{imp} \geq y_t^{imp} \quad \forall t \tag{3.11b}$$

### $CO_{2eq}$-inventory for Net-zero Emission

**Paper III** introduces a long-term price signal based on emission from electricity for end-users. The state variable for $CO_{2eq}$-inventory $e_{CO_{2eq}}$ is based on the initial emission quantity for this decision stage, and the interaction with the grid during this period, given in Eq. (3.12). $f_t^{CO_{2eq}}$ contains information on the time-dependent average $CO_{2eq}$-intensity of electricity in the distributional grid, based on the electricity mix and electricity transfer between bidding zones. This $CO_{2eq}$-intensity value enables compensation of emissions to be performed by exporting electricity to the grid, where compensation is based on the current intensity value.

$$e_{CO_{2eq}} = E^0_{CO_{2eq}} + \sum_{t \in \mathcal{T}} (y_t^{imp} - y_t^{exp}) \cdot f_t^{CO_{2eq}} \tag{3.12}$$

### Short- and Long-term Flexible Assets

It is also possible to couple flexible assets to the EFCCs as long-term price signals. This was done in **Paper IV** for an STES, in which the seasonal coupling of the

asset is necessary to use it optimally. As described in **Paper IV**, this is achieved by coupling the storage level at the last time step to the EFCC, for instance, $E_{\mathcal{T}}^{STES}$. The EFCC then captures the future value given the end storage level at this stage. The price signals captured within the EFCC would then correspond to the long-term value of flexibility from this flexible asset directly, in terms of change in storage level. This formulation is extendable to any type of flexible asset within this work, for instance, EV, BESS, and SH, but this has yet to be investigated further.

# 4 Results and Discussion

This chapter presents the results and findings from this PhD, which are primarily based on the published articles given in Chapter 1.4. Some of the published works have led to further results that are not stated in the published work but are still highly relevant for this thesis. These additional results are mentioned here. The overall findings are compiled into three categories, as shown in Fig. 4.1. This layout is the basis of this chapter. The first category examines the long-term value of flexibility for energy building operation, and how long-term price signals can be formulated and represented to short-term operation. The second category considers more closely the flexible assets in buildings and their long-term performance on operation. This includes short-term flexible assets and long-term flexible assets. The last category provides a technical overview of representing more detail in the long-term strategy framework.

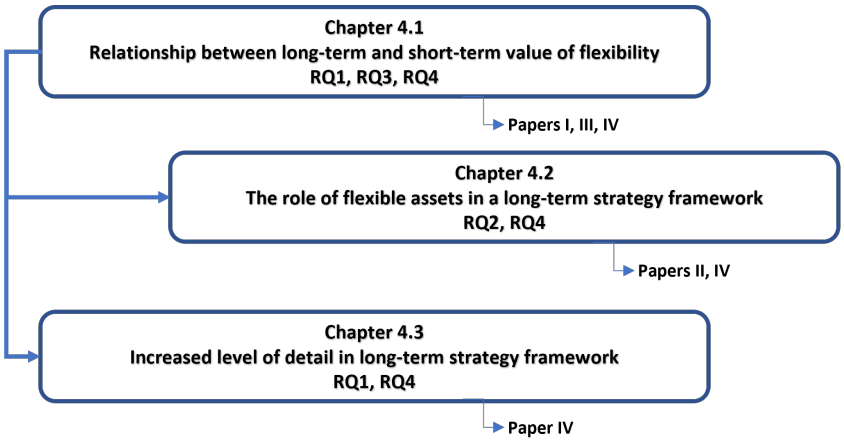


Figure 4.1: Overview of the structure for Chapter 4, and each subchapters relation to published work and research questions.

## 4.1 Relation between Long-term and Short-term Value of Flexibility

The main focus of this thesis has been to explore the long-term value of flexibility, in light of different price signals. The overall goal has been to generate a long-term strategy framework, which can be coupled to a short-term operational model

to improve overall performance. This section outlines the different long-term strategies that have been investigated in the published works, and presents a detailed exploration of what added value the long-term strategy framework offers to performance. The first part addresses the relevant articles and their long-term price signals, while the second part compares the price signals investigated and discusses their influence on operation.

### 4.1.1 The Value of Including Long-term Price Signals

#### Paper I: Monthly Capacity-based Grid Tariff

In this paper, an early version of the LOSTFUTURE toolbox in Chapter 3 was created to analyze the long-term value of flexibility for operating the energy system of a Norwegian building. The motivation for long-term consideration stems from a monthly demand charge grid tariff, which imposes a cost each month based on the highest single-hour electricity import. This price signal motivates a flat import profile over the month. Since the overall period is included in the grid tariff cost, the need to consider a strategic optimal peak-import level from the start of the period will benefit cost of operation, and resulted in this framework being put to the test.

The flexible assets in this building comprise of a BESS, a uni-directional EV charger, and SH. With this flexibility portfolio available, electricity import can be controlled to maintain a cost-optimal peak-import level, while also considering the limitations within the flexible assets. The LOSTFUTURE toolbox generates multiple EFCCs for each decision stage throughout the month, that show the future cost increase of adjusting peak-import. Each EFCC considers the future cost for all days in the future, so the closer to the start of the month, the more information about the future is captured in the EFCCs, since a backward SDP is applied.

The marginal EFCCs (MEFCCs) for specific days are presented in Fig. 4.2, which shows the change in marginal future cost based on peak-import. With more days included, the curves account for two distinct occurrences that influence strategy of operation. First, the curves account for high-demand days, which would put the lower-bound on peak-import. Since the grid tariff is based on the highest single-hour, a highly asymmetric state variable, the worst-case scenario in terms of peak demand gives the set-point. Second, the benefit from RTP cost could motivate higher peak-import levels. If the variation in spot prices are high, the increased incentive on having more flexibility on import timing to save RTP cost, could be higher than the cost of peak-import. For one specific day, the marginal cost of peak-import on a monthly level would most likely not cover the RTP variations, but the more days included, the more opportunities for this marginal

peak-import cost increase to be covered over the month. This trend is captured in Fig. 4.2, where comparison of MEFCCs for day 1 and 15, indicates that day 15 has, in general, a higher marginal future cost for all peak-import levels. The offset of these two curves are both based on higher peak-demand scenarios, but also due to more days with RTP benefits being captured in day 1 MEFCC.

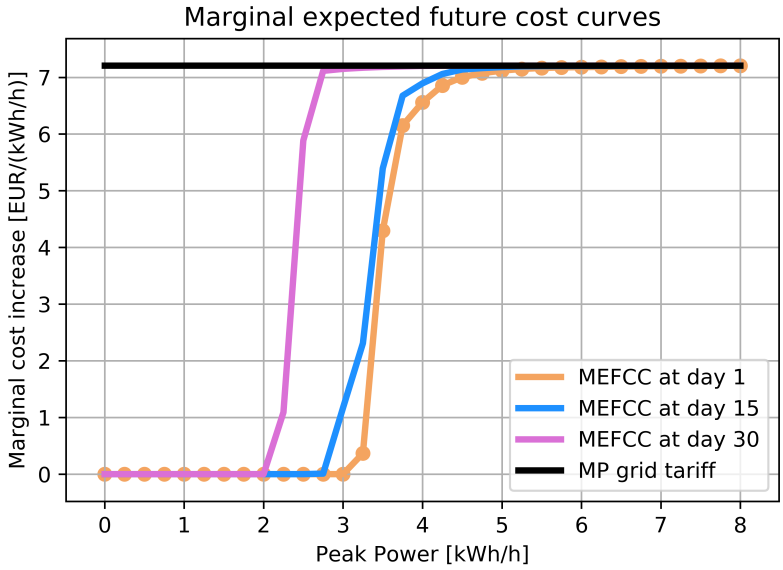


Figure 4.2: Overview over marginal EFCCs for different days over the month. Figure taken from **Paper I**.

The findings in this paper showed that the LOSTFUTURE toolbox represents the long-term price signals and long-term value of flexibility during operation. The EFCCs reveal the cost-optimal initial peak-import level to aim for at the beginning of the month. During operation, each EFCC contributes to a continuously updated consideration of the future value of flexibility in terms of peak-import levels, based on the current decision stage. The framework was compared to two different simple strategies that could handle the long-term price signal. One ignores the long-term price signal during operation, which had the highest total cost of operation due to high demand charge cost. The other strategy tried to minimize peak-import level due to no knowledge of the future cost of operation. It achieved a lower average peak-level than the LOSTFUTURE framework did but had a higher total cost of operation over the month. This is due to more use of flexibility earlier in the month to keep peak-import levels low, which in most cases was readjusted later in the month. This approach leads to extra cost of flexibility use without any savings in return. The LOSTFUTURE framework performs better since it has a representation of the future cost of operation, which

makes it start the month on a peak-import level closer to the achieved level. It could for some few scenarios start on a higher peak-import level than what would be possible to achieve over the month, caused since the strategy accounts for uncertainty and finds the expected future value of flexibility. In addition, it considers the added value of increasing peak-import to increase RTP savings, which the other strategies do not consider at all.

### Paper III: Net-zero Emission during Yearly Operation of Energy System in Buildings

**Paper III** explores a different type of price signal, where emission compensation during operation in a ZEB is analyzed. The long-term strategy is to achieve net-zero emission during operation over a year while taking into account building-embedded emissions. The analysis considers that hourly average $CO_{2eq}$ emission factors for electricity in the distributional grid are accounted for during operation, based on the electricity mix in each NordPool bidding zone. Emission is accumulated and compensated based on import/export of electricity to the distributional gird, based on the average emission factor for the specific hour of operation. As stated in [49], the operational phase is deemed critical for achieving net-zero emission for a ZEB, and at least zero-emission should be achieved during this phase. Therefore, there is high motivation to identify the appropriate operational strategy over the year, to achieve net-zero emission for such a building.

Currently, cost of emission is not considered for end-users and normally not part of the operational decision for buildings. However, this was included in the objective function by representing it as a cost-based price signal, making the overall goal multi-objective. The cost is only considered for the ending $CO_{2eq}$-inventory at the end of the year, where the cost is based on the yearly accumulated $CO_{2eq}$-emission and a user-defined penalty cost. The penalty cost allows the user to define how much it should prioritize emission compensation versus cost of operation, to co-optimize both over the year. With this multi-objective formulation, a user-defined cost of emission is compared to the real monetary cost of operation, where the penalty cost weight influences the priority during operation.

This price signal on emission compensation is embedded in the LOSTFUTURE framework and in EFCCs as a long-term price signal, given at the end of the year. The strategy framework then generates EFCCs that consider the change in future cost based on the $CO_{2eq}$-inventory at each week of the year. The long-term value of flexibility captures the future opportunity cost of compensating emissions, which is achieved through flexibility from the flexible assets. The strategy compares if the marginal cost of emission compensation in the current operational stage is cost-efficient to perform now, or in the future. In addition, the EFCCs account for the whole year, which includes seasonal variation in strategies

to deal with emission compensation. During the summer, excess production is exported, and during winter, timing of import of electricity is focused.

The influence of varying penalty cost for emission compensation is captured in Fig. 4.3. Here, the MEFCC for the first week of the year is shown, with varying penalty costs. Since this curve considers the rest of the year, it highlights the compensation potential over the year with the different penalty costs. At negative inventory (meaning surplus of compensation), the marginal cost is close to zero. At zero cost, the current inventory level is satisfactory to reach net zero-emission during the year, and emission compensation can be disregarded during operation. With higher inventory, the marginal cost increases, implying that some compensation must be performed during the year to reach zero-emission. This marginal cost reflects the expected future cost increase to compensate for this specific inventory level. The curve flattens with increasing emission inventory at their corresponding penalty cost. The penalty cost sets the limit on how much the user is willing to pay for marginal compensation increase. At these points, it is expected that some leftover emission is present at the end of the year, and a marginal $CO_{2eq}$-inventory increase would increase the total cost of emission paid at the end. Should there be some flexibility remaining to perform this marginal emission compensation, it is deemed more costly than the penalty cost, and as such, the cost-optimal solution is to pay the penalty. With increasing penalty costs, more cost-optimal compensation opportunities exist in the future to reach net zero-emission. These opportunities show how much compensation can be achieved through flexibility, and that there is a wide range of options during the year, with different costs for flexibility behind them.

The results in **Paper III** for a Norwegian building located in NO2, found that with increasing penalty cost, the ending $CO_{2eq}$-inventory decreased, with close to zero-emission being achievable at around 1 $\frac{EUR}{kgCO_{2eq}}$. With the increased focus on emission compensation, the cost of operation increased, implying that the shift of focus affected the economical performance for the building. However, at 1 $\frac{EUR}{kgCO_{2eq}}$, the yearly cost increase compared to ignoring emission compensating only came to 4.5%, despite a penalty cost almost 40-times larger than the highest cost for $CO_{2eq}$-quotas in 2019 [74]. The International Energy Agency (IEA) reported that by 2050 the $CO_{2eq}$-price could reach up to 0.25 $\frac{\$}{kgCO_{2eq}}$ [75], which is only about a quarter of the 1 $\frac{EUR}{kgCO_{2eq}}$ penalty cost tested here.

The interaction on purchase of electricity exhibited a change in behavior with increasing penalty cost. The work in [76] found that the Norwegian bidding zone NO2 has tendencies of opposite peaks between electricity price and $CO_{2eq}$-intensity, which was also the case in our study. With increasing penalty cost, and higher need for compensation, this motivates the operational strategy to import during times with high electricity price, and export during off-peaks. The reason for this is primarily that the high share of hydropower enables increased production when the prices are high, and allows the interconnectors to Denmark

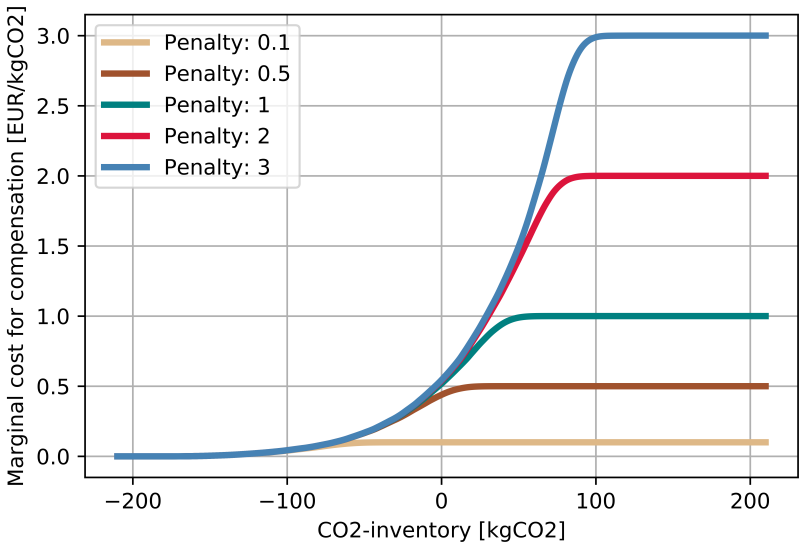


Figure 4.3: MEFCCs for different penalty costs, at week 0. Taken from **Paper III**.

and the Netherlands supply electricity when the price is low. This strategy works against the desired behavior on use of flexibility in buildings, and could in large-scale cases increase risk of congestion in the system. This trend was observed in our work, where the strategy changed with increasing penalty cost. The increasing penalty cost motivates the system to increase import at high electricity-price hours, due to low $CO_{2eq}$-intensity.

The analysis of the Norwegian case study in NO2 was compared to a Danish case in DK1. In DK1, net zero-emission was achieved regardless of penalty cost. This was due to the electricity mix, and the timing of electricity price and $CO_{2eq}$-intensity. With a high presence of wind power, the variation in $CO_{2eq}$-intensity was greater than in NO2, and the intensity followed the variation of electricity prices, with low intensity during low price-hours. The strategic planning from the SDP-algorithm still showed possible compensation potential in the future, although it was not necessary to use flexibility toward emission compensation to achieve the net-zero emission criteria. By considering emission obtained during other phases of the ZEB in the emission compensation goal over the year, this strategy would be able to use the available flexibility to increase compensation further. The comparison between DK1 and NO2 showed that the low variation in $CO_{2eq}$-intensity in Norway, together with dispatchable hydropower, makes emission compensation a non-preferred operational strategy for the building.

### Paper IV: Seasonal Thermal Storage with Monthly Capacity-based Grid Tariff

The work on the LOSTFUTURE framework in **Paper IV** increased the dimensions of the EFCC to include two long-term price signals. The strategy for the building in this work combines an STES unit, together with the monthly demand charge grid tariff. This makes the overall long-term objective to store heat from summer to winter, while keeping the peak-import level under control for each month of the year. The recurring monthly demand charge required a change to the framework, which led to the extension of the SDP-algorithm, described in Chapter 3.2.4. This extension enables the EFCCs to capture the long-term strategy even when a signal is repeating and only valid for shorter periods at a time.

The operational strategy acquired by the SDP algorithm manages to account for both long-term price signals, including their influence on each other. The MEFCCs generated are valid for each marginal direction available, and thus one for both the demand charge and STES is generated for each stage. Figs 4.4, 4.5 present the MEFCC for each long-term price signal for day 140, which is about 45 days before the winter period initiates. Looking at the demand charge MEFCC in Fig. 4.4, the STES SoC heavily influence the strategy for peak-import. With higher SoC, less peak-import is needed. This profile implies that the strategy here is influenced by how prepared the STES is for the winter period, with high priority on increasing peak-import to store heat in the STES if necessary. Likewise, the STES MEFCC in Fig. 4.5 shows that the future opportunity value for heat decreases with higher SoC. With high SoC, lowering peak-import level increases the added value of storing heat, which indicates that with limited electricity import, each marginal heat storage increase is more valuable in the future. As demonstrated here, the EFCCs generated captures the long-term value of flexibility for both price signals, and how they influence each other. A strategy for one of the price signals influences the strategy for the other, and thus they work together to achieve an optimal long-term strategy for the energy system.

During the operational analysis, the findings in **Paper IV** revealed that the long-term strategy balances both the STES and demand charge throughout the year, as showcased in Fig. 4.6. For each month, the strategy regarding the demand charge is clear and without too much variation, and also well-tied to the STES SoC. During summer, the STES influences the peak-import in September and October, increasing peak-import to aggressively store heat for the winter period. This added peak is primarily only meant to increase STES SoC, supported by the MEFCCs in Figs. 4.4, 4.5. Had the SoC been higher, the peak-import would have been decreased, which occured in the case in **Paper IV** where PV was included in the energy system. During the winter period in Fig. 4.6, the peak-import is significantly reduced by discharging the STES, and sees little variation throughout the winter. The last two months are the ones with the most variation

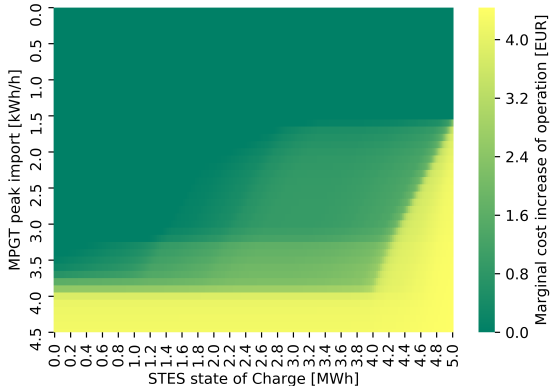


Figure 4.4: MEFCC for demand charge in day 140. Taken from **Paper IV**.

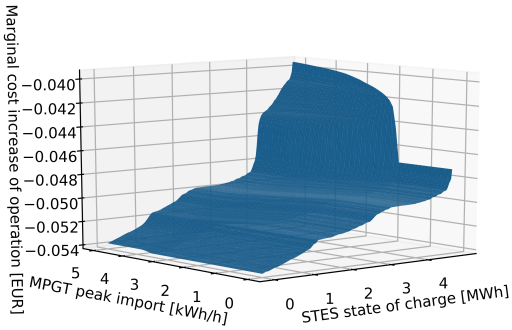


Figure 4.5: MEFCC for STES in day 140. Taken from **Paper IV**.

in profiles, whereas the initial STES SoC at the start of March influences the planned peak-import level for the two months, to properly distribute the remaining heat and reduce demand charge cost. This shows that the two price signals work together to minimize the cost of operation over the year, and their strategy is well-captured by the EFCCs generated with the LOSTFUTURE framework.

### 4.1.2 Long-term Value of Flexibility with Long-term Price Signals

The three papers mentioned above have all described different types of long-term price signals. When comparing these to each other, their behavior and influence

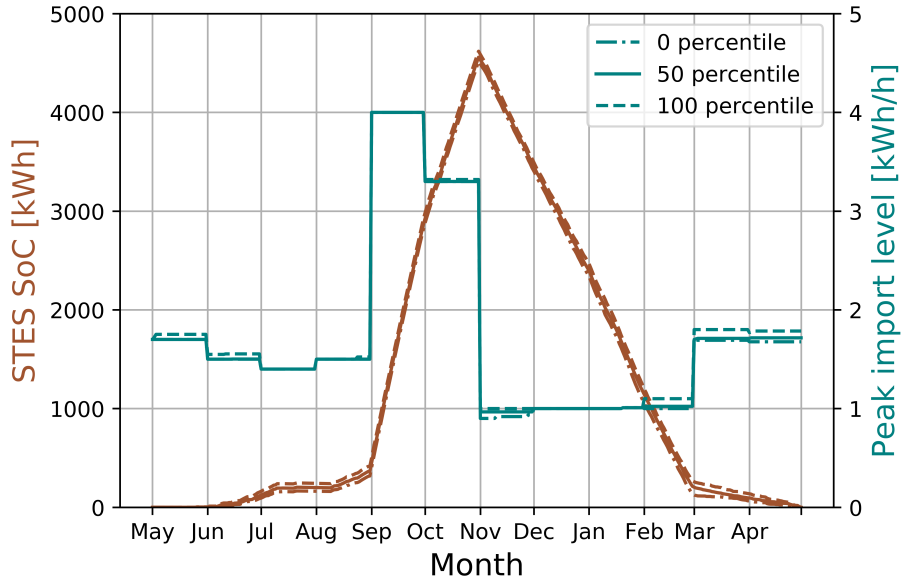


Figure 4.6: Operational performance with STES and monthly demand charge, without PV. Taken from **Paper IV**.

on operation differ noticeably, which we will try to sum up and discuss here.

The monthly demand charge is a cost based on your import profile, measured based on the interaction with the electricity grid. The motivation for the price signal is to have a predictable and flat consumption profile over the month, and avoid short unnecessary peaks. With higher peak import, this influences the strategy going forward, and there is no way to counter an unnecessary peak, except by making the best out of the available flexibility. This asymmetric price signal values a carefully thought out strategy to handle peak import. By accounting for the grid tariff through EFCCs, this enables the available flexibility to consider this grid tariff directly and also how this flexibility influences RTP variation in the future.

The $CO_{2eq}$-inventory has no direct influence on the user's electricity bill, as emission inventory is not paid explicitly by the end-users. The way it was formulated in **Paper III** is based on the willingness to let the consumption profile account for emission. By considering emission compensation, this will lead to an increase in cost of operation, given that compensation is necessary. The internal goal of net zero-emission would impact users' interaction with the distributional grid. If the timing and variation between RTPs and $CO_{2eq}$-intensity is off, it would promote going against an economical optimal solution. However, this way of rep-

resenting $CO_{2eq}$-inventory enables consideration of the whole year of operation, and the possibilities of compensation in the future. During winter, accumulation of $CO_{2eq}$-inventory is expected, since compensation can be achieved through export during summer. As such, variation on a seasonal level is accounted for with this long-term price signal. Without a long-term price signal, for instance having a flat penalty cost on emission accumulation during short-term operation, this would result in higher use of flexibility and increased cost of operation, and it would be difficult to reach the exact end-goal of $CO_{2eq}$-inventory. With the EFCCs, the long-term value of flexibility on the price signal is captured, preventing unnecessary use for short-term price arbitrage.

Long-term price signals in form of flexible assets provide us a broader use of flexibility. Long-term flexible assets, such as an STES, try to take advantage of seasonal variation of the energy system. Within short-term models, capturing the long-term advantage of these flexible assets is difficult. As such, representing them as long-term price signals within EFCCs enables this advantage to be accounted for during operation. The STES in **Paper IV** aimed to decrease cost of operation during winter by storing cheaper electricity from the summer period. This provides an increased benefit to the energy system, reducing the overall cost of operation. The long-term value of flexibility for flexible assets can be captured directly, and improve operation of energy systems.

Another point is how the long-term price signals influence each other, as was investigated in **Paper IV**. There, both an STES and monthly demand charge were coupled and represented by the EFCCs. These two price signals have different goals during operation, and as such, do collide with each other and their long-term strategy. However, in this work, the STES managed to take advantage of its long-term flexibility to influence the monthly demand charge and lower the grid tariff cost over the whole year. By increasing peak-import during summer, the STES could assist in reducing the peak-import during winter even lower than without the STES. Both price signals reacted based on each other, proving that this long-term strategy framework managed to create synergy between them. Thus, by including multiple price signals, the performance could improve and lead to further interesting results. As was described in **Paper III**, considering $CO_{2eq}$-inventory leads to a strategy that increases risk of congestion. However, the introduction of long-term flexible assets or other price signals might make it possible to reduce this risk. Therefore, combination of long-term price signals could counteract the flaws each of them have, and improve the overall operational performance.

## 4.2 The Role of Flexible Assets in a Long-term Strategy Framework

The flexible asset available are making it possible to operate buildings to reduce the cost of operation or to react to long-term price signals. The flexible assets enable the system to adjust the consumption profile, and each asset available have different roles and characteristics when performing flexibility. This section aims to investigate the flexible assets that have been presented in this work in the context of performance toward long-term price signals. Here, we focus primarily on short- and long-term flexible assets, since both has been studied in the published work.

### 4.2.1 Short-term Flexible Assets

#### Paper II: Long-term Value of Flexibility from Short-term Flexible Assets

**Paper II** extended the work denoted in **Paper I**, by investigating the role short-term flexibility played regarding the monthly demand charge long-term price signal. The flexible assets, being an BESS, an uni-directional EV charger, and SH, make up the chosen flexibility within the building that can be controlled and adjusted accordingly in this work. The monthly demand charge is an asymmetric price signal that penalizes unnecessary peak-import levels, and thus motivates well thought-out strategies on optimal peak-import. Since an increase in peak-import cannot be reversed later, this tariff enables a careful consideration of how the flexible assets are capable of influencing long-term price signals and reacting to long-term strategies.

A sensitivity analysis on the boundaries and capacities on the short-term flexible assets were performed in this work. The sensitivity included analyzing for battery capacity of 5 kWh and 10 kWh, 2.3 kW and 3.7 kW EV chargers, and indoor temperature boundaries of 20-24 $°C$ and 21-23 $°C$. In addition, only one flexible asset was activated at a time, whereas the other assets had a specified passive behavior. This made the individual contribution to the long-term value of flexibility apparent.

The operational performance of each flexible asset, to capture their influence on long-term flexibility, is illustrated in Fig. 4.7. This figure shows the ending peak-import level during operation for each case analyzed. The economic performance, where total cost of operation including the monthly demand charge at the end of the month is accounted for, is shown in Fig. 4.8. The reference case, in which

all flexible assets are passive, has the highest ending peak and the largest cost of operation. As seen here, all flexible assets achieve a peak-import reduction and reduction in cost of operation, but the degree of reduction is coupled to each respective asset. The boxplots show the median value by with an orange line, and each box represents the interquartile range (IQR) of the results. The whiskers are shown as lines outside the box, covering the 1.5*IQR, and the dots are the outliers.

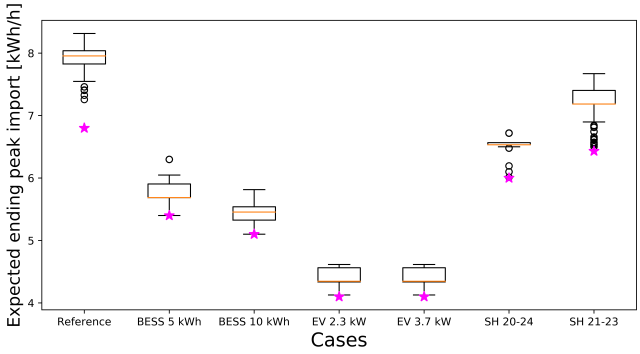


Figure 4.7: Sensitivity analysis of operational performance for each flexible asset in terms of ending peak-import level. Taken from **Paper II.**

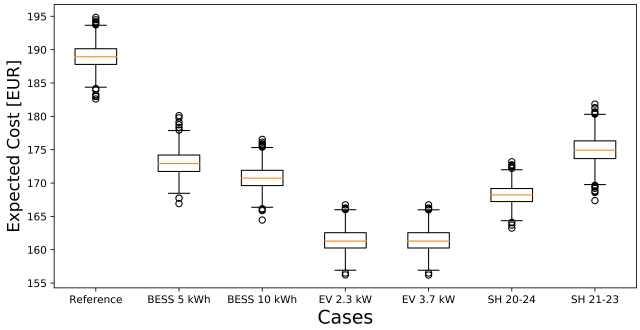


Figure 4.8: Sensitivity analysis of expected total cost over the month for each flexible asset. Taken from **Paper II.**

The BESS provides flexibility to the energy system in terms of peak shaving. The BESS stores electricity during off-peak hours, and discharges when the consumption profile is higher than the aimed peak-import level. Thus, a BESS is very capable of effectively aiding in reducing peak-import levels for the building, and reducing the long-term price signal costs. The flexible behavior of the BESS is unique compared to the other flexible assets investigated, since it is not naturally part of the consumption profile, having no internal load to cover. The case analyzed here had a fixed inverter capacity at 2.5 kW, which limits the peak-import reduction. However, the storage capacity plays a role in storing sufficient elec-

tricity to support during the peak hours. For a 5 and 10 kWh storage capacity, average peak-reductions came at 2.20 and 2.50 kW, respectively. This highlights the need for sufficient storage capacity to peak-shave for the entire peak-periods but that doubling the storage capacity only gave a small peak-reduction.

The EV cases saw almost identical results regardless of charger capacity. Achieving an average of 3.54 kW peak-reduction, which is almost equivalent to the 3.7 kW passive charger present in the reference case, smart control of EV chargers is vital to avoid unnecessary peaks during operation. The EV is available for charging 15 hours per day, giving the EV plenty of opportunities to charge to the desired SoC without conflicting with the non-flexible demand. The charger capacity is not binding to the problem with so many hours available for charging. Additionally, if the EV charger would be bi-directional, it could enhance operation of the building further, inheriting some of the characteristics from the BESS. This was not investigated in this work.

For SH, the indoor temperature boundary influences operation in regards to peak-reduction. A higher temperature boundary gives more flexibility in terms of load-shifting. With a temperature boundary between 21-23 $°C$, the peak-reduction is significantly lower than the other flexible assets, including the boundary of 20-24 $°C$. The 20-24 $°C$ boundary manage to converge on a stable ending-peak, with little deviation despite the uncertainty in the problem. The difference in the two SH cases shows the influence on the temperature boundary, where a higher boundary gives more capacity on load-shifting to avoid high RTP-hours. The case study was for a winter month, with high thermal demand. This means there is much benefit to gain from optimal operation while considering RTP. Thus, the temperature boundary not only influences flexibility, but also seems to correspond to different optimal balances between peak and RTP-benefits. However, prioritizing both RTP and monthly demand charge means there is some cost-based balance within the long-term strategy. Increasing peak-import levels to increase RTP-benefits is possible; it depends on the load-shifting capability and the cost-difference between the two price signals.

Regarding the total cost of operation, captured in Fig. 4.8, each flexible asset contributes to lowering the cost in different ways. The total cost sees a noticeable decrease with the BESS compared to the reference case, with the 5 kWh BESS achieving a 8.4% cost reduction compared to the reference case, but small changes between the two storage capacities. The cost reduction is primarily coupled to the decrease in demand charge cost, indicating limited interaction to deal with RTP-variation. The EV chargers see almost identical cost-reduction compared to the reference case, at a 14.6% cost-reduction. The EV charger has the highest cost-reduction of the flexible assets here, coupled to the increased cost on the demand charge with a passive charging strategy. The identical cost show that the EV chargers do not use their full capacity when charging. The SH cases show varying total cost based on the temperature boundary, with the 20-24 $°C$

boundary achieving the highest cost-reduction of the two. Compared to the reference case, the 20-24 $°C$ boundary ended with a 11.0% cost-reduction. Despite having a lower peak-reduction than both BESS cases, the total cost is lower than the BESS manage. This is coupled to the interaction to cost of operation from RTP-variation, where the savings from load shifting leads to an overall lower cost than by primarily reducing peak. This showcase the value of flexibility from not only prioritizing the long-term price signals, but also the cost of operation along the period.

### Additional Results on the Basis of Paper II

The analysis in **Paper II** on SH showed that the long-term strategy balanced RTP-benefits and cost of monthly demand charge. However, how this synergy changes when adjusting one of the price signals was not investigated, prompting further studies on this balance. Therefore, this was analyzed afterward, studying how increasing the monthly demand charge cost influences the long-term strategy. This was not part of the work conducted in **Paper II**.

The analysis included adjusting the demand charge cost from 0.2-4 times the original cost used in **Paper II**. The performance for the SH case with a 20-24 $°C$ temperature boundary can be found in Fig. 4.9, which captures a decreasing ending peak-import level with increasing demand charge cost. This trend implies that SH has sufficient load-shifting potential to reduce peak-import, but that it does not necessarily aim for the lowest possible peak-import level. This strategy is dependent on the relation between demand charge cost, RTP variation, and scenarios influencing heat demand. Note that for this case, RTP was deterministic for the month. With higher demand charge cost, the boxplots including outliers decrease toward lower peaks. There is some variety in change of operation, where some increase of demand charge only leads to smaller operational adjustments, and while some leads to significant peak-import reduction. The latter is very present in the shift between a multiplication factor of 2.2 to 2.4, which sees a 0.5 kW peak-reduction. Here, this decrease of peak implies the long-term price signal has a higher cost than the benefits from RTP-variations that was seen as economically beneficial with a lower demand charge cost.

For the temperature boundary between 21-23 $°C$, the trend is the same, as shown in Fig. 4.10. With increasing demand charge cost, the ending peak-import level decreases, due to load-shifting. However, a noticeable comparison between the two temperature boundaries is that 21-23 $°C$ have much larger variation with low demand charge cost than 20-24 $°C$. This is linked to uncertainty and the range of heat demand needed in each scenario, and that load-shifting to reduce peak might not be cost-effective compared to RTP-variation. With increasing demand charge cost, the boxplots tighten more, and the two temperature boundaries become similar in average ending peak-import levels at around 2x. However, the

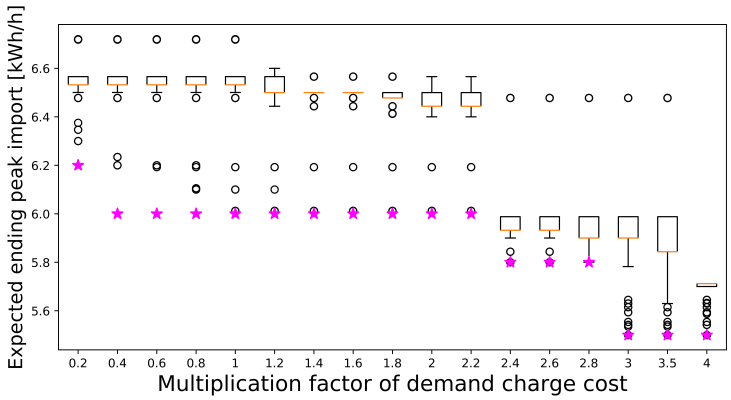


Figure 4.9: Sensitivity analysis of increasing demand charge cost with SH between 20-24 $°C$.

plots show that 21-23 $°C$ has less cost-effective flexibility on load-shifting and operates with higher peaks.

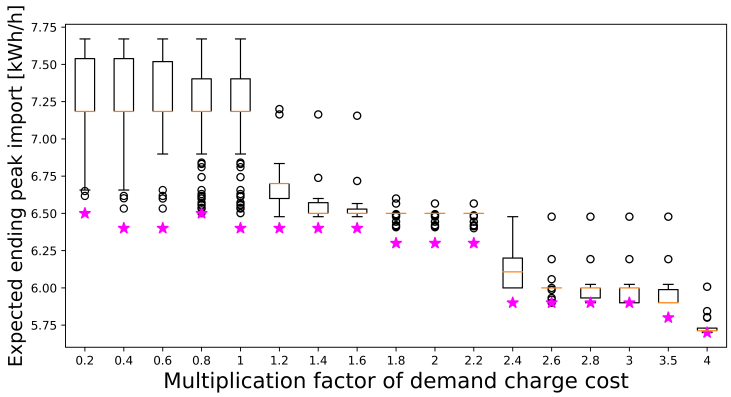


Figure 4.10: Sensitivity analysis of increasing demand charge cost with SH between 21-23 $°C$.

An apparent difference between the two temperature boundaries lies within the initial peak-import levels at the first decision stage, indicated by the purple stars in each figure. For 21-23 $°C$, this initial level is closer to the actual ending peaks, but for 20-24 $°C$, the deviation is larger. This suggests that during operation, the latter case initiates with lower peaks, due to the uncertainty in the future regarding heat demand. The potential future savings in keeping a low peak outweigh the increased savings by increasing the peaks early. The plots do show that corrections are done most of the time during operation, with a few outliers. With increasing demand charge cost, this initial value decreases, but the deviation from the expected ending-peak level is tighter. Thus, there are always some

benefits in comparing RTPs versus demand charge cost, but uncertainty plays a role in what is cost-effective.

These results prove that the flexible SH is coupled well to the selected cost for monthly demand charge during the long-term strategy. As the operational strategy from LOSTFUTURE accounts for scenarios, demand charge cost, and RTP-variations, the flexibility within SH are comparing the cost of operation toward the long-term price signal cost. With increasing demand charge cost, it actively tries to lower this cost by shifting heating to decrease the peak-import level. To compare, having a strategy that would only prioritize minimizing peaks without knowing the future cost of operation, similar to the comparison done in **Paper I**, could lead to significant cost increase from RTPs higher than the peak-reduction benefits. Thus, the long-term value of SH flexibility can have significant influence on cost of operation when long-term price signals are present.

### 4.2.2 Long-term Flexible Assets

#### Paper IV: Seasonal Thermal Energy Storage (STES)

The role of the STES unit in **Paper IV** was to decrease use of electricity during winter to provide heat. By storing thermal energy during summer, this could be supplied to cover the significant heating demands during winter.

The STES could contribute to three important areas for the building during winter. First, it could provide long-term load-shifting and peak-shaving from the thermal system, to lessen the need of electricity during winter that would increase peak-import. Second, it could make better use of cheaper electricity during summer and local production from PV, and store this for use during winter. And third, it could enable the short-term flexible assets like BESS and the EV charger to have more room for flexibility with electricity from the grid during critical periods in winter. **Paper IV** includes an analysis for the energy system of a building located in Norway, with and without both PV and STES. The economic performance of the four cases are shown in Table. 4.1.

The work in **Paper IV** compared the influence the STES had on building operation over a year, with and without STES and PV installed. When comparing the influence of STES alone, it was apparent that it contributed to decreasing peak-import during winter. This led to a 23.9% decrease in demand charge cost over the year, and a 4.6% decrease in yearly cost of operation, when comparing Case 2 to Case 1. Although the yearly import quantity increased to cover losses by the STES, this was cost-effective due to the benefits from demand charge and seasonal RTP-variation. When including PV production, as in Case 4, this provided an additional source of electricity during the summer. The STES led

Table 4.1: Average economic results on cost of operation, monthly demand charge cost, import/export of electricity, and PV production. The table is taken from **Paper IV**.

| Case | Total Cost [EUR] | Monthly Demand Charge Cost [EUR] | Total Import [kWh] | Total Export [kWh] | PV Generation [kWh] |
|---|---|---|---|---|---|
| Case 1: No PV No STES | 1336.17 | 209.53 | 13974.02 | 0 | 0 |
| Case 2: No PV With STES | 1275,15 | 159.36 | 14443.96 | 0 | 0 |
| Case 3: With PV No STES | 1026.50 | 187.07 | 10029.29 | 240.86 | 4294.46 |
| Case 4: With PV With STES | 950.78 | 128.03 | 10361.91 | 0 | 4294.46 |

to decreased export of electricity from the building compared to the case without STES, increasing the self-sufficiency from local production. The increased benefit of using local production came at a 7.4% yearly cost decrease for Case 4, when compared to Case 3. This cost decrease indicates that, with the STES, the seasonal variations in PV production came to better use for the building economically, and contributed to the energy system over the year.

The operation of the STES follows a behavior similar to hydropower operation. As hydropower make use of seasonal inflow to store and discharge water when the cost-optimal opportunity is there, it carefully optimizes use of the resources available. The STES applies the same consideration, using the summer season to store more heat and provide this during winter. The value of storing heat for the future is captured during operation, and the system continuously considers the benefit of storing additional heat. In the EFCCs in Fig. 4.5, the added value of storing heat is captured, but the marginal value of storing heat is never zero, despite the operational performance not using the full capacity of the STES. The cost-optimal strategy found the additional capacity not being necessary during the year, despite having some future value for operation. It could have made use of the additional heat, but this would not be cost-optimal toward the cost of purchasing it. When the PV was included, the SoC increased, since the local production has zero cost; however, this did not lead to maximum capacity, as the local production also played a role for the other flexible assets. Thus, we see a continuous planning of storing and delivering heat over the year, following similar trends as hydropower does.

### Additional Results regarding Paper IV

The results from **Paper IV** have been investigated further to see the balance between the STES and thermal production during winter. Thermal demand can be covered by both the STES and HP during winter, and the synergy between them will be shown here. This analysis is not part of the work in **Paper IV**.

The operational performance for three selected winter days are presented in Fig. 4.11. Here, the thermal energy sources in the buildings are presented, alongside the indoor temperature for SH. Other thermal demands like DHW are not included here but are also covered. The STES is providing much thermal energy to the system, while the HP is only occasionally providing thermal energy. Typically, the HP produces during the day, when the EV is not present and load demand is expected to be lower. The increase in temperature at the end of each day is primarily to meet the set-point temperature at 22 $°C$, a limitation as the indoor temperature is not part of the EFCCs.

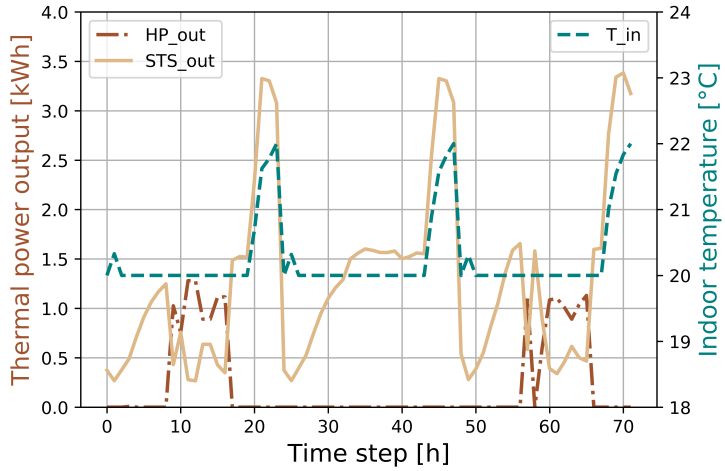


Figure 4.11: Thermal energy supply and indoor temperature for three selected days during early winter, for Case 2 in **Paper IV**.

The STES would supply the system heat during peak-periods, having the role of a peaker-unit. However, in this analysis, it supplies heat almost continuously. With no other technologies than the HP to provide heat, the other choices are limited. And, since the electricity system has a monthly demand charge to consider, and other load demands, this influences cost from electricity to cover thermal demand. The demand charge induces a cost-based restriction on high electricity use, which limits the cost-optimal contribution from the HP. Looking at the EFCC for STES during winter, shown in Fig. 4.12, the added value of storing heat when the SoC is very low during winter, is noticeable high. This is dependent on both RTPs

during winter, but also the cost from demand charge, should this provoke increase of peak-import. In a way, these EFCCs act as future fuel cost for the electricity system to provide heat, and vary significantly depending on the situation for demand charge, and current STES SoC. Thus, the baseload from the HP can be very costly, and the STES and the heat it provides is deemed much more cost-optimal to use.

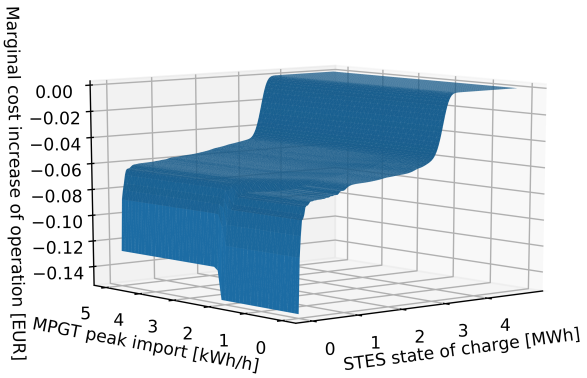


Figure 4.12: 3D-plot of the marginal EFCC for the STES, for day 280, for Case 2. The picture is taken from **Paper IV**.

Taking this analysis in the direction of installation of capacity in an energy system, the baseload unit, being the HP, has a variable cost derived from RTPs, while the "installation cost" for baseload during operation is dependent on the demand charge. The more peak-import capacity is purchased, the more baseload it can cover. As the peak-import level, which also should cover other electrical loads, is very costly, it is preferable for the peaker unit, being the STES, to supply heat most of the time. The installation cost for baseload is set on a monthly basis, and the case studied has different demand charge costs during summer and winter. The summer period works with a 4.458 $\frac{EUR}{kW \cdot month}$ demand charge cost, and triple that amount at 13.375 $\frac{EUR}{kW \cdot month}$ during winter, motivating peak-reduction during the winter period. Operation over the year has a lower demand charge cost during summer, so the system finds it more cost-effective to purchase peak-import then, to make the STES more dominant during winter and decrease baseload-import during that period. As such, the system takes advantage of the seasonal flexibility, to make the thermal system less dependent on the electricity system during winter, by purchasing peak-import capacity during summer. With this strategy, the STES peaker unit has an expected dominant role during winter, charged up by the baseload unit from earlier in the year.

## 4.3 Technical Experiences of Representing Long-term Value of Flexibility

Representing the future cost of operation involves having a detailed overview over the change in cost during operation. Each work has investigated at least one long-term price signal that needs to be represented to improve short-term operation. The SDP-framework allows for extending the number of state variables, and thus the number of long-term price signals considered. This enables multiple long-term price signals to be accounted for at once. In addition, it would be possible to consider coupling price signals where one is recurring multiple times during the overall period. Also, the work has encountered some complexity on the monthly demand charge coupled with other price signals. These topics will be discussed and presented in this subchapter.

### 4.3.1 Multi-period Price Signals

The work in **Paper IV** investigated how to couple two different price signals in the long-term strategy framework. The STES acts as a long-term flexible asset, capturing seasonal variations in operation and creating a strategy for yearly operation, while the monthly demand charge price signals impose a cost on peak-import levels for each month of the year. The latter price signal reoccurs for every month of the year, and each demand charge month is independent of each other. However, these recurring price signals influence the STES, and indirectly each other through the STES, and as such, this coupling must be captured in the EFCCs accurately. Representing the long-term strategy over the year makes it important to adjust the information in the EFCCs during transition between months. At these points, information on the deactivated price signals, activated price signals, and the dependencies both have on other price signals, must be handled correctly. Accounting for this, the need to properly describe the accurate future value of flexibility, led to the formulation of the extension to the SDP-framework described in Chapter 3.2.4, Alg. 2. For a detailed description of how this extension works, refer to Chapter 3.2.4.

This algorithm and extension played a vital role in the results obtained and discussed in **Paper IV**. This extension and formulation in Chapter 3.2.4, enabled the long-term strategy to capture the long-term value of flexibility for both the STES and every monthly demand charge in the future. Only the present monthly demand charge is directly captured in the EFCC, but the future demand charge periods are indirectly captured by the STES future cost. The future value of flexibility in the STES accounts for the future periods where the monthly demand charge is renewed, and via the marginal cost of thermal energy storage, can make the long-term strategy account for lowering future peak-import levels through the

STES. The strategy, displayed in Fig. 4.6, captures this coupling. The strategy to increase peak-import levels during summer, to charge the STES, provided peak-import level reduction during the winter. The long-term value of flexibility through the STES captures the long-term influence on monthly demand charges. This coupling between different price signals provides more accurate information on the future, and the algorithm extension in Alg. 2 enables this to be achieved. The strategy framework has more tools available for accurately capturing long-term price signals, to achieve cost-optimal operational performance for longer periods.

### 4.3.2 Convexity Issues

During the expansion of the SDP framework to include multiple variables in the generation of EFCCs, convexity-issues were encountered. This has not been described in detail within in **Paper IV** but will be detailed here.

The non-convexity issue stems from coupling the monthly demand charge price signal with other price signals within the energy system of the building. This example uses the STES and monthly demand charge as long-term price signals. When keeping the SOS2-nature of the build up of the EFCC, mathematically described in Chapter 3.3.8, the EFCC experienced non-convex behavior after a few decision stages. The MEFCCs for both the monthly demand charge and STES SoC are shown in Figures 4.13 and 4.14, respectively. Fig. 4.14 shows a non-convex trend on parts of the overall curve, specifically at lower initial values for the monthly demand charge state variable. These plots are made up of a deterministic case study from **Paper IV**, with 41 discrete demand charge states between 0-5 $\frac{kWh}{h}$ and 41 discrete STES SoC states between 0-500 kWh. This example is only meant to explain the behavior.

The influence of the MEFCC for the monthly demand charge state variable, denoted as highest peak-import level, is shown in Fig. 4.13. At zero initial value for the highest peak-import level, the marginal cost is zero since it is necessary to increase the import quantity. It is then influenced by the storage quantity of the STES, the stochastic variables in the current scenario, and by the indicators from the EFCC for the future decision stages. The slope of the peak-import level is very steep when going from zero marginal cost up to the monthly demand charge cost. This curve illustrates that when trying to find the cost-optimal peak-import level, the boundary between zero cost and demand charge cost is narrow. This emphasizes an accurate and detailed representation of this state variable around the change in marginal cost. If the representation is too coarse with few discrete states, then it could miscalculate the optimal peak-import level. Should the cost-optimal peak-import level be between two discrete points, it would achieve a lower value than the optimal level, due to the convex marginal cost increase. This could cause readjustment later during operation, where the peak-import level needs to

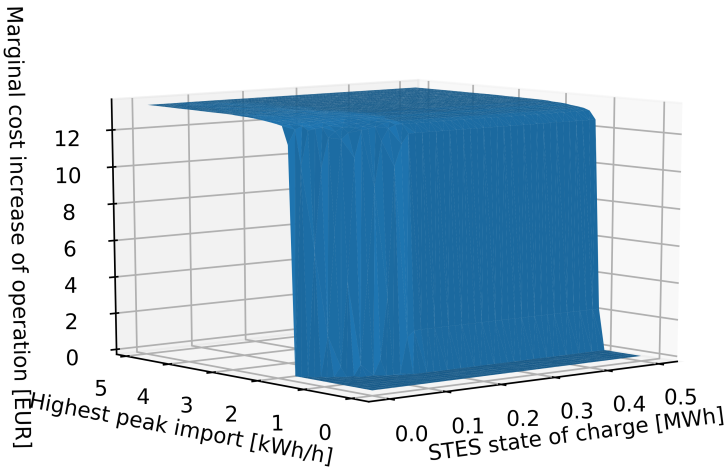


Figure 4.13: Marginal expected future cost curve for marginal peak-import level change.

be increased. If it is increased, the use of flexibility earlier to keep it at the lower level would have been wasted. This is due to the asymmetrical behavior of this grid tariff. This was also mentioned in **Paper I** and Chapter 4.1.1 where the SDP-algorithm was compared to a simplified strategy where minimizing the peak-import level was emphasized. This loss of flexibility would then result in an increased cost of operation compared to what would be possible with an accurate peak-import level from the start.

The non-convex behavior in Fig. 4.14 is related to the accuracy of discretizing the state variables within the SDP-algorithm, especially for the peak-import level. When increasing the number of state variables in the SDP-algorithm, the re-adjustment of the monthly demand charge peak could be influenced by other state variables as well. For an increasing STES SoC, there is more thermal energy available to reduce the electricity need from the grid, which could reduce the peak-import level during the decision stage. However, if the cost-optimal peak-import level is between two discrete states, this could lead to undershooting the optimal value, which would be corrected later. Thus, for each increasing STES SoC, the optimal peak-import level changes and could be between two discrete points, leading to an offset. The offset in the peak-import level can be random, but will be dependent on the accuracy of the discrete points for the peak-import level. This, in turn, leads to the non-convex behavior in the Fig. 4.14, which is

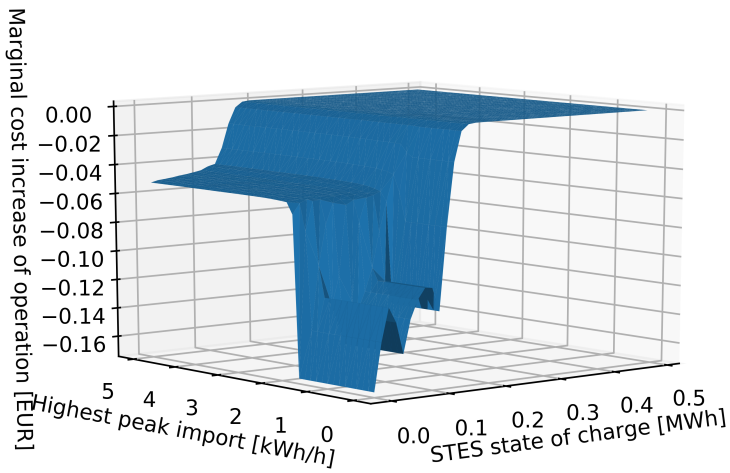


Figure 4.14: Marginal expected future cost curve for marginal STES SoC change. The curve shows non-convexity at low initial peak-import levels.

the result of different offsets on the peak-import level, caused by discretization error.

The operational performance is not continuously influenced by the non-convex behavior in the EFCCs. The non-convex behavior of the plot is primarily apparent during the first decision stage of the month, where there is no historical peak-import level given. After the first decision stage, the peak-import level would be at a close level or within the convex region of the EFCC. However, the strategy set after the first day could be off due to the inaccuracy, which in turn could lead to re-adjustments later. Thus, having an accurate representation of the monthly demand charge state variable would still be beneficial to decrease the offset and improve the strategy within the EFCCs.

There exist multiple ways to deal with this non-convexity in the EFCCs. Removing the non-convexity in the EFCCs could be achieved by removing the SOS2-nature when formulating the EFCC in Chapter 3.3.7. This does not solve the issue with inaccurate measures due to discretization, but convexifies the curve. Removing the SOS2-nature was done in **Paper IV**, as the analysis saw almost no changes in the operational performance over the yearly operation. An example of the MEFCC without the SOS2-nature is illustrated in Fig. 4.15. This is a viable option for a linear programming problem, where the piecewise-linearity

from the SOS2-nature would not be crucial to capture the future value of flexibility. However, should non-convexity be introduced to the SDP-framework, for instance, non-convex efficiency on the STES, the SOS2-nature would be necessary. Another alternative to decrease the non-convexity would be to increase the number of discrete points for the state variables. With an increased accuracy in the curve, the offset in optimal peak-import level would be decreased. Increasing the number of states increases the computational time use due to a larger discretization, posing a computational time versus accuracy challenge.

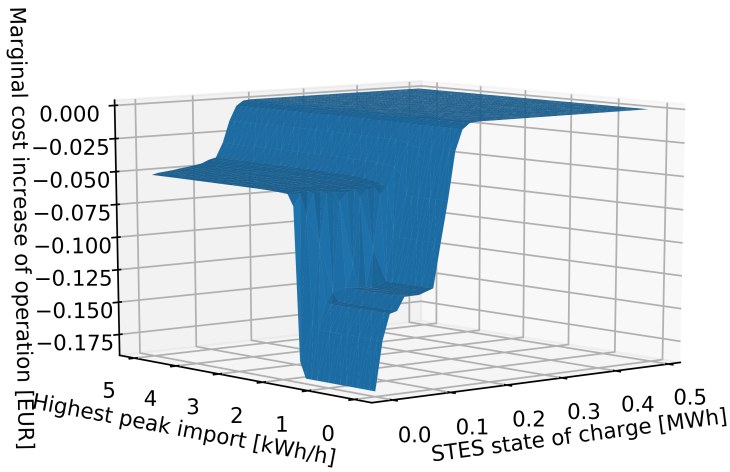


Figure 4.15: Same case as in Fig. 4.14, but where the problem is convexified. To enable this, the SOS2-nature on the state variables is disabled in the EFCC formulation in Chapter 3.3.7.

# 5 Conclusion and Future Work

Capturing the long-term value of flexibility into operational models for energy systems in residential buildings will improve overall operation and cost performance. Having more information on the long-term impact of operation enables more accurate decisions to be made. In addition, this provides a possibility of accurately representing long-term price signals into operational models, where the long-term value of flexibility on these price signals can also be accounted for. This thesis has presented and investigated a framework for dealing with the long-term value of flexibility and how to represent long-term price signals for esidential building operation.

## 5.1 Main Results

The results from the work presented have revealed how to represent the long-term value of flexibility for residential building operation, providing more accurate operational decisions in the short term. This long-term consideration is not limited in layout and types of case studies, as it enables long-term price signals of different characteristics to be embedded, alongside an understanding of how the future flexibility use performs on the price signals. Within the LOSTFUTURE toolbox, the long-term strategy is captured and enables all of these factors to be represented for short-term operational models.

The short-term flexible assets within the building have improved operational performance with the presence of the long-term strategy framework. Without considering the long-term value of flexibility, the use of flexible assets will optimize for the short-term period only. But when including the long-term strategy, as was seen in **Paper I**, balancing both short- and long-term with the use of flexibility increases the economic performance. The short-term flexible assets are not required to be part of the future cost curves to contribute to long-term performance, which indicates that not all flexible assets must be part of the long-term strategy. This was the case in **Paper II**, where the individual contribution from BESS, EV charging, and SH were analyzed regarding monthly demand charge. All flexible assets had a significant contribution to the long-term price signal, despite only being able to use short-term flexibility within 24-hours at a time. Regardless of the characteristics behind each flexible asset, they all contributed to improve long-term performance. This demonstrates the synergy flexible assets have with both the short- and long-term value of flexibility.

The long-term price signals that can be embedded in the long-term strategy

framework are not limited in structure. As has been shown in the published works, different types of price signals can be represented in the generated future cost curves, based on the overall goal of long-term operation. Grid tariffs for end-users, internal motivation and goals for operation like emission compensation, and long-term flexible assets have all been investigated and accurately represented by this strategy framework. The diversity of the price signals suggest that the strategy framework is general and can have a wide span of possibilities for representing long-term price signals. The strategy framework is not limited by these but could also be extended to consider other types of long-term signals. This general formulation is valuable considering what energy systems in buildings could be exposed to now, and in the future.

Long-term flexible assets are provided an opportunity to be operated strategically in short-term models with the presence of future cost curves. With this framework, their long-term consequence of operation is captured, and this provides a detailed here-and-now versus long-term impact comparison, making a cost-optimal use of the flexible asset. This enables seasonal variation to be accounted for during operation, as this is included in the future cost curve representation. As for the STES in **Paper IV**, the long-term value of flexibility on storing heat is accounted for, and the value this provides is enough to alter other long-term price signals. The monthly demand charge was increased during summer to reduce cost during winter, enabled by the STES. This strategic decision was only possible due to the STES, and showed a considerate cost-reduction over the whole year. The long-term flexible asset provided valuable flexibility to influence not only the energy system but also other long-term price signals, providing flexibility on multiple signals and considerations during operation.

Coupling multiple long-term price signals is a possibility in the strategy framework, even when they have different characteristics. This was the case in **Paper IV**, with several monthly demand charge costs applied together with STES. Accounting for the change in active price signals has been enabled through extending the SDP-algorithm within the LOSTFUTURE toolbox. This makes it possible to couple different complex price signals and retain their valuable influence on each other in the strategy framework. As was also shown, keeping the coupling between them during price signal transition enables the strategy to account for future price signals that will be active later. This provides key information on how to operate the energy system and how to be prepared for these future price signals.

The behavior of several long-term price signals operating together in the strategy framework proved to complicate the overall operational problem. This was the case not only in terms of complexity and computation time given the SDP-algorithm within the toolbox and framework, but also in that non-convex coupling of price signals could occur. With an asymmetric price signal as the monthly demand charge, strategic planning with this and other price signals together was

found to complicate the problem with the presence of non-convexity when trying to enforce a piecewise-linear behavior. Further analysis of such price signals in the future will provide more understanding on this issue and how best to create optimal strategies.

The LOSTFUTURE toolbox offers an option for short-term models to account for more information, providing a layout for operational planning of energy system operation of a building. As within hydropower, decomposing the operation of buildings into a short- and long-term aspect enables the expansion of the possibilities of operation. We can analyze the long-term aspect and make strategies based on these, and provide the results to short-term models to make the accurate decisions. This work has set the course and shown the value of the long-term aspect with this toolbox, motivating further work and analysis of how this can assist short-term models to achieve the common goal: optimal operation of the energy systems for the end-users and residents in buildings.

## 5.2 Conclusion

This thesis has created and formulated a long-term strategy framework for operation of energy systems in buildings. Several long-term price signals have been formulated and analyzed with this framework, to capture the long-term value of flexibility. Different flexible assets have been considered to evaluate their influence on long-term operation. The main conclusions comprising the contributions of this thesis can be summarized as follows:

- A long-term strategy framework toolbox for building operation has been created. The toolbox **Long-term strategy framework for future building operation (LOSTFUTURE)** calculates the long-term value of flexibility for building operation, and represents this as future cost curves. The framework allows long-term price signals to be represented and accounted for, to improve the overall operational decision by considering the long-term impact.
- By accounting for the long-term value of flexibility during operation, more cost-optimal flexibility use can be performed in the short-term operation. The coupling of short- and long-term operation provides more information on future consequence of operation and also allows long-term price signals to be accounted for.
- Flexible assets such as batteries, uni-directional EV charging, and space heating can use their flexibility to balance both the short- and long-term value of flexibility. With the long-term strategy framework, the flexible assets are able to react to long-term price signals, leading to more cost-optimal long-term decisions.

- Space heating flexibility manages to cost-optimally balance the value of varying spot prices and monthly demand charge cost during winter months. With the long-term strategy, cost-optimal peak-import levels are found that achieve benefits in short-term operation through load shifting. Changing the indoor temperature boundary, which influences load shifting capacity, impacts what peak-import levels are cost-optimal, and the system finds suitable strategies based on the limitations in the energy system.

- When considering emission compensation during operation of a ZEB, a long-term strategy assists in making more cost-optimal decisions. With varying penalty costs for leftover emission inventory at the end of the year, the strategy captures the cost-effective future opportunities based on both the users' willingness to pay for compensation and the future scenarios. These scenarios include seasonal variation in compensation opportunities, accounting for the different strategies on compensation during summer and winter.

- Emission compensation during operation of a ZEB is strongly connected to the correlation between electricity prices and emission intensity in the grid. The long-term strategy is influenced by this correlation, and a Norwegian case saw increased import of electricity during peak-hours due to the low emission intensity during those periods. This can lead to increased risk of congestion to the system, and also increased cost of operation due to the conflicts between operational cost and compensation. This behavior was not seen in a Danish case comparison, where the timing of electricity prices and $CO_{2eq}$-intensity in the electricity grid favored compensation by primarily accounting for variation in electricity prices.

- The operational strategy for seasonal thermal energy storage is represented with the long-term strategy framework. This enables seasonal impact and long-term influence on the long-term seasonal storage unit to be captured and represented for accurate use in the short term. The long-term value of storing extra energy is presented and assists in making cost-based decisions on long-term strategy.

- Multi-period monthly demand charge over a year has been captured alongside seasonal thermal energy storage in the long-term strategy framework. The coupling between the seasonal storage and each monthly demand charge is accounted for, so that their dependencies on each other are retained. This achieves cost-efficient use of seasonal flexibility to influence demand charge cost for all periods, and reduces overall demand charge cost and cost of operation.

## 5.3 Suggestions for Future Work

The work carried out is fresh in the context of the field of energy systems in buildings, and as such further work could be done in several directions. The following suggestions for new research directions focus not only on the methodological expansions on the decomposition techniques but also on the energy system described in the optimization problem.

A key research direction would be to apply the LOSTFUTURE toolbox to a detailed short-term operational model to analyze its influence on operation. As this work has mainly focused on capturing the long-term value of flexibility, the short-term coupling has been simplified. How the LOSTFUTURE toolbox should be used is also an interesting topic for analysis, for instance, once or multiple times during a long-term period. Regardless, investigating the long-term value of flexibility for more sophisticated short-term models is of high interest to progress this research approach.

Further investigation on the long-term value of flexibility for energy systems with more uncertainty present can be extended in the future work. Using data from more extensive scenario generation models would further test the effectiveness of the long-term strategy.

Extending the energy system to consider multiple buildings or neighborhoods would provide valuable analysis of long-term influence on operation. For a neighborhood, the long-term value of flexibility would be a means of putting a cost or value on the internal flexibility, not only in the short-term but also long-term. This could lead to more accurate use of flexibility and would also enable long-term seasonal storage to be operated within the neighborhood.

Altering the LOSTFUTURE framework to consider a system perspective is another step that would enable researchers investigate buildings' contribution of flexibility to the system. The current energy systems modeled focus on lowering the cost from the building perspective, ignoring the benefits and interaction with the surrounding system, with the exception of spot prices and grid tariffs. However, analyzing the system perspective enables more investigation of the value of flexibility the buildings can provide to the system, for a system benefit. Especially when applying the framework to large-scale buildings or neighborhood, this interaction can be valuable for all parts of the system and act as a source of local flexibility.

Other important further works relate to investigating other price signals and the long-term value of flexibility they provide. As the LOSTFUTURE framework is general, other price signals of different natures could be modeled and represented as long-term price signals. This could also be applied to incentive-based demand response programs, where the flexibility of the building could be sold as an asset

to local markets. These market interactions could be converted and represented as long-term price signals, to make the most out of the flexibility available in the system. In addition, coupling multiple long-term price signals, as in **Paper IV**, is also an area that could be explored further.

Exploring other decomposition techniques and how they are able to represent the long-term value of flexibility for energy systems in buildings is important. Using SDDP within this model formulation would be a natural approach to investigate going forward, as both SDP and SDDP have clear advantages and disadvantages compared to each other. Having multiple techniques applied would offer more context regarding what kind of circumstances favour the different approaches. There will most likely be valuable uses of both techniques and others within this field in the future.

Improving the algorithm surrounding multi-period price signals could enhance the level of detail that can be captured within the EFCCs. The formulation given in this work was specified for two state variables and providing a general formulation of this approach could make it more available. Also, **Paper IV** mentioned how the algorithm allows for stochastic initial conditions for price signals, which could be extended to include this. That would provide more possibilities in sophisticated price signals. In addition, testing this algorithm with an SDP-framework outside of the work done in this thesis would verify the value of this extension. For instance, applying the algorithm to a case study surrounding hydropower scheduling would provide valuable understanding on the value of this extension.

The framework could be coupled to large-scale seasonal storage, as a means to portray the long-term value of flexibility. The work in **Paper IV** introduced this framework to seasonal storage units and captured the value of representing the long-term impact of using the seasonal storage. The operational strategy for large-scale storage does not need to be explicitly toward buildings but could be used in any setting where a storage unit is needed, for instance, offshore hydrogen storage.

# Bibliography

[1] The European Commision, "Stepping up Europe's 2030 climate ambition Investing," 2020. [Online]. Available: https://knowledge4policy.ec.europa.eu/publication/communication-com2020562-stepping-europe\OT1\textquoterights-2030-climate-ambition-investing-climate_en

[2] The European Commision, "Proposal for a DIRECTIVE OF THE EUROPEAN PARLIAMENT AND OF THE COUNCIL on Energy Efficiency (recast)," 2021. [Online]. Available: https://eur-lex.europa.eu/legal-content/EN/TXT/?uri=CELEX%3A52021PC0558

[3] EMBER, "EU Power Sector in 2020." [Online]. Available: https://ember-climate.org/insights/research/eu-power-sector-2020/

[4] International Energy Agency, "Status of Power System Transformation 2019: Power system flexibility." [Online]. Available: https://www.iea.org/reports/status-of-power-system-transformation-2019

[5] A. Akrami, M. Doostizadeh, and F. Aminifar, "Power system flexibility: an overview of emergence to evolution," *Journal of Modern Power Systems and Clean Energy*, vol. 7, no. 5, pp. 987–1007, 9 2019.

[6] L. Gelazanskas and K. A. Gamage, "Demand side management in smart grid: A review and proposals for future direction," pp. 22–30, 2 2014.

[7] H. Shareef, M. S. Ahmed, A. Mohamed, and E. Al Hassan, "Review on Home Energy Management System Considering Demand Responses, Smart Technologies, and Intelligent Controllers," *IEEE Access*, vol. 6, pp. 24 498–24 509, 4 2018.

[8] M. Beaudin and H. Zareipour, "Home energy management systems: A review of modelling and complexity," *Renewable and Sustainable Energy Reviews*, vol. 45, pp. 318–335, 5 2015.

[9] ACER, "Report on Distribution Tariff Methodologies in Europe," 2021. [Online]. Available: https://documents.acer.europa.eu/Media/News/Pages/ACER-reports-on-electricity-distribution-tariff-methodologies-in-Europe-and-recommends-how-to-improve-them.aspx

[10] I. Andresen, "Towards Zero Energy and Zero Emission Buildings—Definitions, Concepts, and Strategies," *Current Sustainable/Renewable Energy Reports*, vol. 4, no. 2, pp. 63–71, 6 2017. [Online]. Available: https://link.springer.com/article/10.1007/s40518-017-0066-4

[11] C. W. Gellings and J. H. Chamberlin, "Demand-side management: Concepts and methods," 1 1987. [Online]. Available: https://www.osti.gov/biblio/5275778

[12] E. Sarker, P. Halder, M. Seyedmahmoudian, E. Jamei, B. Horan, S. Mekhilef, and A. Stojcevski, "Progress on the demand side management in smart grid and optimization approaches," *International Journal of Energy Research*, vol. 45, no. 1, pp. 36–64, 1 2021. [Online]. Available: https://onlinelibrary.wiley.com/doi/full/10.1002/er.5631

[13] The Norwegian Water Resources and Energy Directorate (NVE), "Smart metering (AMS)," 2021. [Online]. Available: https://2021.nve.no/norwegian-energy-regulatory-authority/retail-market/smart-metering-ams/

[14] H. Li, Z. Wang, T. Hong, and M. A. Piette, "Energy flexibility of residential buildings: A systematic review of characterization and quantification methods and applications," *Advances in Applied Energy*, vol. 3, p. 100054, 8 2021.

[15] M. A. Hannan, S. B. Wali, P. J. Ker, M. S. Rahman, M. Mansor, V. K. Ramachandaramurthy, K. M. Muttaqi, T. M. Mahlia, and Z. Y. Dong, "Battery energy-storage system: A review of technologies, optimization objectives, constraints, approaches, and outstanding issues," *Journal of Energy Storage*, vol. 42, p. 103023, 10 2021.

[16] D. Mariano-Hernández, L. Hernández-Callejo, A. Zorita-Lamadrid, O. Duque-Pérez, and F. Santos García, "A review of strategies for building energy management system: Model predictive control, demand side management, optimization, and fault detect & diagnosis," *Journal of Building Engineering*, vol. 33, p. 101692, 1 2021.

[17] R. K. Bonthu, H. Pham, R. P. Aguilera, and Q. P. Ha, "Minimization of building energy cost by optimally managing PV and battery energy storage systems," *2017 20th International Conference on Electrical Machines and Systems, ICEMS 2017*, 10 2017.

[18] Power Sonic, "What is a Battery C Rating?" 2021. [Online]. Available: https://www.power-sonic.com/wp-content/uploads/2021/02/What-is-a-battery-C-rating.pdf

[19] N. Sadeghianpourhamami, N. Refa, M. Strobbe, and C. Develder, "Quantitive analysis of electric vehicle flexibility: A data-driven approach," *International Journal of Electrical Power and Energy Systems*, vol. 95, pp. 451–462, 2018. [Online]. Available: http://dx.doi.org/10.1016/j.ijepes.2017.09.007

[20] Easee, "Home Electric Vehicle Chargers." [Online]. Available: https://easee.com/uk/home-charging/

[21] G. Van Kriekinge, C. De Cauwer, N. Sapountzoglou, T. Coosemans, and M. Messagie, "Peak shaving and cost minimization using model predictive control for uni- and bi-directional charging of electric vehicles," *Energy Reports*, vol. 7, pp. 8760–8771, 11 2021.

[22] R. Elsland, T. Fleiter, M. Jakob, U. Reiter, R. Harmsen, P. Mines, P. Rivière, and F. Dittmann, "Heating and cooling (facts and figures) - the transformation towards a low-carbon heating & cooling sector," 06 2017.

[23] G. Thomaßen, K. Kavvadias, and J. P. Jiménez Navarro, "The decarbonisation of the EU heating sector through electrification: A parametric analysis," *Energy Policy*, vol. 148, p. 111929, 1 2021.

[24] "DIRECTIVE (EU) 2018/844 OF THE EUROPEAN PARLIAMENT AND OF THE COUNCIL of 30 May 2018 amending Directive 2010/31/EU on the energy performance of buildings and Directive 2012/27/EU on energy efficiency (Text with EEA relevance)," Tech. Rep.

[25] Y. Chen, P. Xu, J. Gu, F. Schmidt, and W. Li, "Measures to improve energy demand flexibility in buildings for demand response (DR): A review," *Energy and Buildings*, vol. 177, pp. 125–139, 10 2018.

[26] M. Berge and H. M. Mathisen, "Perceived and measured indoor climate conditions in high-performance residential buildings," *Energy and Buildings*, vol. 127, pp. 1057–1073, 9 2016.

[27] V. Lakshmanan, H. Sæle, and M. Z. Degefa, "Electric water heater flexibility potential and activation impact in system operator perspective – Norwegian scenario case study," *Energy*, vol. 236, p. 121490, 12 2021.

[28] M. Pipattanasomporn, M. Kuzlu, S. Rahman, and Y. Teklu, "Load profiles of selected major household appliances and their demand response opportunities," *IEEE Transactions on Smart Grid*, 2014.

[29] O. Erdinc, "Economic impacts of small-scale own generating and storage units, and electric vehicles under different demand response strategies for smart households," *Applied Energy*, vol. 126, pp. 142–150, 8 2014.

[30] S. Kuboth, F. Heberle, A. König-Haagen, and D. Brüggemann, "Economic model predictive control of combined thermal and electric residential building energy systems," *Applied Energy*, vol. 240, pp. 372–385, 4 2019.

[31] R. Palma-Behnke, C. Benavides, F. Lanas, B. Severino, L. Reyes, J. Llanos, and D. Saez, "A microgrid energy management system based on the rolling horizon strategy," *IEEE Transactions on Smart Grid*, vol. 4, no. 2, pp. 996–1006, 2013.

[32] A. Gjelsvik, M. M. Belsnes, and A. Haugstad, "An algorithm for stochastic medium-term hydrothermal scheduling under spot price uncertainty," *13th PSCC*, pp. 1079–1085, 1999.

[33] Y. Sun, S. Wang, and G. Huang, "A demand limiting strategy for maximizing monthly cost savings of commercial buildings," *Energy and Buildings*, vol. 42, no. 11, pp. 2219–2230, 11 2010.

[34] Lnett, "New tariffs postponed," 2022. [Online]. Available: https://www.l-nett.no/nynettleie/new-tariffs-postponed

[35] Agder Energi Nett, "Nettleiepriser 2019," 2019. [Online]. Available: https://www.aenett.no/globalassets/publikasjoner/nettleiepriser-2019-privat.pdf

[36] S. Bjarghov, H. Farahmand, and G. Doorman, "Capacity subscription grid tariff efficiency and the impact of uncertainty on the subscribed level," *Energy Policy*, vol. 165, p. 112972, 6 2022. [Online]. Available: https://linkinghub.elsevier.com/retrieve/pii/S0301421522001975

[37] S. Backe, G. Kara, and A. Tomasgard, "Comparing individual and coordinated demand response with dynamic and static power grid tariffs," *Energy*, vol. 201, p. 117619, 6 2020.

[38] L. Xu, S. Wang, and F. Xiao, "An adaptive optimal monthly peak building demand limiting strategy considering load uncertainty," *Applied Energy*, vol. 253, p. 113582, 11 2019.

[39] L. Xu, H. Tang, and S. Wang, "Adaptive optimal monthly peak building demand limiting strategy based on exploration-exploitation tradeoff," *Automation in Construction*, vol. 119, p. 103349, 11 2020.

[40] F. Luo, W. Kong, G. Ranzi, and Z. Y. Dong, "Optimal home energy management system with demand charge tariff and appliance operational dependencies," *IEEE Transactions on Smart Grid*, vol. 11, no. 1, pp. 4–14, 1 2020.

[41] B. Mo, O. B. Fosso, N. Flatabø, and A. Haugstad, "Short-term and Medium-term Generation Scheduling in the Norwegian Hydro System under a Competitive Power Market," Tech. Rep., 2002. [Online]. Available: https://www.researchgate.net/publication/306446062

[42] P. Aaslid, M. Korpås, M. M. Belsnes, and O. B. Fosso, "Pricing electricity in constrained networks dominated by stochastic renewable generation and electric energy storage," *Electric Power Systems Research*, vol. 197, p. 107169, 8 2021.

[43] P. Aaslid, M. Korpas, M. M. Belsnes, and O. Fosso, "Stochastic Optimization of Microgrid Operation With Renewable Generation and Energy Storages," *IEEE Transactions on Sustainable Energy*, 2022.

[44] P. Aaslid, M. M. Belsnes, and O. B. Fosso, "Optimal microgrid operation considering battery degradation using stochastic dual dynamic programming," *SEST 2019 - 2nd International Conference on Smart Energy Systems and Technologies*, 9 2019.

[45] P. Aaslid, M. Korpås, M. M. Belsnes, and O. B. Fosso, "Stochastic Operation of Energy Constrained Microgrids Considering Battery Degradation," 11 2021. [Online]. Available: https://arxiv.org/abs/2111.03313v1

[46] European Parliament, "Directive 2010/31/EU on the energy performance of buildings (EPBD) - recast," *Official Journal of the European Union*, 2010. [Online]. Available: https://eur-lex.europa.eu/legal-content/EN/TXT/?uri=celex%3A32010L0031

[47] FME ZEB, "The Research Centre on Zero Emission Buildings - Final Report," Tech. Rep., 2017. [Online]. Available: http://zeb.no/index.php/en/final-report

[48] FME ZEN, "Research Centre on Zero Emission Neighbourhoods in Smart Cities." [Online]. Available: https://fmezen.no/

[49] F. Selamawit, R. Schlanbudch, K. Sørnes, M. Inman, and I. Andresen, *A Norwegian ZEB Definition Guideline*, 2016, no. January. [Online]. Available: zeb.no

[50] A. E. Fenner, C. J. Kibert, J. Woo, S. Morque, M. Razkenari, H. Hakim, and X. Lu, "The carbon footprint of buildings: A review of methodologies and applications," *Renewable and Sustainable Energy Reviews*, vol. 94, pp. 1142–1152, 10 2018. [Online]. Available: https://www.sciencedirect.com/science/article/pii/S1364032118305069

[51] Standard Norge, "Norsk Standard NS 3720:2018," Tech. Rep., 2018. [Online]. Available: https://www.standard.no/no/Nettbutikk/produktkatalogen/Produktpresentasjon/?ProductID=992162

[52] C. Good, T. Kristjansdottír, A. Houlihan Wiberg, L. Georges, and A. G. Hestnes, "Influence of PV technology and system design on the emission balance of a net zero emission building concept," *Solar Energy*, vol. 130, pp. 89–100, 6 2016. [Online]. Available: https://linkinghub.elsevier.com/retrieve/pii/S0038092X16000621

[53] I. Graabak, B. H. Bakken, and N. Feilberg, "Zero emission building and conversion factors between electricity consumption and emissions of greenhouse gases in a long term perspective," *Environmental and Climate Technologies*, vol. 13, no. 1, pp. 12–19, 2014.

[54] K. B. Lindberg, G. Doorman, D. Fischer, M. Korpås, A. Ånestad, and I. Sartori, "Methodology for optimal energy system design of Zero Energy Buildings using mixed-integer linear programming," *Energy and Buildings*, vol. 127, pp. 194–205, 9 2016.

[55] J. . Clauß, S. . Stinner, C. . Solli, K. Lindberg, . Byskov, H. . Madsen, and L. Georges, "General rights Evaluation method for the hourly average CO2eq. Intensity of the electricity mix and its application to the demand

response of residential heating," *Downloaded from orbit.dtu.dk on*, 2019. [Online]. Available: https://doi.org/10.3390/en12071345

[56] B. Tranberg, O. Corradi, B. Lajoie, T. Gibon, I. Staffell, and G. B. Andresen, "Real-time carbon accounting method for the European electricity markets," *Energy Strategy Reviews*, vol. 26, p. 100367, 11 2019.

[57] D. Pinel, M. Korpås, and K. B. Lindberg, "Impact of the CO2 factor of electricity and the external CO2 compensation price on zero emission neighborhoods' energy system design," *Building and Environment*, vol. 187, p. 107418, 1 2021.

[58] C. Lausselet, V. Borgnes, and H. Brattebø, "LCA modelling for Zero Emission Neighbourhoods in early stage planning," *Building and Environment*, vol. 149, pp. 379–389, 2 2019.

[59] D. Pinel, "Clustering methods assessment for investment in zero emission neighborhoods' energy system," *International Journal of Electrical Power and Energy Systems*, vol. 121, p. 106088, 10 2020.

[60] H. Blanco and A. Faaij, "A review at the role of storage in energy systems with a focus on Power to Gas and long-term storage," *Renewable and Sustainable Energy Reviews*, vol. 81, pp. 1049–1086, 1 2018.

[61] P. Gabrielli, A. Poluzzi, G. J. Kramer, C. Spiers, M. Mazzotti, and M. Gazzani, "Seasonal energy storage for zero-emissions multi-energy systems via underground hydrogen storage," *Renewable and Sustainable Energy Reviews*, vol. 121, p. 109629, 4 2020.

[62] H. T. Walnum and E. Fredriksen, "Thermal Energy Systems in ZEN: Review of technologies relevant for ZEN pilots," *68*, 2018. [Online]. Available: https://sintef.brage.unit.no/sintef-xmlui/handle/11250/2503718

[63] A. Hesaraki, S. Holmberg, and F. Haghighat, "Seasonal thermal energy storage with heat pumps and low temperatures in building projects—A comparative review," *Renewable and Sustainable Energy Reviews*, vol. 43, pp. 1199–1213, 3 2015.

[64] S. K. Shah, L. Aye, and B. Rismanchi, "Seasonal thermal energy storage system for cold climate zones: A review of recent developments," *Renewable and Sustainable Energy Reviews*, vol. 97, pp. 38–49, 12 2018.

[65] T. Yang, W. Liu, G. J. Kramer, and Q. Sun, "Seasonal thermal energy storage: A techno-economic literature review," *Renewable and Sustainable Energy Reviews*, vol. 139, p. 110732, 4 2021.

[66] B. McDaniel and D. Kosanovic, "Modeling of combined heat and power plant performance with seasonal thermal energy storage," *Journal of Energy Storage*, vol. 7, pp. 13–23, 8 2016.

[67] T. Brown, D. Schlachtberger, A. Kies, S. Schramm, and M. Greiner, "Synergies of sector coupling and transmission reinforcement in a cost-optimised, highly renewable European energy system," *Energy*, vol. 160, pp. 720–739, 10 2018.

[68] R. Egging-Bratseth, H. Kauko, B. R. Knudsen, S. A. Bakke, A. Ettayebi, and I. R. Haufe, "Seasonal storage and demand side management in district heating systems with demand uncertainty," *Applied Energy*, vol. 285, p. 116392, 3 2021.

[69] R. Bellman, "A MARKOVIAN DECISION PROCESS -," 1957.

[70] V. N. Gudivada, D. Rao, and V. V. Raghavan, "Big Data Driven Natural Language Processing Research and Applications," in *Handbook of Statistics*. Elsevier, 1 2015, vol. 33, pp. 203–238.

[71] R. C. Sonderegger and R. C., "Dynamic models of house heating based on equivalent thermal parameters," *PhDT*, 1978.

[72] P. Bacher and H. Madsen, "Identifying suitable models for the heat dynamics of buildings," *Energy and Buildings*, vol. 43, no. 7, pp. 1511–1522, 7 2011.

[73] E. M. L. Beale and J. J. H. Forrest, "GLOBAL OPTIMIZATION USING SPECIAL ORDERED SETS," Tech. Rep., 1976. [Online]. Available: https://link.springer.com/content/pdf/10.1007%2FBF01580653.pdf

[74] Markets Insider, "CO2 European Emission Allowances Spot Price Chart." [Online]. Available: https://markets.businessinsider.com/commodities/co2-european-emission-allowances

[75] I. Energy Agency, "Net Zero by 2050 - A Roadmap for the Global Energy Sector," 2050. [Online]. Available: www.iea.org/t&c/

[76] J. Clauß, S. Stinner, I. Sartori, and L. Georges, "Predictive rule-based control to activate the energy flexibility of Norwegian residential buildings: Case of an air-source heat pump and direct electric heating," *Applied Energy*, vol. 237, pp. 500–518, 3 2019.

# Publications

# Paper I



Cite as:
K. E. Thorvaldsen, S. Bjarghov and H. Farahmand
"Representing Long-term Impact of Residential Building Energy Management using Stochastic Dynamic Programming"
*2020 International Conference on Probabilistic Methods Applied to Power Systems (PMAPS)*, Aug 2020
DOI: 10.1109/PMAPS47429.2020.9183623
URL: `https://doi.org/10.1109/PMAPS47429.2020.9183623`

# Paper II



The paper **"Long-term Value of Flexibility from Flexible Assets in Building Operation"** is published by **Elsevier** in **International Journal of Electrical Power & Energy Systems**. The final published paper is reprinted here without changes in compliance with the CC-BY 4.0 license[1] it is published under.

Cite as:
K. E. Thorvaldsen, M. Korpås, and H. Farahmand
"Long-term Value of Flexibility from Flexible Assets in Building Operation"
*International Journal of Electrical Power and Energy Systems*, vol. 138, June 2022
DOI: 10.1016/j.ijepes.2021.107811
URL: `https://doi.org/10.1016/j.ijepes.2021.107811`

[1] See `https://creativecommons.org/licenses/by/4.0/` for license details.

Electrical Power and Energy Systems 138 (2022) 107811

Contents lists available at ScienceDirect

International Journal of Electrical Power and Energy Systems

journal homepage: www.elsevier.com/locate/ijepes

# Long-term Value of Flexibility from Flexible Assets in Building Operation

Kasper Emil Thorvaldsen *, Magnus Korpås, Hossein Farahmand

*Department of Electric Power Engineering, Norwegian University of Science and Technology, 7491 Trondheim, Norway*

ARTICLE INFO

*Keywords:*
Demand-side management
Grid tariff
Operational planning
Stochastic dynamic programming
Expected future cost curve

ABSTRACT

In this work, we investigate how flexible assets within a residential building influence the long-term impact of operation. We use a measured-peak grid tariff (MPGT) that puts a cost on the highest single-hour peak import over the month. We apply a mathematical model of a Home Energy Management System (HEMS) together with Stochastic Dynamic Programming (SDP), which calculates the long-term impact of operating as a non-linear expected future cost curve (EFCC) from the end of the scheduling period to the start. The proposed model is applied to a case study for a Norwegian building with smart control of a battery energy storage system (BESS), Electric vehicle (EV) charging and space heating (SH). Each of the flexible assets are investigated individually with MPGT and for an energy-based grid tariff. The results showed that EV charging has the highest peak-power impact in the system, decreasing the total electricity cost by 14.6% with MPGT when controllable compared to a reference case with passive charging. It is further shown how the EFCC helps achieve optimal timing and level of the peak demand, where it co-optimizes both real-time pricing and the MPGT.

## 1. Introduction

With the roll-out of smart meters, it is possible to implement more dynamic price structures so the end-users can react to price signals on their own accord. This introduces the potential of participating in price-based Demand Response (DR) programs, which ideally should be able to represent the grid operators' actual system cost of operating the grid. However, it is important that the system cost is accurately represented in their programs.

The electricity bill from the grid operator for the end-user is currently in a period of transition, where the cost is going from a passive volumetric charge cost to a combination of volumetric and capacity-based costs, in line with recommendations [1]. The measured-peak grid tariff (MPGT) and subscribed capacity have been presented by the Norwegian Water Resources and Energy Directorate (NVE) as possible new grid tariffs in Norway [2]. MPGT introduces a capacity-based tariff determined by the highest single-hour energy consumption over an hour for a given period. The MPGT is already implemented for end-users with a total yearly consumption rate over 100 MWh, for a monthly period [3]. If such a grid tariff is implemented for smaller consumers, a Home Energy Management System (HEMS) can help consumers achieve a more cost-optimal utilization of local energy resources in response to such tariffs if they are capable of operating while considering the whole period. However, with a long-term price signal such as a monthly MPGT, it is crucial to operate the building appropriately over the whole month. This price signal creates a need to be able to account for the whole period during short-term operation, and thus a long-term operational strategy would assist the HEMS during operation.

In this study, we focus on the impact of flexible assets in a HEMS, such as battery energy storage system (BESS), thermal flexibility from space heating (SH) and electric vehicles (EVs). In [4], different BESS alternatives are investigated in an economic overview for an average residential consumer in the US with the overall goal of shaving electrical peaks under a Time-of-use demand tariff. A thermal storage tank was used in [5] for a building consisting of multiple smart homes with wind production and BESS to reduce peak electricity consumption from the grid. The work in [6] analyzed thermal comfort and temperature zoning in residential buildings with user feedback to analyze performance. Trying to charge an EV optimally given the uncertainty in driving pattern was investigated in [7], where the stochastic nature gave a noticeable impact on charging strategies. In [8], the EV was used together with a HEMS and a charge–discharge management framework to charge the EV optimally while lowering the PV curtailment and reduce total residential operation cost.

A HEMS will operate and control the energy input and output from the different flexible assets, adjusting the flow of energy based on what is deemed the optimal decision for the HEMS to consider. In most cases, this control of flexible assets is used to optimize the total cost of electricity within the period that the HEMS considers. However, the

* Corresponding author.
*E-mail address:* kasper.e.thorvaldsen@ntnu.no (K.E. Thorvaldsen).

https://doi.org/10.1016/j.ijepes.2021.107811
Received 5 February 2021; Received in revised form 26 September 2021; Accepted 12 November 2021

## Nomenclature

### Index sets

| | |
|---|---|
| $S_g$ | set of state variables |
| $\mathcal{T}$ | Set of time steps within the day |
| $\mathcal{G}$ | set of days within the month |

### Parameters

| | |
|---|---|
| $\dot{E}^{B,dch}, \dot{E}^{B,ch}$ | Discharge/charge capacity for battery [$\frac{\text{kWh}}{\text{h}}$] |
| $\dot{E}^{Max}$ | Maximum EV charging capacity [$\frac{\text{kWh}}{\text{h}}$] |
| $\dot{Q}^{sh}$ | Capacity for space heating radiator [$\frac{\text{kWh}}{\text{h}}$] |
| $\eta^{B}_{dch}, \eta^{B}_{ch}$ | Discharge/charge efficiency for battery [$p.u$] |
| $\eta^{EV}_{ch}$ | EV charging efficiency [$p.u$] |
| $\eta^{PV}$ | Total efficiency for PV system [$p.u$] |
| $C^{grid}$ | DSO energy tariff for imported energy [$\frac{\text{EUR}}{\text{kWh}}$] |
| $C^{peak}$ | DSO capacity-based tariff for highest peak import [$\frac{\frac{\text{EUR}}{\text{kWh}}}{\text{h}}$] |
| $C^{imp}_n$ | Expected future cost for point $n$ [EUR] |
| $A^{PV}$ | PV system area [$\text{m}^2$] |
| $C_i, C_e$ | Heat capacity for interior and building envelope [$\frac{\text{kWh}}{^\circ\text{C}}$] |
| $D^{EV}$ | EV discharge when not connected [kWh] |
| $E^{B,Cap}$ | Battery storage capacity [kWh] |
| $E^{B,min}, E^{B,max}$ | Battery SoC limits [kWh] |
| $E^{EV,Cap}$ | EV storage capacity [kWh] |
| $E^{EV,min}, E^{EV,max}$ | Min/Max EV SoC capacity [kWh] |
| $N_P$ | Number of discrete peak power values |
| $N_S$ | Number of nodes for stochastic variables |
| $P^{imp,max}$ | Maximum power import to building [$\frac{\text{kWh}}{\text{h}}$] |
| $P^{imp}_0$ | Initial peak power [$\frac{\text{kWh}}{\text{h}}$] |
| $P^{imp}_n$ | Peak power at point $n$ [$\frac{\text{kWh}}{\text{h}}$] |
| $R_{ie}, R_{eo}$ | The thermal resistance between the interior-building envelope and building envelope-outdoor area [$\frac{^\circ\text{C}}{\text{kWh}}$] |
| $T^{in,min}_t, T^{in,max}_t$ | Lower/upper interior boundary [°C] |
| $VAT$ | Value added tax for purchase of electricity [$p.u$] |

### Decision variables

| | |
|---|---|
| $\alpha^{future}_{p^{imp}, s^e_{t+1}}$ | Expected future cost from peak power [$\frac{\frac{\text{EUR}}{\text{kWh}}}{\text{h}}$] |
| $\gamma$ | SOS-2 variables for the Expected future cost curve |
| $E^B_t$ | State of charge for Battery for time step t [kWh] |
| $E^{EV}_t$ | State of charge for EV for time step t [kWh] |
| $p^{imp}$ | Peak of imported energy [$\frac{\text{kWh}}{\text{h}}$] |
| $q^{sh}_t$ | Power usage for space heating [$\frac{\text{kWh}}{\text{h}}$] |
| $T^{in}_t, T^{e}_t$ | Interior and building envelope temperature [°C] |
| $y^{B,ch}_t, y^{B,dch}_t$ | Power to/from the battery for time step t [$\frac{\text{kWh}}{\text{h}}$] |
| $y^{EV,ch}_t$ | Input power to EV for time step t [$\frac{\text{kWh}}{\text{h}}$] |
| $y^{imp}_t, y^{exp}_t$ | Energy imported/exported to household [$\frac{\text{kWh}}{\text{h}}$] |
| $y^{PV}_t$ | Power produced from PV system [$\frac{\text{kWh}}{\text{h}}$] |

### Stochastic variables

| | |
|---|---|
| $\delta^{EV}_t$ | EV connected to building $\{0, 1\}$ |
| $C^{spot}_t$ | Electricity spot price in time step t [$\frac{\text{EUR}}{\text{kWh}}$] |
| $D^{el}_t$ | Consumer-specific load in time step t [kWh] |
| $I^{Irr}_t$ | Solar irradiation at building in time step t[$\frac{\text{kWh}}{\text{m}^2}$] |
| $T^{out}_t$ | Outdoor temperature in time step t [°C] |

information that the HEMS consider for operation of the energy system, is subject to uncertainty. A literature review was conducted in [9] regarding uncertainty within building energy systems, showcasing how weather effects, the modeling of the building envelope, and occupant behavior are different kinds of input data uncertainty that should be accounted for. In [10], an overview over DR-programs and their development was done, commenting on the importance of smart control systems for residential buildings to participate efficiently in these programs. In addition, different modeling techniques for a residential building and control algorithms for a HEMS were presented. However, they also raised the issue that appropriate tariff structures depend on the end-users capability of controlling their own consumption.

Within the operation of a HEMS, multiple optimization methods and approaches have been presented in the research literature. A mixed-integer linear problem (MILP) definition was defined within a HEMS in [11]. The HEMS included photovoltaics (PV), BESS and EV with bi-directional power flow, and the model optimizes the system operation with dynamic pricing and peak power limits. Another approach was used for a smart building consisting of PV, heat pump, thermal storage and BESS in [12], where the authors used a model predictive control (MPC) approach on a stochastic problem to optimize each of the flexible assets. A rolling horizon strategy was deployed in [13] to operate an energy management system for a microgrid. The microgrid consisted of PV, wind turbines, a diesel generator and a BESS, together with demand-side management (DSM). A HEMS with a bi-level optimization-based bidding strategy in [14] was used to schedule the loads and flexible assets within a smart building. This approach minimized cost associated with day-ahead energy commitment, while accounting for uncertainty in loads, prices and local production.

The authors in [15] apply a deterministic dynamic programming (DP) model to analyze the cost-optimal control for a building with varying degree of PV installed. The application resulted in cost savings compared to a rule-based approach which maximizes PV self-consumption. The work presented in [16] developed a deterministic DP model that optimized the state-of-charge for either a BESS or EV battery over a year for a household with PV. For a power-based grid tariff, cost savings at 13.3% with optimal battery control, or 16.6% for optimal EV battery control were achieved. The use of stochastic DP (SDP) in a HEMS has been investigated in [17], where the authors utilized SDP to optimize both EV charging and frequency regulation bids given the expected future costs calculated by SDP. A smart building model is presented in [18] that used SDP to optimize energy management for EV and PV with uncertainty in generation, consumption and EV availability. The approach found potential cost savings of almost 500% for a Tesla Model S compared to no optimal control, and load shifting potential for interaction with the grid. The work was further carried on in [19] where the authors analyzed several operating modes of the EV, such as V2G, V2H and G2V. The study found that by utilizing V2G in a grid with real-time pricing (RTP) and limited bi-directional grid capacity during certain times of the day, 75.5% cost savings could be achieved compared to a case without a plug-in EV. Ref [20] investigated an energy consumption scheduling problem with uncertain future prices. The SDP algorithm was used to describe an optimal scheduling algorithm for non- and interruptible loads based on price thresholds.

Most of the work here using SDP considers a short-time horizon of up to a day, except for [15,16], both considering a year, but not indicating that their models could be used as a short-term operational

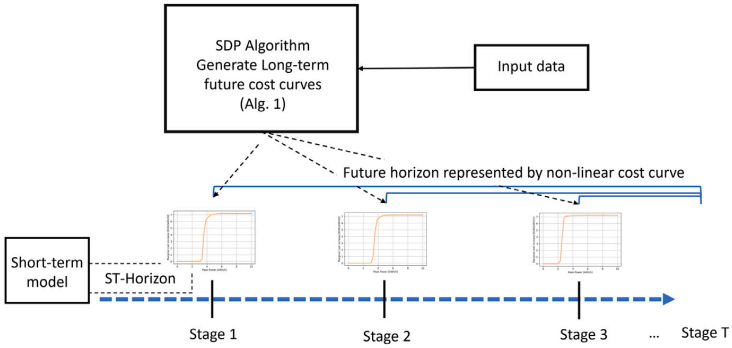


**Fig. 1.** Overview over the coupling of long-term future cost curves generated by the SDP framework in this work and in [22], and a short-term operational model. Alg. 1 will be further explained in Section 2.

model. One of the most valuable takeaways from the use of SDP is that the scheduling period is decomposed into smaller decoupled segments, only coupled through expected future cost curves which depict the future consequence of altering the state variables. Therefore, SDP can contribute on foreshadowing the expected impact of the system beyond the current scheduling horizon.

Based on a review of the literature, the relationship between long-term and short-term value of energy flexibility has not yet been specified or investigated in full detail. To the best of the authors' knowledge, the inclusion of long-term price signals in building operational models was first introduced in [21], where the monthly MPGT was introduced as an operational problem. Their work presented a HEMS dealing with the long-term cost for peak import using a metaheuristic method. The objective was to find the potential cost increment for MPGT at the end of the month, when the value from RTP and MPGT was balanced during operation. This work used a user-defined weighting constant as a signal for how costly the future could be, and did not take into account any information about what the building could expect in the future regarding operation.

Another approach to this problem regarding long-term price signals was done in [22], which is the basis for the work presented in this paper. There, we applied SDP in a MPGT setting over a month to calculate the operational strategy to deal with the long-term price signal. The methodology presented decomposed one month (long-term horizon) into smaller daily stages (short-term horizon) and generated non-linear expected future cost curves (EFCC). The EFCC describes the future consequence of flexibility utilization within a HEMS at each stage, and can be given as an input to a detailed short-term operational model. This approach is quite different compared to the metaheuristic method in [21], which did not use information about the future to set the appropriate import peak level. In [22], we compared the current operational decision to what could occur in the future, to make a global optimum operation. Therefore, there is more accuracy and information on what happens beyond the real-time operation with the use of SDP to represent the future cost of operation. The coupling of the proposed long-term operation to a short-term operating model is showcased in Fig. 1.

The SDP algorithm is used to generate EFCCs, showcasing the change in the expected cost beyond the decisions taken up to each stage. The SDP algorithm determines how a HEMS would react to a number of possible future scenarios, and calculates the cost-optimal decision backward, which then is put together into a weighted future cost curve and used in a short-term operational model. This approach is similar to hydropower scheduling, where long- and medium-term models are used to generate cost curves as showcased in Ref. [23], which are given as input to a short-term operational model [24]. This paper focuses on the generation of these future cost curves.

There exist other decomposition techniques than SDP, that could be applied to assist in foreshadowing the expected impact for a system. One such method is stochastic dual-dynamic programming (SDDP), which represents EFCCs as linear cuts generated in an iterative process by going back and forth in the scenario tree to represent the future cost of operation [25]. In Ref. [26], a receding horizon control optimization algorithm was developed to operate a community with a shared BESS, to reduce an MPGT cost for the shared community over one month. To deal with a potentially large scenario tree, the horizon beyond the control horizon was simplified into three scenarios to capture the long-term influence needed to account for the MPGT cost.

For capturing the long-term effects of operation for a HEMS, the SDP method is suitable for this kind of problem. It decomposes a bigger optimization model into smaller deterministic problems consisting of multiple stages, scenarios, and discrete values of the long-term variable. This approach allows the possibility of choosing finer state variable resolution, and adjusting for increased accuracy. The SDP algorithm can also solve non-linear problems, whereas other models such as SDDP require linearity in the problem to be solvable. However, the SDP method has some short comings, for instance the curse of dimensionality if the number of discrete values, scenarios and stages are too many. Also, the method will lose some information when decomposing the problem, since variables except the state variables must have a fixed start/end parameter value at the start/end of each stage to be feasible for transition.

Expanding on the work presented in [22], the main contributions here are as follows:

- We present a general SDP framework for optimal energy management of HEMS exposed to a monthly MPGT. The HEMS considers that SH, EV charging and a BESS can be utilized to keep the peak import at the cost-optimal level, influenced by the implications given by the EFCC calculated
- The output of the SDP framework is further analyzed for each individual flexible asset, to capture the different characteristics each asset contains in a long-term operational setting
- In a numerical case study based on real Norwegian conditions, the model is applied to two different electricity grid tariffs, and tested where each flexible asset can be controlled individually. The analysis showcases their impact and value of flexibility based on the peak import level, and each asset and the different schemes are compared against each other

The paper progresses as follows. Section 2 introduces the SDP framework methodology of the HEMS. The case study used for the analysis is presented in Section 3, while the results and discussion are found in Section 4. The conclusion and future work are given in Section 5.

## 2. Methodology

The overall objective of a HEMS is to minimize the expected total electricity cost from interaction with the distributional grid, consisting of electricity purchase and grid tariff payments. The scheduling horizon depends on the value of utilizing load shifting over longer periods, and the duration of any long-term price signals that are included. This work considers the long-term price signal from the MPGT, paid at the end of the horizon. Thus, the objective will be to find the optimal operation to obtain the minimum expected operating cost for the HEMS, as shown in Eq. (1):

$$min\mathbb{E}\{\sum_{t=1}^{T_{sub}}[C_t^{spot}\cdot(y_t^{imp}-y_t^{exp})+C^{grid}\cdot y_t^{imp}]+\Phi(p^{imp})\} \quad (1)$$

We deal with this issue in a similar fashion to hydropower scheduling [27], by assuming that we only want to optimize the HEMS for a pre-determined period between $t=1$ and $T_{sub}$ of the total horizon. For this pre-determined period to be capable of operating optimally and still consider the cost paid at the end of the horizon, the future impact must be included. Here, the function $\Phi(p^{imp})$ represents the cost for the peak import beyond the present period, into the future. Thus, the peak import $p^{imp}$ is coupled in time, giving a dynamic connection of the optimization problem. Hence, the formulation represents a multi-stage multi-scenario optimization problem, and we can apply decomposition techniques to simplify the problem. We utilize an SDP approach for multi-stage in a backwards procedure [28]. The function $\Phi(p^{imp})$ from Eq. (1) is represented as a piecewise-linear future cost curve calculated through an SDP algorithm.

The original problem is decomposed into several smaller single-stage deterministic problems to decrease the computational complexity. The decomposition is performed through a set of state variables $\mathcal{S}_g$, which consists of all information that is carried over between the decision stages $g-1$ to $g$. This set consists of two unique subsets; subset $\mathcal{S}_{S,g}$, which consists of realized values for the stochastic variables for each decision stage $g$, and subset $\mathcal{S}_{P,g}$, which contains state variables in the optimization problem. Based on the set $\mathcal{S}_g$, a decomposed decision problem for the HEMS to solve is defined based on the state $s_g^s, s_g^p \in \mathcal{S}_g$ for a decision stage $g$, which is given by the current scheduling for that decision stage, and the weighted impact of the future cost for all scenarios. The decomposed decision problem is presented in Section 2.1.

To perform valid coupling between the stages, the conditions at the end of one stage to the next corresponding stage must be identical. If not ensured, the transition is not feasible and will result in inaccurate results. In a building, this would be connected to the energy levels and connectivity of certain shiftable units. If these variables are not tied to the state variable subset $\mathcal{S}_{P,g}$, such that the future impact of any changes are included, then it is possible to lock their start/end values between stages to make the transition feasible. This work has a set start/end condition for each stage for the flexible assets, described in Section 2.2.

The stages are considered to be decoupled from each other, while the scenarios between stages are tied together through a transition probability, represented as a Markov decision process (MDP). To enable a method for generating future cost curves in a backwards DP strategy, the problem is represented as a Markov decision [29]. The scenarios generated specify the uncertain parameters in the system, referred to as stochastic variables. For a specific stage and scenario, the stochastic variables are realized as input for the HEMS. The future impact beyond the stage is affected by transitioning the scenarios forward and their probabilities. The transition probabilities are assumed to have a Markov property, which specifies the stochastic process is memoryless [30]. The transitioning scenarios and their impact in the future are represented as the future cost $\Phi(p^{imp})$, making it an MDP. Therefore, the impact of the future scenarios in the MDP can be represented in the present scenario as an EFCC. By combining the different discrete scenarios $\mathcal{N}_S$ in $\mathcal{S}_{S,g+1}$, the EFCC illustrates the weighted cost-based impact towards the future.

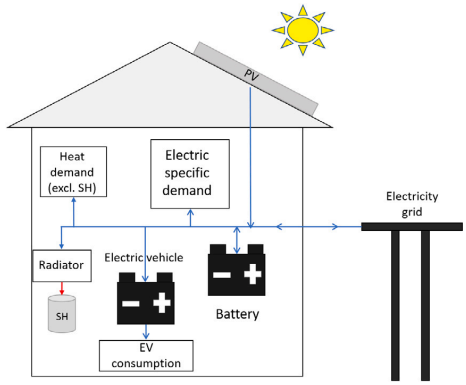


**Fig. 2.** Overview of building structure and energy system.

### 2.1. Decomposed decision problem

The decomposed decision problem is formulated as an optimization model for a given stage $g$, scenario $s_g^s$, and initial peak import power $P_0^{imp}$. The optimization model described in this subsection consists of a residential building connected to the power grid with bi-directional power flow capability, as illustrated in Fig. 2, operated through a HEMS. The electric-specific demand and heat demand from a water tank must be met at all times and these are treated as non-shiftable loads $D_t^{El}$. The smart control covers SH, BESS control, EV charging, and a roof-mounted photovoltaic (PV) system.

#### 2.1.1. Objective function

The objective function in (2) minimizes the total electricity cost for the end-user. The electricity cost is the cost or benefit of importing/exporting electricity from the grid, respectively, and the future long-term cost for operating beyond this stage based on the highest single-hour peak import power $p^{imp}$, based on the EFCC. The objective function will co-optimize both short-term and long-term implications, where it balances the marginal cost increase of short-term operation versus the marginal cost savings in the long-term when lowering the peak import.

$$min\{\sum_{t\in\mathcal{T}}[C_t^{spot}\cdot(y_t^{imp}-y_t^{exp})+C^{grid}\cdot y_t^{imp}]+\alpha^{future}_{p^{imp},s^s_{g+1}}\} \quad (2)$$

#### 2.1.2. Energy balance

The electric energy balance of the house is given in (3). The exchange between the grid, together with production from the PV system and interaction from the BESS, must cover the needed load for the building.

$$y_t^{imp}-y_t^{exp}+y_t^{PV}+y_t^{B,dch}=D_t^{El}+y_t^{EV,ch}+q_t^{sh}+y_t^{B,ch}\quad \forall t \quad (3)$$

#### 2.1.3. Expected future cost curve

The EFC for this problem is depicted within (4a) to (4f). The highest amount of power that is imported to the building is denoted by $p^{imp}$, which is bounded by the highest peak within the decision stage (4b) and the initial value from earlier periods (4a). The peak import power achieved at the end is used to set the EFC included in the objective function, which consists of discretized values of $P_n^{imp}\ n\in\mathcal{N}_P$ represented through SOS-2 variables [31].

$$p^{imp}\geq P_0^{imp} \quad (4a)$$

$$p^{imp}\geq y_t^{imp}\quad \forall t \quad (4b)$$

$$\alpha^{future}_{p^{imp},s^s_{g+1}} = \sum_{n\in\mathcal{N}_P} \gamma_n \cdot C^{imp}_n \tag{4c}$$

$$p^{imp} = \sum_{n\in\mathcal{N}_P} \gamma_n \cdot P^{imp}_n \tag{4d}$$

$$\sum_{n\in\mathcal{N}_P} \gamma_n = 1 \tag{4e}$$

$$\gamma_n \geq 0 \quad \forall n,\ SOS\text{-}2 \tag{4f}$$

#### 2.1.4. Electric vehicle

The behavior of the EV is formulated in (5a) to (5c). The EV is modeled as a uni-directional battery that can be charged at a continuous rate, with an availability pattern based on the stochastic variable $\delta^{EV}_t$. If the EV is not available at the building, the EV cannot be charged and a constant load discharges the battery to simulate consumption from driving. The EV must stay within a specific range in its state-of-charge (SoC) in (5c), whereas the boundary is time-dependent to include traveling preferences.

$$E^{EV}_t - E^{EV}_{t-1} = y^{EV,ch}_t \eta^{EV}_{ch} \delta^{EV}_t - D^{EV}(1-\delta^{EV}_t) \quad \forall t \tag{5a}$$

$$0 \leq y^{EV,ch}_t \leq \dot{E}^{Max} \quad \forall t \tag{5b}$$

$$E^{EV,min}_t \leq E^{EV}_t \leq E^{EV,max}_t \quad \forall t \tag{5c}$$

#### 2.1.5. Battery energy storage system

A bi-directional BESS is available within the building with the characteristics shown in (6a) to (6d). The battery can be discharged and charged at a continuous rate, with limitations on power capacity and a storage capacity range to ensure optimal operation without risk of damage.

$$E^B_t - E^B_{t-1} = y^{B,ch}_t \eta^B_{ch} - \frac{y^{B,dch}_t}{\eta^b_{dch}} \quad \forall t \tag{6a}$$

$$0 \leq y^{B,ch}_t \eta^B_{ch} \leq \dot{E}^{B,ch} \quad \forall t \in \mathcal{T} \tag{6b}$$

$$0 \leq y^{B,dch}_t \leq \dot{E}^{B,dch} \quad \forall t \in \mathcal{T} \tag{6c}$$

$$E^{B,min}_t \leq E^B_t \leq E^{B,max} \quad \forall t \tag{6d}$$

#### 2.1.6. Photovoltaic system

A roof-mounted PV system is connected to the electrical system through a controllable system. The HEMS is assumed to change the power output in a similar fashion to the work presented in [32].

$$0 \leq y^{PV}_t \leq A^{PV} \cdot \eta^{PV} \cdot I^{Irr}_t \quad \forall t \in \mathcal{T} \tag{7}$$

#### 2.1.7. Space heating

All considerations regarding heating of the building are formulated in (8a) to (8d). The building has an electric radiator for SH that can be operated continuously. The heat dynamics in the building are shown as a gray-box model, in which the physical behavior is formulated using linear state–space models [33,34]. The dynamics between the interior temperature and the outdoor temperature can be captured alongside disturbances as heat input, which will include the impact of time-dependent temperature deviations. Thus, the heat system can be represented through an RC-network model. In an RC-network model, resistors (R) represents thermal resistance between measuring points, capacitors (C) capture the heat capacity of the measuring point, and $q^{sh}$ is the heat flux from heat sources. In addition, the outdoor temperature impact is included as a voltage source ($T^{out}$).

The RC-network layout depends on the number of zones and inputs into each existing zone [34]. This optimization problem utilizes a 2R2C model, which divides the system into three zones: the interior or indoor of the building, the envelope acting as the physical separator between the interior and outdoors, and the outdoor area. The layout is shown in Fig. 3. The interior temperature is measured by the control system for the building, which can utilize the electric heater to regulate the temperature in response to impact from the envelope and outdoor temperature.

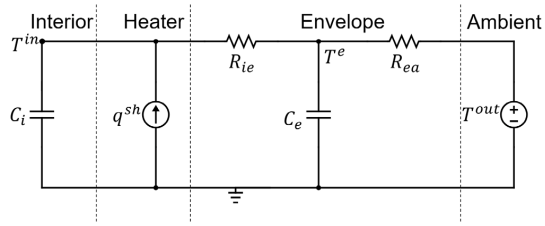


**Fig. 3.** RC-network for the SH dynamics given in Eqs. (8c) to (8d).

$$0 \leq q^{sh}_t \leq Q^{sh} \quad \forall t \tag{8a}$$

$$T^{in,min}_t \leq T^{in}_t \leq T^{in,max}_t \quad \forall t \tag{8b}$$

$$T^{in}_t - T^{in}_{t-1} = \frac{1}{R_{ie}C_i}[T^e_{t-1} - T^{in}_{t-1}] + \frac{1}{C_i} q^{sh}_t \quad \forall t \tag{8c}$$

$$T^e_t - T^e_{t-1} = \frac{1}{R_{ie}C_e}[T^{in}_{t-1} - T^e_{t-1}] + \frac{1}{R_{eo}C_i}(T^{out}_{t-1} - T^e_{t-1}) \quad \forall t \tag{8d}$$

### 2.2. Solution strategy

**Algorithm 1:** The SDP algorithm

```
1 for g = G, G − 1, .., 1 do
2     for n ∈ N_P do
3         P^imp_0 ← P^imp_n
4         for s^s_g ∈ N_S do
5             {C^spot_t, D^El_t, δ^EV_t, I^Irr_t, T^out_t} ← Γ(g, s^s_g)
6             C^imp_i ← Φ(i, s^s_g, g + 1) for i = 1..N_P
7             C_{s^s_g,n} ← Optimize(2)–(8)
8         for s^s_{g−1} ∈ N_S do
9             Φ(n, s^s_{g−1}, g) = Σ_{s^s_g=1}^{N_S} C_{s^s_g,n} · ρ(g, s^s_g | s^s_{g−1})
```

The complete optimization problem is solved through the SDP algorithm solution strategy as shown in Algorithm 1. This process will generate EFCCs for every stage of the overall problem.

The SDP algorithm initiates at the last stage of the horizon, and computes the overall cost of the decomposed decision problem in Section 2.1 for the number of discrete points of the state variable $n \in \mathcal{N}_P$, and the number of scenarios $s^s_g \in \mathcal{N}_S$. For each scenario, we realize the stochastic variables with values from $\Gamma$ in line 5 as input into the specific problem, and in line 6 the EFCC for the future scheduling day $g+1$ is realized for each discrete point in $C^{imp}_i$. $\Gamma$ contains the realized stochastic variables based on the scheduling day $g$ and scenario $s^s_g$. The EFCC used are the results from the previous stage $g+1$, and for the initial case $g = \mathcal{G}$, the end cost for peak import by the MPGT is used.

In line 7, the optimization problem for the HEMS is solved in order to find the objective function value, which is affected by both the cost for operating within the stage and the resulting EFC beyond the period. To enable a feasible transition between stages, $T^{in}_t$, $T^e_t$, $E^{EV}_t$ and $E^B_t$ have a start/end condition the optimization problem must hold. There is a high penalty cost included for the SH variables if this condition cannot be met, but this penalty cost is not included in the generation of EFCCs as it has no further influence on the decision-making.

The result from the problem is then used to derive the EFCC $\Phi(n, s^e_{g-1}, g)$ for $n \in \mathcal{N}_P$. The calculation of the EFCC is performed in

line 8–9, where the EFC for a specific state variable point is derived. For a state variable value $n$, the EFC representation for stage $g$ is calculated as the weighted future cost value for all scenarios that can occur in this stage, to be used in the previous stage $g-1$. The EFC is calculated for each scenario that occurs in stage $g-1$ through the loop in line 8, and the weight of each EFC is based on the corresponding transition probabilities $\rho(g, s_g^s | s_{g-1}^s)$, which depends on the probability of arriving at scenario $s_g^s$ when originally at scenario $s_{g-1}^s$. This process is performed for all state variables until the whole EFCC has been calculated for all scenarios $s_{g-1}^s \in \mathcal{N}_S$. These results are then used as the basis for stage $g-1$, until we have arrived at the first stage and have derived EFCCs for all stages and scenarios.

## 3. Case study

The presented model has been applied to a realistic case study of a Norwegian building in which the presented MPGT is included in the electricity bill. The building is a single-family house (SFH) placed in the south-eastern part of Norway, and the HEMS controls the different flexible assets available. The analysis is for January 2017 with hourly time resolution per day, and the stochastic variables consist of historical data or synthetic data from supporting literature.

### 3.1. Building structure

The PV system on the roof consists of 4.65 kW installed capacity, connected through an MPP inverter with a combined constant conversion and MPP efficiency at 95% [35].

The inelastic demand originates from two sources: The electric-specific electricity consumption from users, and non-flexible domestic hot water (DHW) consumption covered by a water tank. The data for the electric-specific electricity are obtained from the Distributional Operator (DSO) Ringerikskraft from January 2017 [36]. The DHW-consumption profile is based on measurement of 49 water heaters at Norwegian households through the "Electric Demand Knowledge - ElDek"[1] research project by SINTEF Energy Research [37]. The RTP electricity prices from bidding zone NO1 in Nordpool for year 2017 are used [38]. As the end-user is a small consumer in the grid, the spot prices are given as input, and we assume the end-user is a price-taker.

#### 3.1.1. Heat dynamics

The layout in Fig. 3 represents the heat dynamics of the building, and is based on observed values from the Living Lab building built by Zero Emission Building (FME ZEB)[2] and NTNU [39,40]. The Living Lab is a pilot project used to study various technologies and design strategies with the overall goal of reaching the zero emission target and analyzing thermo-physical properties [41]. The space heating is performed through a 3 kW radiator, which can operate continuously. The default temperature boundary that the HEMS uses is a range of 20–24 °C, which from Ref. [6] is the threshold end-users find comfortable.

#### 3.1.2. Electric vehicle

A 24 kWh EV is selected for this study, with an operational range between 20%–90% of total capacity at all times, with a range between 60%–90% when departing to prevent range anxiety. The EV consumes electricity from the battery when it has departed to simulate driving.

The EV consumption rate over a weekday has been simplified as a deterministic input. Based on [42], the mean driving distance of 52 km has been used, under the assumption that the EV consumes 18 kWh/100 km, which puts the hourly discharge rate at 1.02 kWh/h for $D^{EV}$ with a 9-hour offline timeframe. The EV is assumed to always be connected during stage transition, and as the optimization model in Section 2.1 has deterministic info for each stage and scenario analyzed, the HEMS can charge the EV so it ensures enough SoC for the trip.

[1] https://www.sintef.no/prosjekter/eldek-electricity-demand-knowledge/.
[2] www.fmezen.no/.

#### 3.1.3. Battery energy storage system

The BESS installed in this system is based on a battery from SonnenBatterie [43] with a rated power input/output of 2.5 kW measured at the output of the inverter. The tolerated SoC is set at between 10%–100% SoC, and a round-trip efficiency of 85% in line with efficiency settings from [44]. Any cost or performance associated with battery degradation is left out of this analysis.

#### 3.1.4. Initial conditions

As mentioned in Section 2.2, the following variables have been given a start/end value to enable a feasible stage transition: $T_0^{in} = 22$ °C, $T_0^e = 20$ °C, $E_0^{EV} = 14.4$ kWh, $E_0^B = 2.5$ kWh.

#### 3.1.5. Grid tariff structure

The grid tariff structure consists of multiple layers of payment. A conversion rate of 1 EUR = 10 NOK has been used for this work. The first is a fixed consumer cost given as a volumetric cost at 0.024 $\frac{\text{EUR}}{\text{kWh}}$ in 2017. The rest contains the cost provided by the DSO, which depends on the tariff scheme. In 2017, the DSO Ringerikskraft provided only a volumetric cost at 0.02425 $\frac{\text{EUR}}{\text{kWh}}$. With the proposed MP capacity-based grid tariff from NVE, accumulated for a monthly period [2], the volumetric cost would be at 0.00625$\frac{\text{EUR}}{\text{kWh}}$, and a monthly capacity-based cost at 7.2075 $\frac{\text{EUR}}{kW_{peak}}$.

### 3.2. Scenario generation

The HEMS together with the SDP algorithm allows the possibility for multiple input data to be uncertain in the period of operation. To limit the range of uncertainty, the work here considers uncertainty within the EV behavior, outdoor temperature and solar irradiation. Information such as electricity price and electric-specific demand is considered deterministic.

In total, 9 scenarios per day have been generated for this case study, where 3 scenarios have been generated from both weather effects and EV behavior. It is assumed that the sources are independent of each other, resulting in 9 combinations. The stochastic nature of the input data is based on a normal distribution with the mean and standard deviation as the discrete scenarios, giving a probability distribution at $\rho_\mu = 68.2\%, \rho_\sigma = 15.9\%$ for each source.

The normal distribution of EV behavior for a weekday is based on [42], with an expected departure/arrival time from 9 AM to 5 PM, and a standard deviation of 90 min (as this work considers an hourly time step, the standard deviation is rounded up to 2 h). Moreover, authors in [45] show that the expected arrival time when charging near home does not change dramatically between weekdays and weekends. Thus, we assume the same departure/arrival time pattern for the weekend.

Data for both the outdoor temperature and solar irradiation have been obtained from Rygge weather station in South-east Norway [46]. Hourly data from 2014–2019 for the month of January have been used to create hourly normal distributions, to generate three discrete scenarios.

### 3.3. Model cases

The scope of this work will be to investigate the flexibility contribution each flexible asset can provide, both for MPGT and energy-based grid tariff (EBGT) structures, both given $MPGT$ and $EBGT$ as case names, respectively. This extends the analysis in [22] by investigating the long-term value each flexible asset offers individually instead of combined. For each case with a specified flexible asset, the other assets will have a passive behavior. The passive manner for each of the assets is the following: The BESS is turned off, the EV charging will charge to max capacity at 90% whenever it can and has an initial condition of $E_0^{EV} = 22.6$ kWh during transition. The space heating will maintain a constant indoor temperature at $T_t^{in} = 22$ °C $\forall t$. Moreover, the flexible

**Table 1**
Flexible asset parameters for the different cases. Values in bold are default values when considering the asset as passive.

| Component | Parameter(s) | Cases |
|---|---|---|
| Battery energy storage system | $E^{B,Cap}$ | **5 kWh**, 10 kWh |
| Space heating | $T^{in,min}$, $T^{in,max}$ | **[20, 24]**, [21, 23] |
| Electric Vehicle | $\dot{E}^{Max}$ | 2.3 kW, **3.7 kW** |

assets will be investigated for several input parameter values to analyze the change of impact, as showcased in Table 1.

The analysis will be carried out by first generating the EFCCs for each case using the SDP algorithm in Alg. 1. The state variable subset $S_{P,g}$ will consist of 100 discrete initial values of $p^{imp}$, ranging from 0–10 $\frac{\text{kWh}}{\text{h}}$. This leads to 27 900 unique decomposed problems to solve per case. After this, the value of the EFCCs will be analyzed through a simulation phase, where each day is run sequentially for the whole month to see the overall economical performance, where the peak import level will be carried over between stages and the final grid tariff cost is set at the end. To account for the range of uncertainty in the input data, the simulation phase analyze this month 1000 times with different stochastic scenario realizations based on their scenario probability. The sequential coupling between two stages is done by randomly drawing a future scenario for the next stage transition, where the odds for each scenario is based on their probability. This leads to multiple scenario combinations per month.

## 4. Results & discussion

The SDP algorithm showcased in Algorithm 1 creates EFCC from the last day of the month, and by working backwards to create an accurate EFCC for the first stage, that presents the future cost associated with the peak import state variable. To obtain an overview of the capabilities and potential given by the generation of the EFCCs, case $MPGT$ will be analyzed first, with the economic performance and EFCCs presented in Section 4.1. Furthermore, $MPGT$ will be compared to $EBGT$ in Section 4.2.

### 4.1. Long-term price signal performance $MPGT$

#### 4.1.1. Economic performance

As the case study presented here involves uncertainty, the economic performance will vary based on the sequence of scenario realizations. To capture the tendencies and dispersion of the data, the expected total cost for the month based on the different cases is plotted as a boxplot in Fig. 4. Within the boxplot, the median value is indicated by the orange line, whereas the box specifies the interquartile range (IQR) of the results. The lines outside the boxes are whiskers, representing the 1.5*IQR, while the outliers show the few results that are outside of the 1.5*IQR.

Fig. 4 illustrates how every flexible asset manages to decrease the cost in comparison to the reference case. Both EV charging cases have the highest impact with an expected cost decrease of 14.6% compared to the reference case, with $SH_{20,24}$ being the second best with a 10.9% decrease, in which the latter had a noticeable positive cost change compared to the other SH case. The 10 kWh BESS had a 9.6% cost reduction, coming up close to the best SH case. The range of possibilities in total cost due to the uncertainty, shows that the cost has a specific span of possible results, in which all cases have a similar IQR and whisker range.

As the economic performance in Fig. 4 is affected by the MPGT in addition to RPT, the ending peak level for each case is showcased in Fig. 5 to illustrate the MPGT impact. All cases achieve a reduction in ending peak level, although the amount depends on which flexible asset is activated.

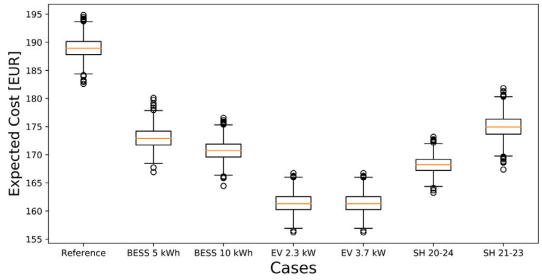


**Fig. 4.** Boxplot of expected monthly total cost for the different cases for scheme $MPGT$.

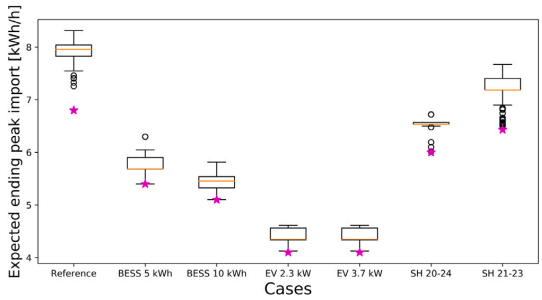


**Fig. 5.** Overview of expected ending peak for the different cases for $MPGT$. The star is the initial peak import level from day 1.

For the BESS cases, they can charge/discharge strategically to reduce the peak import as shown in Fig. 5. The battery is not a natural load within the building, making the value of flexibility unique compared to the rest with no risk of any rebound effect. With an inverter of 2.5 kW, the expected peak reduction from the reference case is at 2.20 kW and 2.50 kW for the 5 and 10 KWh BESS, respectively. Thus, there is a correlation to not only power capacity, but also storage capacity, indicating that the peaks last for multiple hours. However, the 5 kWh BESS manages to reduce a relatively large proportion of the peak compared to the 10 kWh BESS. For the EV charger cases, the flexible contribution provides the highest peak import reduction, with an expected peak import cut by 3.54 kW. As the peak result is similar for both capacities, with the reference case utilizing a 3.7 kW charger, this showcases how significant an impact the passive EV charging strategy has, and how vital flexible EV charging is. As it is possible to charge for 15 h per day, there is a high range of flexibility to choose from, making the charging capacity minor if flexible. However, as the EV is uni-directional, it can only decrease peak from its own demand.

For space heating, the performance improves as the indoor temperature boundary increases. The heater is used diligently during this cold winter month to keep the temperature in check. Case $SH_{21,23}$ has the lowest total cost reduction and peak import reduction compared to the other cases. The cost decrease is derived from both the peak reduction, and by the utilization of flexibility for RTP adjustments, whereas the latter seems to have the most impact. However, by looking at the peak import, the capability of load shifting in peak hours for $SH_{21,23}$ is deemed less critical in the long run. If the boundary was increased further to 20–24 °C, the total cost will be reduced as well as the peak is declined further. The deviation between the two SH cases shows how the temperature boundary affects the load shifting capability, where a higher boundary gives more capacity of pre-heating the interior before peak hours while avoiding high RTP hours as a rebound effect, allowing a longer idle period. Based on the differences, the 21–23 °C boundary,

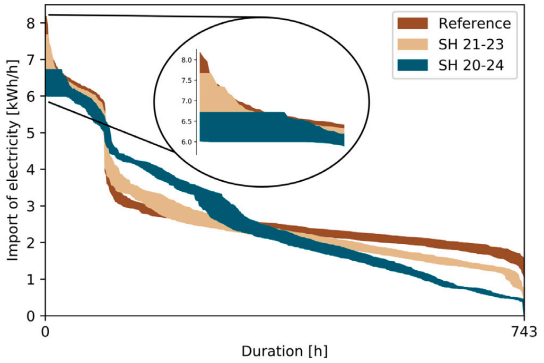


**Fig. 6.** Duration curve for the specified space heating cases over a month, with the uncertainty of scenarios included.

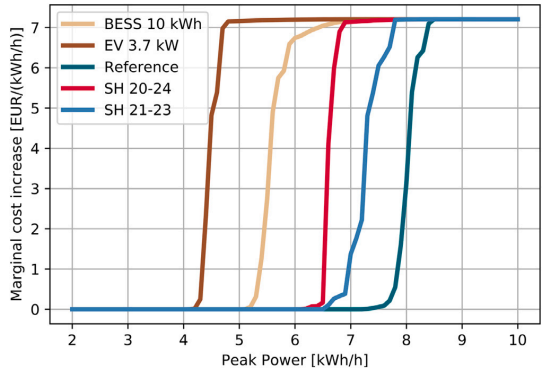


**Fig. 7.** Plot of the MEFCC for the different cases on day 1.

with the limitations in continuous idle hours, shows it to be more cost-optimal to increase peak to decrease RTP costs. Both cases find the threshold for peak power that gives the optimal balance of MPGT and RTP costs seen together, and continuously considers the marginal MPGT increase vs decreasing RTP costs for each scheduling day.

An interesting takeaway from the SH results, is the peak import for both cases, which from Fig. 5 is likely to change during scheduling from the initial point. Case $SH_{21,23}$ has a much wider range of ending peak import than the other. In $SH_{20,24}$, the first and third quartiles, as well as the whiskers, are very tight for the peak import, indicating that the added flexibility gives it more room to reach the same ending peak import, almost regardless of the scenarios realized. Moreover, the deviation from the initial point is smaller than for $SH_{21,23}$, which shows the latter case is more prone to scenario realizations, as that would affect RTP costs. For $SH_{20,24}$, these results show how adjustable SH can be regarding peak import, since as the total cost has a wider spread, it keeps the peak import stable, and instead utilizes load shifting which increases RTP costs, but which is deemed as less costly than the increased grid tariff cost. It is worth mentioning that when increasing the temperature boundary beyond $SH_{20,24}$, the changes are marginal, indicating that this boundary gives the most valuable flexibility capability increase for this case, fitting well with the observation from [6].

Moreover, Fig. 6 illustrates the import duration curve for the reference and the two SH cases. The most prominent behavior is how case $SH_{20,24}$ manages to cut the peak through the use of flexibility, whereas case $SH_{21,23}$ has higher peak demand as some critical scenarios makes a higher peak more beneficial than increasing RTP cost as a rebound effect, overlapping with the reference case at the peaks.

For SH, which has considerable consumption during this winter month, variation in RTP influences operation. RTP impacts how costly the load shifting to reduce peak should be, and if the highest peak should be adjusted to increase RTP benefits. As the current problem has uncertainty in ambient temperature, low temperatures and high thermal demand influences the appropriate peak level. However, the variation in RTP for each day would play a bigger role if it was stochastic. If RTP had multiple scenarios at each stage, the future cost curves would include information on how much load shifting benefit there is in the future, based on both variation in RTP in each scenario and the ambient temperature. With high RTP variation, increasing the peak would be more beneficial to counter the cost of load shifting, and with lower variation the need for increased peak is reduced.

#### 4.1.2. Marginal expected future cost curves

To demonstrate how the EFCC changes, the different cases are shown in Fig. 7, plotted as marginal EFCC (MEFCC) to make a better comparison of the marginal change based on the peak import.

In general, the curves can be divided into three main areas. For marginal cost increase at 0, the initial peak power will not be economically suitable to stay at this level, either because of the lack of flexibility potential, or through costly use of flexibility that is not worth it. Likewise, for the part where the marginal cost increase is equal to the grid tariff cost at 7.25 $\frac{\text{EUR}}{kW_{peak}}$, there is no future cost–benefit other than the increasing grid tariff at the end. Between these two areas, the curve is increasing in cost from 0 to the grid tariff cost, which shows the value of enabling more flexibility from peak import levels. This area is influenced by the reaction of flexible assets towards peak levels, and the uncertainty of the problem. In comparison to the flexible assets, all assets manage to shift this intersection towards the left, thus highlighting the capability to cut peak import.

The 10 kWh BESS decreases the peak import by charging during non-peak hours, and discharge during critical hours, cutting the peak by around 2.5 kW compared to the reference case. The curve has a marginal cost increase with increasing peak power, which shifts to the right to a higher degree than all the other cases, due to scenario realizations and efficiency loss savings with less usage. By increasing the inverter capacity, the peak shaving could be more substantial, however this could lead to the situation with the 5 kWh BESS where the power-energy rating would come into question for the behavior of the MEFCC. The MEFCC of EV charger has the highest peak import level reduction compared to the reference case. The EV charger cuts the peak level substantially by being flexible in charging, which is primarily due to the significant impact the charger gives if being passive, such as in the reference case. Finally, the MEFCC for both $SH_{20,24}$ and $SH_{21,23}$ have different behavior. As stated in Section 4.1, the temperature boundary affected the peak demand level and the variance significantly, which is confirmed by the shape of the curves. The $SH_{21,23}$ curve has the smallest peak level decrease from the reference case, and is scenario sensitive with the shift towards the right, whereas the $SH_{20,24}$ curve shows little scenario impact due to the almost vertical cost increase.

### 4.2. The economic comparison of MPGT and EBGT

The economic performances of all cases are found in Table 2, showing the average total cost.

By analyzing each scheme separately, we can see how the expected total cost decreases compared to the reference case when the flexible assets are enabled to be controlled. For $EBGT$, the cost decrease is tied to the load-shifting capability to utilize the RTP deviations. For this electricity scheme, it is mostly defined for the SH cases, as the high use for heating during winter months leads to increased consumption, which gives higher cost saving potential if controllable.

**Table 2**
The economic performance of all sensitivity cases on both electricity schemes. Values given in EUR.

| Case \ Scheme | EBGT | MPGT |
|---|---|---|
| Reference | 169.49 | 188.95 |
| BESS 5 kWh | 169.07 | 173.02 |
| BESS 10 kWh | 168.86 | 170.77 |
| EV 2.3 kW | 167.49 | 161.44 |
| EV 3.7 kW | 167.45 | 161.44 |
| $SH_{20,24}$ | 155.87 | 168.23 |
| $SH_{21,23}$ | 158.6 | 175.0 |

When comparing the schemes, it is evident that the average cost of $MPGT$ is higher than for $EBGT$, except when activating smart EV control, which achieves the lowest expected total cost with the $MPGT$ scheme. In addition, $SH_{20,24}$ manages to achieve the next best result in $MPGT$ despite having a higher ending peak than the batteries, due to load shifting to balance peak power and RTP costs. The utilization of load shifting for RTP is also seen in the $EBGT$ scheme, demonstrating the high potential in cost reduction by utilizing flexibility for both peak power and RTP. The 10 kWh BESS has a marginal contribution to RTP alone in the $EBGT$ scheme, but provides a much higher cost reduction within the $MPGT$ scheme by reducing the peak import.

However, what these two electricity schemes provide is an overview of the future value of the flexibility that the assets can offer. With the $EBGT$ scheme that only benefits RTP deviations, the cost decrease of smart control is generally lower than with the MPGT, compared to the reference cases. Given that the grid tariff is needed to reflect the cost of operating more accurately, more time-based cost deviations might occur or be presented, which as presented here can provide much more cost savings than if we remain with the default behavior. Flexible assets are valuable even during current operation, however their potential can only increase in the future, both in regards to short- and long-term price signals as we have presented here.

## 5. Conclusion

We have presented a model that aims to illustrate the expected future cost for a building operation model with a long-term price signal. The future cost is based on the expected succeeding cost for operation for a building and the long-term price signal, in this work being a measured-peak grid tariff. This model was applied to a Norwegian household. The primary goal was to analyze the contribution from a battery energy storage system (BESS), a smart Electric vehicle (EV) charger, and controllable space heating (SH) individually with varying input parameters, to see how they react to cope with the long-term price signal. The performance was compared to two electricity schemes, with and without the long-term price signal.

The results from the generation of expected future cost curves showed that all flexible assets contribute to lower the peak import level compared to a reference case, but revealed that their flexibility characteristics affect the long-term performance. The generation of expected future cost curves enables us to represent the future impact of current short-term decision-making, which can provide more cost-optimal flexibility usage over the total period. The controllable EV managed to cut expected cost by 14.6% compared to the reference case, by load shifting the EV charging to reduce peak import. In second came SH, which reduced the expected cost by 10.9% compared to the reference case, despite having the lowest peak import reduction compared to both EV and BESS. Despite SH having the lowest peak import reduction, the load shifting gave additional savings from considering the added value from real-time prices of electricity import.

The work here has shown a general method for representing the long-term value building operation, which can increase the accuracy of operation when combined to a short-term operational model. The method is not limited to a specific case and is adjustable to temporal changes as well as different structures for electricity cost. Therefore, the work here promotes and makes it possible to further investigate the value of this approach with different price structures and temporal locations. Other potential future work includes the long-term value of flexible assets under different price signals, to acquire a broader understanding of their capabilities. In addition, comparing this SDP approach to other decomposition techniques would give more added value on solving long-term operational problems.

## CRediT authorship contribution statement

**Kasper Emil Thorvaldsen:** Conceptualization, Data curation, Formal analysis, Investigation, Methodology, Software, Writing – original draft, Writing – review & editing. **Magnus Korpås:** Conceptualization, Formal analysis, Investigation, Supervision, Writing – original draft, Writing – review & editing. **Hossein Farahmand:** Data curation, Formal analysis, Investigation, Methodology, Supervision, Writing – original draft, Writing – review & editing.

## Declaration of competing interest

The authors declare that they have no known competing financial interests or personal relationships that could have appeared to influence the work reported in this paper.

## Acknowledgments

This work was funded and supported by the Research Council of Norway (Grant Number : 257626/257660/E20) and several partners through FME ZEN and FME CINELDI. The authors gratefully acknowledge the financial support from the Research Council of Norway and all partners in FME CINELDI and FME ZEN.

## References

[1] EDSO for Smart Grids. Adapting distribution network tariffs to a decentralised energy future. Tech. rep., (September). 2015.
[2] Norges vassdrags- og energidirektorat. Forslag til endring i forskrift om kontroll av nettvirksomhet. Tech. rep., 2017.
[3] Agder Energi | AE.no.
[4] Zheng M, Meinrenken CJ, Lackner KS. Smart households: Dispatch strategies and economic analysis of distributed energy storage for residential peak shaving. Appl Energy 2015;147:246–57. http://dx.doi.org/10.1016/j.apenergy.2015.02.039.
[5] Zhang D, Shah N, Papageorgiou LG. Efficient energy consumption and operation management in a smart building with microgrid. Energy Convers Manage 2013;74:209–22. http://dx.doi.org/10.1016/j.enconman.2013.04.038.
[6] Berge M, Mathisen HM. Perceived and measured indoor climate conditions in high-performance residential buildings. Energy Build 2016;127:1057–73. http://dx.doi.org/10.1016/j.enbuild.2016.06.061.
[7] Iversen EB, Morales JM, Madsen H. Optimal charging of an electric vehicle using a Markov decision process. Appl Energy 2014;123:1–12. http://dx.doi.org/10.1016/j.apenergy.2014.02.003.
[8] Angenendt G, Zurmühlen S, Rücker F, Axelsen H, Sauer DU. Optimization and operation of integrated homes with photovoltaic battery energy storage systems and power-to-heat coupling. Energy Convers Manage: X 2019;1:100005. http://dx.doi.org/10.1016/j.ecmx.2019.100005.
[9] Tian W, Heo Y, de Wilde P, Li Z, Yan D, Park CS, et al. A review of uncertainty analysis in building energy assessment. Renew Sustain Energy Rev 2018;93:285–301. http://dx.doi.org/10.1016/j.rser.2018.05.029.
[10] Pallonetto F, De Rosa M, D'Ettorre F, Finn DP. On the assessment and control optimisation of demand response programs in residential buildings. Renew Sustain Energy Rev 2020;127:109861. http://dx.doi.org/10.1016/j.rser.2020.109861.
[11] Erdinc O. Economic impacts of small-scale own generating and storage units, and electric vehicles under different demand response strategies for smart households. Appl Energy 2014;126:142–50. http://dx.doi.org/10.1016/j.apenergy.2014.04.010.
[12] Kuboth S, Heberle F, König-Haagen A, Brüggemann D. Economic model predictive control of combined thermal and electric residential building energy systems. Appl Energy 2019;240:372–85. http://dx.doi.org/10.1016/j.apenergy.2019.01.097.
[13] Palma-Behnke R, Benavides C, Lanas F, Severino B, Reyes L, Llanos J, et al. A microgrid energy management system based on the rolling horizon strategy. IEEE Trans Smart Grid 2013;4(2):996–1006. http://dx.doi.org/10.1109/TSG.2012.2231440.

[14] Nizami MS, Hossain MJ, Amin BM, Fernandez E. A residential energy management system with bi-level optimization-based bidding strategy for day-ahead bi-directional electricity trading. Appl Energy 2020;261:114322. http://dx.doi.org/10.1016/J.APENERGY.2019.114322.
[15] Salpakari J, Lund P. Optimal and rule-based control strategies for energy flexibility in buildings with PV. Appl Energy 2016;161:425–36. http://dx.doi.org/10.1016/j.apenergy.2015.10.036.
[16] Bjarghov SN. Utilizing ev batteries as a flexible resource at end-user level. NTNU; 2017.
[17] Donadee J, Ilić M. Stochastic co-optimization of charging and frequency regulation by electric vehicles. In: 2012 North American power symposium. 2012, http://dx.doi.org/10.1109/NAPS.2012.6336373.
[18] Wu X, Hu X, Moura S, Yin X, Pickert V. Stochastic control of smart home energy management with plug-in electric vehicle battery energy storage and photovoltaic array. J Power Sources 2016;333:203–12. http://dx.doi.org/10.1016/j.jpowsour.2016.09.157.
[19] Wu X, Hu X, Yin X, Moura SJ. Stochastic optimal energy management of smart home with PEV energy storage. IEEE Trans Smart Grid 2018;9(3):2065–75. http://dx.doi.org/10.1109/TSG.2016.2606442.
[20] Kim TT, Poor HV. Scheduling power consumption with price uncertainty. IEEE Trans Smart Grid 2011;2(3):519–27. http://dx.doi.org/10.1109/TSG.2011.2159279.
[21] Luo F, Kong W, Ranzi G, Dong ZY. Optimal home energy management system with demand charge tariff and appliance operational dependencies. IEEE Trans Smart Grid 2020;11(1):4–14. http://dx.doi.org/10.1109/TSG.2019.2915679.
[22] Emil Thorvaldsen K, Bjarghov S, Farahmand H. Representing long-term impact of residential building energy management using stochastic dynamic programming. In: 2020 International conference on probabilistic methods applied to power systems. IEEE; 2020, p. 1–7. http://dx.doi.org/10.1109/PMAPS47429.2020.9183623.
[23] Gjelsvik A, Belsnes MM, Haugstad A. An algorithm for stochastic medium-term hydrothermal scheduling under spot price uncertainty. In: 13th PSCC; 1999, p. 1079–85.
[24] Fodstad M, Henden AL, Helseth A. Hydropower scheduling in day-ahead and balancing markets. In: International conference on the European energy market. IEEE Computer Society; 2015, http://dx.doi.org/10.1109/EEM.2015.7216726.
[25] Morillo JL, Zéphyr L, Pérez JF, Lindsay Anderson C, Cadena A. Risk-averse stochastic dual dynamic programming approach for the operation of a hydro-dominated power system in the presence of wind uncertainty. Int J Electr Power Energy Syst 2020;115:105469. http://dx.doi.org/10.1016/J.IJEPES.2019.105469.
[26] Skoglund IE, Rostad M, Thorvaldsen KE. Impact of shared battery energy storage system on total system costs and power peak reduction in commercial buildings. Proc CISBAT Int Conf 2021, J. Phys.: Conf. Ser. 2021;2042:012108. http://dx.doi.org/10.1088/1742-6596/2042/1/012108.
[27] Helseth A, Gjelsvik A, Mo B, Linnet U. A model for optimal scheduling of hydro thermal systems including pumped-storage and wind power. IET Gener Transm Distrib 2013;7(12):1426–34. http://dx.doi.org/10.1049/iet-gtd.2012.0639.
[28] Birge JR, Louveaux F. Introduction to stochastic optimization. Springer series in operations research and financial engineering, (1):Springer; 2011, p. 485. http://dx.doi.org/10.1007/978-1-4614-0237-4.
[29] Bellman R. A Markovian decision process. 1957.
[30] Gudivada VN, Rao D, Raghavan VV. Big data driven natural language processing research and applications. In: Handbook of statistics, Vol. 33. Elsevier; 2015, p. 203–38. http://dx.doi.org/10.1016/B978-0-444-63492-4.00009-5.
[31] Beale EML, Forrest JJH. Global optimization using special ordered sets. In: Mathematical programming, Vol. 10. North-Holland Publishing Company; 1976, p. 52–69.
[32] Jain C, Singh B. An adjustable DC link voltage-based control of multifunctional grid interfaced solar PV system. IEEE J Emerg Sel Top Power Electron 2017;5(2):651–60. http://dx.doi.org/10.1109/JESTPE.2016.2627533.
[33] Sonderegger RC, C R. Dynamic models of house heating based on equivalent thermal parameters. [PhDT], 1978.
[34] Bacher P, Madsen H. Identifying suitable models for the heat dynamics of buildings. Energy Build 2011;43(7):1511–22. http://dx.doi.org/10.1016/j.enbuild.2011.02.005.
[35] Valentini M, Raducu A, Sera D, Teodorescu R. PV Inverter test setup for european efficiency, static and dynamic MPPT efficiency evaluation. In: 11th International conference on optimization of electrical and electronic equipment. 2008, p. 433–8. http://dx.doi.org/10.1109/OPTIM.2008.4602445.
[36] Ringerikskraft - https://www.ringerikskraft.no/.
[37] SINTEF Energy Research KMB project 190780/S60. ElDeK, Electricity Demand Knowledge. SINTEF Energy Research, KMB project, 190780/S60.
[38] Nord Pool - https://www.nordpoolgroup.com.
[39] ZEB Living Lab - https://www.zeb.no.
[40] Vogler-Finck PJC, Clauß J, Georges L, Sartori I, Wisniewski R. Inverse model identification of the thermal dynamics of a Norwegian zero emission house. Springer, Cham; 2019, p. 533–43. http://dx.doi.org/10.1007/978-3-030-00662-4{_}44.
[41] Finocchiaro L, Goia F, Grynning S, Gustavsen A. The ZEB Living Lab: A multi-purpose experimental facility. Gent expert meeting.
[42] Lakshmanan V, Bjarghov S, Olivella-Rosell P, Lloret-Gallego P, Munné-Collado I, Korpås M. Value of flexibility according to the perspective of distribution system operators — a case study with a real-life example for a Norwegian scenario, Working Paper; 2020.
[43] sonnenBatterie - https://sonnengroup.com.
[44] Jafari M, Korpås M, Botterud A. Power system decarbonization: Impacts of energy storage duration and interannual renewables variability. Renew Energy 2020;156:1171–85. http://dx.doi.org/10.1016/j.renene.2020.04.144.
[45] Sadeghianpourhamami N, Refa N, Strobbe M, Develder C. Quantitive analysis of electric vehicle flexibility: A data-driven approach. Int J Electr Power Energy Syst 2018;95:451–62. http://dx.doi.org/10.1016/j.ijepes.2017.09.007.
[46] LandbruksMeteorologisk Tjeneste (LMT) - https://lmt.nibio.no/.

# Paper III

The paper **"A stochastic operational planning model for a zero emission building withe mission compensation"** is published by **Elsevier** in a special section of **Applied Energy (APEN)** as an invitation after the proceedings of the **2020 MIT A+B Applied Energy Symposium**. The final published paper is reprinted here without changes in compliance with the CC-BY 4.0 license[2] it is published under.

Cite as:
K. E. Thorvaldsen, M. Korpås, and H. Farahmand
"Long-term Value of Flexibility from Flexible Assets in Building Operation"
*Applied Energy, Special section on MIT "A+B" 2020*, vol. 302, Nov 2021
DOI: 10.1016/j.apenergy.2021.117415
URL: `https://doi.org/10.1016/j.apenergy.2021.117415`

[2]See `https://creativecommons.org/licenses/by/4.0/` for license details.

Applied Energy 302 (2021) 117415

Contents lists available at ScienceDirect

Applied Energy

journal homepage: www.elsevier.com/locate/apenergy

# A stochastic operational planning model for a zero emission building with emission compensation

Kasper Emil Thorvaldsen [a,*], Magnus Korpås [a], Karen Byskov Lindberg [a,b], Hossein Farahmand [a]

[a] Department of Electric Power Engineering, Norwegian University of Science and Technology, Norway
[b] SINTEF Community, Oslo, Norway

ARTICLE INFO

*Keywords:*
Operational planning
Stochastic dynamic programming
Grid interaction
Demand-side management
Hourly $CO_{2eq}$-intensity

ABSTRACT

The primary objective of Zero Emission Buildings (ZEBs) is to achieve net zero emission over the buildings' lifetime. To achieve this goal, accurate cost-effective emission compensation is needed during the operational phase. This paper presents a stochastic planning model comprising an emission inventory for the operation of ZEBs. The operational planning methodology uses stochastic dynamic programming (SDP) to analyze and represent the expected future cost curve (EFCC) for operation based on the electricity price and accumulated $CO_{2eq}$-inventory during the year. Failing to compensate for net zero emission makes the leftover amount subject to a penalty cost at the end of the year. This renders the overall problem multi-objective optimization including emission compensation and cost of operation. The model is applied to a case study of a Norwegian building, tested for a range of penalty costs for leftover $CO_{2eq}$-inventory. The results show that, for a ZEB, including emission compensation demonstrates a significant impact on the operation of the building. The penalty cost puts a limit on how much the operational cost increase for additional compensation should be, influencing the end $CO_{2eq}$-inventory. Increasing penalty costs decreases the end inventory, and a penalty cost of 10 $\frac{EUR}{kgCO_{2eq}}$ resulted in zero emission. The case achieving zero emission had an operational cost increase of 4.8% compared to operating without a penalty cost. This shows the importance of accounting for emissions during the operation of a ZEB, and the value of having an operational strategy that presents the future impact of operation.

## 1. Introduction

In the European Union (EU), buildings account for up to 80% of the total energy consumption [1]. Overall, the building stock amounts to 36% of the total $CO_{2eq}$-emissions in the EU [1].

### 1.1. Zero emission buildings

A considerable volume of research has been conducted on new solutions for Zero Emission Buildings (ZEBs) based on the definition from the Directive on Energy Performance of Buildings (EPBD) [2]. The Zero Emission Building research center[1] has explored how to increase the market penetration of buildings with low or net zero greenhouse gas (GHG) emissions over their lifetime [3]. The net zero emission goal considers the following phases of a building during its lifetime: construction, materials, operation, and end-of-life [4]. The critical phase for net zero emission is the operational phase, where emission compensation is required to cover the other phases [4]. In [5], the authors investigated existing definitions and calculation methodologies for ZEBs and zero energy buildings, identifying critical issues that should be addressed for a common ZEB definition and regulation. One specific issue identified concerned the period of calculating the energy and emission balance, where most methodologies presented used an annual balance.

As described and discussed in [6], the operational phase of a ZEB is affected by building location, energy sources in both the grid and on-site production, and the design choices for the buildings. It was observed that the emission compensation realized through the export of on-site renewable power generation depends on the electricity mix in the grid.

Most previous research on ZEBs uses annual average $CO_{2eq}$-intensities of the grid electricity. The authors in [7] optimized the design of a school building for different energy technologies, designed to be a zero energy building. In addition, emission compensation was included in the analysis through primal energy indicators for each technology. The results showed how the annual average $CO_{2eq}$-intensity

* Corresponding author.
*E-mail address:* kasper.e.thorvaldsen@ntnu.no (K.E. Thorvaldsen).
[1] https://www.zeb.no.

https://doi.org/10.1016/j.apenergy.2021.117415
Received 22 February 2021; Received in revised form 30 June 2021; Accepted 7 July 2021
Available online 12 August 2021

**Nomenclature**

**Index sets**

| | |
|---|---|
| $\mathcal{T}$ | Set of time steps within a week |
| $G$ | Set of weeks within the year |

**Parameters**

| | |
|---|---|
| $\dot{E}^{B,dch}, \dot{E}^{B,ch}$ | Discharge/charge capacity for battery [$\frac{\text{kWh}}{\text{h}}$] |
| $\dot{E}^{Max}$ | Maximum EV charging capacity [$\frac{\text{kWh}}{\text{h}}$] |
| $\dot{Q}^{sh}$ | Capacity for space heating radiator [$\frac{\text{kWh}}{\text{h}}$] |
| $\eta^{B}_{dch}, \eta^{B}_{ch}$ | Discharge/charge efficiency for battery [%] |
| $\eta^{EV}_{ch}$ | EV charging efficiency [%] |
| $\eta^{PV}$ | Total efficiency for PV system [%] |
| $C^{grid}$ | DSO energy tariff for imported energy [$\frac{\text{EUR}}{\text{kWh}}$] |
| $C^{\text{CO}_{2eq}}_{n}$ | Expected future cost for point $n$ [EUR] |
| $C_{\text{CO}_{2eq}}$ | Penalty cost for negative end inventory at end of year [$\frac{\text{EUR}}{\text{kgCO}_{2eq}}$] |
| $A^{PV}$ | PV system area [$\text{m}^2$] |
| $C_i, C_e$ | Heat capacity for interior and building envelope [$\frac{\text{kWh}}{\text{°C}}$] |
| $D^{EV}$ | EV discharge when not connected [kWh] |
| $E^{B,Cap}$ | Battery storage capacity [kWh] |
| $E^{B,min}, E^{B,max}$ | Battery SoC limits [kWh] |
| $E^{EV,Cap}$ | EV storage capacity [kWh] |
| $E^{EV,min}, E^{EV,max}$ | Min/Max EV SoC capacity [kWh] |
| $E^{0}_{\text{CO}_{2eq}}$ | Initial accumulated $\text{CO}_{2eq}$-inventory [$\text{kgCO}_{2eq}$] |
| $E^{n,p}_{\text{CO}_{2eq}}$ | Accumulated $\text{CO}_{2eq}$-inventory at point $n$ [$\text{kgCO}_{2eq}$] |
| $N_P$ | Number of discrete $\text{CO}_{2eq}$-inventory values |
| $N_S$ | Number of nodes for stochastic variables |
| $R_{ie}, R_{eo}$ | The thermal resistance between the interior-building envelope and building envelope-outdoor area [$\frac{\text{°C}}{\text{kWh}}$] |
| $T^{in,min}_{t}, T^{in,max}_{t}$ | Lower/upper interior boundary [°C] |
| $VAT$ | Value added tax for purchase of electricity [p.u] |

**Decision variables**

| | |
|---|---|
| $\alpha^{future}_{e_{\text{CO}_{2eq}}, s^{s}_{g+1}}$ | Expected future cost from end accumulated $\text{CO}_{2eq}$-inventory [EUR] |
| $\gamma$ | SOS-2 variables for the expected future cost curve |
| $E^{B}_{t}$ | State of charge for battery at t [kWh] |
| $E^{EV}_{t}$ | State of charge for EV at t [kWh] |
| $e_{\text{CO}_{2eq}}$ | End accumulated $\text{CO}_{2eq}$-inventory at current decision stage [$\text{kgCO}_{2eq}$] |
| $q^{sh}_{t}$ | Power usage for space heating at t [$\frac{\text{kWh}}{\text{h}}$] |
| $T^{in}_{t}, T^{e}_{t}$ | Interior and building envelope temperature at t [°C] |
| $y^{B,ch}_{t}, y^{B,dch}_{t}$ | Power to/from the battery at t [$\frac{\text{kWh}}{\text{h}}$] |
| $y^{EV,ch}_{t}$ | Input power to EV at t [$\frac{\text{kWh}}{\text{h}}$] |
| $y^{imp}_{t}, y^{exp}_{t}$ | Energy imported/exported at t [$\frac{\text{kWh}}{\text{h}}$] |
| $y^{PV}_{t}$ | Power produced from PV system at t [$\frac{\text{kWh}}{\text{h}}$] |

**Stochastic variables**

| | |
|---|---|
| $\delta^{EV}_{t}$ | EV connected to building $\{0, 1\}$ |
| $C^{spot}_{t}$ | Electricity spot price at t [$\frac{\text{EUR}}{\text{kWh}}$] |
| $D^{El}_{t}$ | Consumer-specific load at t [kWh] |
| $f^{\text{CO}_{2eq}}_{t}$ | $\text{CO}_{2eq}$-intensity of electricity at t [$\frac{\text{kgCO}_{2eq}}{\text{kWh}}$] |
| $I^{Irr}_{t}$ | Solar irradiation at building at t [$\frac{\text{kWh}}{\text{m}^2}$] |
| $T^{out}_{t}$ | Outdoor temperature at t [°C] |

from the grid affected the installation of energy carriers, based on net zero emission targets.

The work in [7] is extended in [8], comparing the use of hourly $\text{CO}_{2eq}$-intensities from the grid to yearly average for designing a Zero Emission Neighborhood (ZEN) in Norway. The findings showed that hourly emission intensity did not change the results significantly compared to using yearly average values.

In recent years there has been a development in the calculation of $\text{CO}_{2eq}$-intensities from the electrical grid. The authors in [9] calculated yearly average and marginal emission values for different zones in Europe based on future scenarios. In [10], average $\text{CO}_{2eq}$-intensities on an hourly resolution have been calculated for different bidding zones in Europe, by tracing the origin of electricity back to the generating unit. Similar work is presented in [11].

A building can be operated by a control system that adjusts flexible assets to shift their consumption. If the operation considers emission compensation, the $\text{CO}_{2eq}$-intensities can impact how the flexible resources are used. A yearly average $\text{CO}_{2eq}$-intensity offers no incentive for load shifting within the year, as the only focus for grid interaction lies in the net exchange over the year. With hourly average intensities, the timing of grid exchange within the year becomes more important. Use of flexible assets to adjust the grid interaction will provide short-term value for emission compensation. Moreover, hourly average intensities will promote import from the grid when the electricity mix in the grid has a low $\text{CO}_{2eq}$-intensity, i.e., has a higher share of renewable energy. Likewise, the export will be more favorable when there is a high $\text{CO}_{2eq}$-intensity in the grid. The definition in Norway regarding emission compensation for buildings uses time-dependent interaction [12], promoting operation considering the hourly $\text{CO}_{2eq}$-intensity as a means of achieving net zero emission.

### 1.2. Long-term building operation

In Norway, the optimal yearly strategy for emission compensation with hourly $\text{CO}_{2eq}$-intensity depends on the season. During winter, flexible assets can shift electricity import to time steps with lower $\text{CO}_{2eq}$-intensity, lowering inventory increase. During summer, local production can export electricity to reduce the $\text{CO}_{2eq}$-inventory. However, it is important to find a way of presenting the necessary contribution during the year, to reach the net zero emission goal. In addition, the uncertainty in operation needs to be accounted for. Uncertainty within load demand and local power production creates further uncertainty in the potential for emission compensation during the year. Providing the long-term impact of operational strategy is a vital tool for accurate performance when considering emission compensation, while including the uncertain impacts.

To the authors' knowledge, only a few studies consider the use of long-term price signals to optimize the short-term operation of buildings. However, this methodology is frequently applied to optimize the operation of other types of dispatchable assets in the power system, such as hydropower. Water values have been defined in hydropower scheduling to represent the future value of storing water in a reservoir, created through long-term scheduling models [13]. The generated

water values can be given as input for short-term scheduling models to consider the consequences of operation beyond the short-term horizon [14,15].

For long-term signals of buildings' operation, different clustering methods were tested in [16] for a ZEN over a year, finding the optimal design to achieve zero emission during operation. In [17], a stochastic dynamic programming (SDP) framework calculated and generated long-term price signals for the operation of a residential building. Future cost curves were generated to represent the change in future cost based on a measured-peak grid tariff (MPGT). The MPGT is a cost based on the highest single-hour peak import over a month. The future cost curves provided information about the full expected cost change for the future, balancing costs for increasing peak consumption and benefits from consumption adjustment with real-time pricing (RTP) costs. The same model was used in [18] to evaluate the individual value of flexibility from different flexible assets within the residential building using the same MPGT. The results showed the value of controlling flexible assets such as a stationary battery, electrical vehicle (EV) charging, and space heating (SH), and how the assets have different flexibility contributions.

The SDP framework from [17] could be implemented for the operation of a ZEB. However, the crucial point to enable this layout would be: How to tie emission compensation into the future cost curves? For the operation of a smart residential building, the overall goal is to minimize the total cost of operation. During operation of a ZEB, it is important to include both costs of operation and emission together, tying emission compensation into the objective function through a conversion factor, making the problem multi-objective. Some previous work has managed to combine the economic performance with emissions through multi-objective models. In [19], a planning framework for a local energy system is proposed, which included conversion factors for emission during operation. Emission reduction was focused upon when the authors in [20] wanted to look at how operating conditions for a cutting process could be tied to emissions, by using a conversion factor for emission based on carbon taxes.

The SDP framework can include the impact of emission compensation through the multi-objective layout, having the future cost curve based on both cost of operation and the penalty cost from net emission inventory. If disregarding the penalty cost for emission, the future cost only represents the expected cost of operation to minimize electricity cost over the year. Adding the penalty cost results in a future cost that co-optimizes operational cost and emission compensation. The SDP framework will generate curves throughout the year to highlight the penalty for emission at the end, generating a plan of operation to minimize the multi-objective cost while accounting for the seasonal variations and current point in time. The operational strategy generated could be given as input into a short-term operational model, so the long-term aspect of operation beyond the short-term horizon is included.

### 1.3. Our contribution

In this paper, we present a modified version of the SDP framework derived in [17], adjusted to capture the long-term economic impact of emission compensation for a ZEB during operation. The goal is to generate future cost curves showing the cost-optimal operational plan for achieving zero emission during building operation. The overall optimization model will be multi-objective, balancing both operational cost for electricity exchange and a penalty cost at the end of the year for remaining deviation from zero emission in the $CO_{2eq}$-inventory. Our contributions are the following:

- We include the future cost of emission compensation based on the current $CO_{2eq}$-inventory in building operation for a ZEB using SDP. The SDP framework defines an operational strategy throughout the year for cost-optimal emission compensation
- We investigate how the $CO_{2eq}$ penalty cost for leftover $CO_{2eq}$-inventory puts an upper cost limit for emission compensation, and how a varying penalty cost changes the operational strategy throughout the year
- We look at how a finer resolution of the $CO_{2eq}$-intensity gives an added value to the use of flexible assets within the ZEB, where the flexible assets are controlled to increase emission compensation based on the variance in hourly $CO_{2eq}$-intensity

The remainder of the paper will be organized as follows: Section 2 describes the mathematical formulation of the multi-objective optimization model and the SDP framework. Section 3 will present the case study, while Section 4 presents and discusses the results and performance. Finally, a conclusion is given in Section 5.

## 2. Model description

The overall objective of the presented framework is to minimize the expected total operational cost of an all-electric residential building, while taking into account the cost of leftover $CO_{2eq}$-inventory at the end of the year. The horizon for this work is the course of a year and includes seasonal variation in emission compensation.

### 2.1. Model overview

A long-term operation model for a residential building is used to optimize the operational strategy of a ZEB over a one-year planning horizon. As mentioned in Section 1.2, the operating strategy acquired through the SDP framework can be used as input for a short-term operating model, to reach optimum long-term operation. The scheduling horizon depends on the long-term targets that the residential building is expected to reach. For instance, the MPGT investigated in [17] had a horizon of one month as the tariff was set based on the consumption over one month. The scope of this work considers a one-year horizon to capture the seasonal variations of $CO_{2eq}$-emissions. The problem is solved for weekly decision stages. For each week, the stochastic variables are known from the start of the week and throughout the week. This work considers the following stochastic variables: outdoor temperature, solar irradiation, electricity prices, hourly $CO_{2eq}$-intensity, consumer-specific load and EV availability.

Over the course of a year, we control the flexible assets within the building to adjust the import and export of electricity from the electricity grid in each week. The exchange of electricity directly impacts the $CO_{2eq}$-inventory, which is supposed to be net zero, otherwise a penalty should be paid for the leftover emission. The objective over the year is to minimize the total operating cost from the import and export of electricity, and the cost associated with the emission penalty:

$$min\mathbb{E}\{\sum_{t=1}^{8760}[C_t^{spot}\cdot(y_t^{imp}-y_t^{exp})+C^{grid}\cdot y_t^{imp}]+\Phi(e_{CO_{2eq}})\} \tag{1}$$

$\Phi(e_{CO_{2eq}})$ represents the cost for leftover accumulated emissions throughout the year. The inventory variable $e_{CO_{2eq}}$ keeps track of the emissions we receive during import of electricity from the grid, and the emissions compensated when exporting to the grid. A negative $e_{CO_{2eq}}$ inventory means that we have compensated more than we have acquired from import, while a positive inventory implies that we need to increase compensation to reach net zero emission at the end. The cost function for emission inventory is shown in Eq. (2), where we put a cost on having insufficiently compensated to reach our target emission inventory, $X$. Any extra emission compensated gives no further benefit, whereas any leftover emission results in a cost based on the leftover and the penalty cost $C_{CO_{2eq}}$.

$$\Phi(e_{CO_{2eq}})=\begin{cases}C_{CO_{2eq}}\cdot(e_{CO_{2eq}}-X), & \text{if } e_{CO_{2eq}}\geq X\\ 0, & \text{otherwise}\end{cases} \tag{2}$$

As the $e_{CO_{2eq}}$ is varying throughout the year and the initial value per week changes the strategy, this variable is coupled in time. With the time-coupling of the inventory, the optimization problem has a dynamic nature, making the overall problem in Eq. (1) a multi-stage stochastic optimization problem.

We apply SDP to solve the multi-stage stochastic optimization problem. With the use of dynamic programming, representing the expected future cost as a piecewise-linear cost curve, the overall problem can be decomposed into weekly deterministic subproblems. Each scenario per week comprises a unique subproblem to be solved. The SDP framework, further explained in Section 2.5, is solved in a backward procedure; we start at the last week of the year, and analyze backwards to the start of the year. With a backward procedure, we generate an operating strategy for each week that captures the future consequences, represented by expected future cost curves (EFCCs).

Using the SDP framework presented in [17] to find the optimal strategy for emission compensation allows us to decouple the year into multiple stages. Decoupling into stages decreases the complexity of each unique case that must be run. However, having too many stages or very high levels of detail in the future cost curves can lead to high run time. Another advantage of the SDP framework is the possibility to include uncertainty in the problem, which the clustering method from [16] did not include.

To enable coupling between the decision stages, we formulate a set $\mathcal{S}_g$ that contains information regarding everything that is carried over between decision stages. Within this set lies two subsets; $\mathcal{S}_{S,g}$ contains information on stochastic variables for the decision stage $g$, while $\mathcal{S}_{P,g}$ comprises the state variables in the optimization problem for formulating the future cost curve. The state variables comprise the discrete number of points for initial $CO_{2eq}$-inventory for each week that we investigate to find the change of the future cost curve with changing inventory values. The range of the discrete initial $CO_{2eq}$-inventories provides a good overview of what strategy one should implement during the year, both when the inventory is very negative or positive. Combined, a decomposed decision problem is defined by both subsets $s_g^s, s_g^p \in \mathcal{S}_g$, which indicates that, for a decision stage $g$, we analyze for a specific scenario and state variable for all combinations. State variables and the EFCC for each decision problem will be explained in Section 2.4.2, while the stochastic variables are described in Section 2.2.

### 2.2. Stochastic behavior

The stochastic scenarios that can occur throughout the year increase the complexity of the overall problem. In addition, uncertainty within weather has a serial correlation. This serial correlation makes it difficult to use a backward procedure, as history defines the current scenarios. To deal with the serial correlation, the scenarios are treated as a Markov decision process (MDP) using discrete states per scenario. The MDP assumes that scenarios are memoryless, meaning they have no information concerning how they got here, but do have information about their next scenario transition and the corresponding probabilities [21,22]. The MDP with the SDP framework makes the backward procedure possible. The coupling between the decision stages and scenarios is implemented as shown in Fig. 1, where a given scenario only contains and considers information on the future scenarios that can occur.

The scenarios represented in Fig. 1 are based on MDP behavior. For each decision stage, we have a finite number of discrete scenarios $s_g^s \in \mathcal{N}_S$ that can occur. Each of these scenario nodes contains values for the stochastic variables in the decomposed decision problem, each having a unique characteristic of the stochastic input. The transition probability $\rho(g, s_g^s | s_{g-1}^s)$ of transitioning from scenario node $s_{g-1}^s$ to $s_g^s$ during week $g-1$ to $g$ is based on the probability function value between the two scenarios.

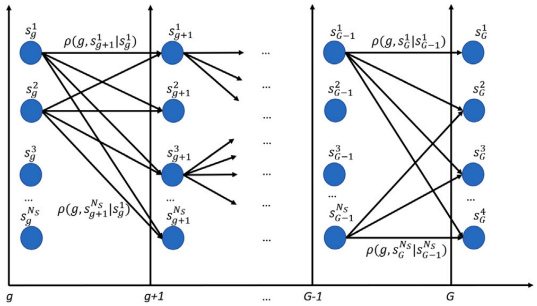


**Fig. 1.** Illustration of the scenario coupling between stage transition.

### 2.3. Decision stages

A given decision week $g$ has an hourly time resolution. For each hour, the electricity demand must be met through exchange with the grid and the use of flexible assets to adjust consumption. At the start of each week, the electricity prices from the grid and all stochastic variables are assumed to be known. The flexible assets have identical start and end values on their energy levels for each decision stage, which for this problem includes a battery, EV, and indoor temperature. This simplification is introduced to ensure that the decision stage transition is feasible with equal values during transition, as their change in energy level and the corresponding future impact is not included in the future cost curve.

### 2.4. Decomposed decision problem

The decomposed decision problem is formulated as an optimization model for operating a ZEB with bi-directional power flow to the power grid. Different flexible assets are being controlled by the optimization model, so the flow of electricity within the building can be adjusted accordingly. The presented optimization model operates for a single deterministic stage of the overall SDP framework, for a given decision stage $g$, scenario $s_g^s$, and initial $CO_{2eq}$-inventory from the state variable $s_g^p$.

Within the building, there are several assets that the optimization model can control: a battery energy storage system (BESS), an EV charger, indoor space heating, and a roof-mounted photovoltaic (PV) system. Each flexible asset is modeled as a constraint-based asset, meaning they cannot operate outside of their given boundaries. The non-flexible electric-specific demand and heat demand for the water tank are assumed to be non-shiftable loads $D_t^{El}$, in which their demand must be met at all time steps.

#### 2.4.1. Objective function

The objective function for the multi-objective problem is to minimize the total electricity cost for the end-user, while considering the expected future cost $\alpha^{future}_{e_{CO_{2eq}}, s^s_{g+1}}$ associated with the accumulated $CO_{2eq}$-inventory at the end of the stage. The cost is then tied to the time-dependent energy demand for the ZEB, RTP, $CO_{2eq}$-intensity over the stage, and the initial $CO_{2eq}$-inventory from the start of the week.

$$min\{\sum_{t\in\mathcal{T}}[C_t^{spot}\cdot(y_t^{imp}-y_t^{exp})+\mathcal{C}^{grid}\cdot y_t^{imp}]+\alpha^{future}_{e_{CO_{2eq}}, s^s_{g+1}}\} \quad (3)$$

#### 2.4.2. Emission compensation and future cost

The constraints regarding emission compensation and the setup for the expected future cost are presented in (4a) to (4e). The accumulated $CO_{2eq}$-inventory for this stage is showcased in (4a), where the accumulated inventory is based on the initial inventory value, and the sum of import and export with the time-dependent $CO_{2eq}$-intensities in the grid. The accumulated total sets the expected future cost variable $\alpha^{future}_{e_{CO_{2eq}},s^s_{g+1}}$ in (4b).

The $\alpha^{future}_{e_{CO_{2eq}},s^s_{g+1}}$ variable is set up using SOS-2 variables for the discrete values $E^{n,p}_{CO_{2eq}}$ $n \in \mathcal{N}_P$ to create a piecewise-linear cost curve based on the accumulated $CO_{2eq}$-inventory [23], named expected future cost curve (EFCC). The EFCC is made up of a number of discrete end $CO_{2eq}$-inventories, and a corresponding future cost based on the emission inventory, representing the expected future cost for the remaining period of the year. Uncertainty from future scenario nodes described in Fig. 1 is included, as the weighted cost is displayed in the EFCC. The EFCC is generated through the SDP framework, presented in Section 2.5.

$$e_{CO_{2eq}} = E^0_{CO_{2eq}} + \sum_{t\in\mathcal{T}} (y^{imp}_t - y^{exp}_t)\cdot f^{CO_{2eq}}_t \tag{4a}$$

$$\alpha^{future}_{e_{CO_{2eq}},s^s_{g+1}} = \sum_{n\in\mathcal{N}_P} \gamma_n \cdot C^{CO_{2eq}}_n \tag{4b}$$

$$e_{CO_{2eq}} = \sum_{n\in\mathcal{N}_P} \gamma_n \cdot E^{n,p}_{CO_{2eq}} \tag{4c}$$

$$\sum_{n\in\mathcal{N}_P} \gamma_n = 1 \tag{4d}$$

$$\gamma_n \geq 0 \quad \forall n,\ SOS\text{-}2 \tag{4e}$$

#### 2.4.3. Energy balance

The energy balance for the electrical system in the building is given in (5). This includes import and export of electricity, local production from PV, charge and discharge from the BESS, load from SH and EV charging, and the non-elastic electrical demand.

$$y^{imp}_t - y^{exp}_t + y^{PV}_t + y^{B,dch}_t = D^{El}_t + y^{EV,ch}_t + q^{sh}_t + y^{B,ch}_t \quad \forall t \tag{5}$$

#### 2.4.4. Electric vehicle

The EV system is formulated as shown in Eqs. (6a) to (6c). The EV has a uni-directional charging capability at a continuous rate, and availability for charging is given by the stochastic variable $\delta^{EV}_t$. During time steps where it is not at the building, a constant discharge $D^{EV}$ from the EV battery is occurring to simulate discharge from driving. The EV battery has a specified state-of-charge (SoC) range given in Eq. (6c), which is time-dependent to enable time-specific SoC preferences.

$$E^{EV}_t - E^{EV}_{t-1} = y^{EV,ch}_t \eta^{EV}_{ch} \delta^{EV}_t - D^{EV}(1-\delta^{EV}_t) \quad \forall t \tag{6a}$$

$$0 \leq y^{EV,ch}_t \leq \dot{E}^{Max} \quad \forall t \tag{6b}$$

$$E^{EV,min}_t \leq E^{EV}_t \leq E^{EV,max}_t \quad \forall t \tag{6c}$$

#### 2.4.5. Battery energy storage system

The building has a bi-directional stationary battery available, which is controllable based on Eqs. (7a) to (7d). Power flow can be operated both ways at a continuous rate, where the limitation lies in power capacity and storage capacity. The storage capacity has a range to ensure optimal operation without damaging the battery.

$$E^B_t - E^B_{t-1} = y^{B,ch}_t \eta^B_{ch} - \frac{y^{B,dch}_t}{\eta^b_{dch}} \quad \forall t \tag{7a}$$

$$0 \leq y^{B,ch}_t \eta^B_{ch} \leq \dot{E}^{B,ch} \quad \forall t \tag{7b}$$

$$0 \leq y^{B,dch}_t \leq \dot{E}^{B,dch} \quad \forall t \tag{7c}$$

$$E^{B,min} \leq E^B_t \leq E^{B,max} \quad \forall t \tag{7d}$$

#### 2.4.6. Photovoltaic system

A roof-mounted PV system is connected to the electrical system through a controllable system that allows the possibility to decrease power output if necessary.

$$0 \leq y^{PV}_t \leq A^{PV}\cdot \eta^{PV}\cdot I^{Irr}_t \quad \forall t \tag{8}$$

#### 2.4.7. Space heating

SH of the building is formulated in (9a) to (9d). Heating of the building is done through an electric radiator with continuous output up to the rated capacity. Heat dynamics are represented as a grey-box model, so the physical behavior is formulated through linear state–space models [24,25].

The SH dynamics are presented as a 2R2C model, dividing the system into three thermal zones: the interior or indoor of the building, the envelope, and the outdoor area. The heat dynamics of the building are modeled without considering internal gains, solar gains or other heating gains except for a radiator. The control system can measure the interior, envelope and outdoor temperature, and operate the radiator to regulate the indoor temperature accordingly.

$$0 \leq q^{sh}_t \leq \dot{Q}^{sh} \quad \forall t \tag{9a}$$

$$T^{in,min}_t \leq T^{in}_t \leq T^{in,max}_t \quad \forall t \tag{9b}$$

$$T^{in}_t - T^{in}_{t-1} = \frac{1}{R_{ie}C_i}[T^e_{t-1} - T^{in}_{t-1}] + \frac{1}{C_i} q^{sh}_t \quad \forall t \tag{9c}$$

$$T^e_t - T^e_{t-1} = \frac{1}{R_{ie}C_e}[T^{in}_{t-1} - T^e_{t-1}] + \frac{1}{R_{eo}C_i}(T^{out}_{t-1} - T^e_{t-1}) \quad \forall t \tag{9d}$$

### 2.5. Solution strategy

**Algorithm 1:** The SDP algorithm to generate EFCCs per decision stage.

```
1 for g = G, G − 1, .., 1 do
2     for n ∈ N_P do
3         E^0_{CO2eq} ← E^{n,p}_{CO2eq}
4         for s^s_g ∈ N_S do
5             {C^spot_t, D^El_t, f^{CO2eq}_t, δ^EV_t, I^Irr_t, T^out_t} ← Γ(g, s^s_g)
6             C^{CO2eq}_i ← Φ(i, s^s_g, g + 1) for i = 1..N_P
7             C_{s^s_g,n} ← Optimize (3) − (9)
8         for s^s_{g−1} ∈ N_S do
9             Φ(n, s^s_{g−1}, g) = Σ_{s^s_g=1}^{N_S} C_{s^s_g,n} · ρ(g, s^s_g | s^s_{g−1})
```

To find the optimal strategy for minimizing electricity cost while performing emission compensation, the SDP algorithm showcased in Algorithm 1 is used in a backwards procedure, starting at the last stage of the horizon. The presented SDP algorithm will for every decision stage $g \in \mathcal{G}$, every discrete point of the state variable $n \in \mathcal{N}_P$, and every scenario $s^s_g \in \mathcal{N}_S$ optimize the decision problem described in Section 2.4 and calculate the economic performance. For each state of an initial $CO_{2eq}$-inventory and scenario given a decision stage $g$, we realize the stochastic variables with scenario-specific values from $\Gamma$ in line 5. In line 6, the EFCC for the next decision stage $g+1$ is specified. For the initial case of $g = \mathcal{G}$, the EFCC is made up of a discrete number of states from Eq. (2). Using these values as input, the multi-objective problem is solved in line 7 to find the objective function value, which is the total cost from that stage and the expected future cost based on emission compensation.

As discussed earlier, transition between stages must be feasible. Therefore, the flexible assets and their energy levels $T^{in}_t$, $T^e_t$, $E^{EV}_t$ and $E^B_t$, have a constant start/end condition that must be encompassed by the optimization problem. For SH, a high penalty cost is included for missing the target, but is not included in the EFCC calculation.

The objective function results in line 7 are part of what makes up the EFCC points $\Phi(n, s^e_{g-1}, g)$ for $n \in \mathcal{N}_P$. The EFCC values are calculated in lines 8–9, where each specific state variable point is derived. The future cost for a given state variable node $n$ is calculated as the weighted future cost value for all scenarios that can occur in stage $g$, which will be representing this stage and state variable for stage $g-1$. The future cost connects stage $g-1$ to stage $g$, coupling the stage transition as shown in Fig. 1. We use the transition probabilities $\rho(g, s^s_g | s^s_{g-1})$ to find the weighted future cost based on the current scenario node from $g-1$. After finding the weighted future cost for each scenario and for all discrete state variables, the complete EFCC is calculated.

After calculating the EFCC for a given stage, the next stage $g-1$ is calculated with the new EFCCs as input for this stage, until arriving at the first stage of the problem. All the generated EFCCs provide an overview of the future cost with a change of operational strategy, capturing the long-term effects of emission compensation at the current time of the year.

## 3. Case study

The model presented has been applied to a residential building located in Southern Norway. This single-family house (SFH) has a control system for the flexible assets, and tracks the import and export of electricity and the corresponding hourly average $CO_{2eq}$-intensity in the grid. The period analyzed is the year 2017, with an hourly time resolution per week over 52 weeks and historical data making up the stochastic variables.

The SFH house is assumed to be part of a ZEN, and that only the community has any limitations on the export of electricity. The demand in the ZEN is assumed to be significant enough that our ZEB can export electricity to any neighboring building without causing any potential harm to the whole electricity system.

### 3.1. Building structure

#### 3.1.1. PV system

The PV system on the roof has an installed capacity of 18.6 kW, which is connected to an MPP inverter with a combined constant conversion and MPP efficiency at 95% [26].

#### 3.1.2. Inelastic consumer demand

The inelastic demand originates from two sources: The passive and user-specific electric-specific electricity consumption, and demand from passive domestic hot water (DHW) consumption. The DHW-consumption profile is based on the measurement of 49 water heaters at Norwegian households through the "Electric Demand Knowledge - ElDek"[2] research project by SINTEF Energy Research [27].

#### 3.1.3. Heat dynamics

The heat dynamics of the building are represented as a single-room building with a 2R2C layout. The characteristics of the building are based on observed values from the Living Lab building built by FME ZEB and NTNU [28,29]. The Living Lab is a pilot project used to study various technologies and design strategies with the overall goal of reaching the zero emission target and analyzing thermo-physical properties [30]. Heating is performed through a 3 kW radiator which can operate continuously. The control system operates the radiator to keep the indoor temperature between 20–24 °C, based on the work in [31].

#### 3.1.4. Stationary battery

The stationary battery is from SonnenBatterie [32] with a rated power input/output of 2.5 kW measured at the output of the inverter. The installed capacity is at 10 kWh, with a tolerated SoC set at between 10%–100% SoC. The round-trip efficiency is set to 85% from [33].

[2] https://www.sintef.no/prosjekter/eldek-electricity-demand-knowledge/.

#### 3.1.5. Electric vehicle

A 24 kWh EV is selected for this study, with an operational range between 20%–90% of total capacity at all times. At departure, the SoC must be between 60%–90% as a countermeasure to range anxiety. The EV consumes electricity from the battery during the time it is offline to simulate driving. For each day, the EV is assumed to leave at 9 AM and arrive at 5 PM, which was found to be the expected departure/arrival time during weekdays for EVs in Norway [34], with an hourly average discharge rate at $D^{EV} = 1.08$ kWh. Moreover, the authors of [35] found small changes on arrival time between weekdays and weekends, and thus we assume the same departure/arrival time for the weekend.

#### 3.1.6. Initial conditions

As mentioned in Section 2.5, the following variables have been given a start/end value to enable a feasible stage transition: $T^{in}_0 = 22$ °C, $T^e_0 = 20$ °C, $E^{EV}_0 = 14.4$ kWh, $E^B_0 = 5$ kWh.

#### 3.1.7. Grid tariff cost

The residential building is assumed to have an energy-only grid tariff with the local DSO, in this case being Ringerikskraft [36]. The total volumetric cost for purchasing electricity in 2017 was at 0.03572 $\frac{\text{EUR}}{\text{kWh}}$ when including both the consumer energy cost and grid tariff cost, plus 25% VAT. The RTP cost of electricity comes in addition to this.

#### 3.1.8. $CO_{2eq}$-intensity and electricity cost

This work has used hourly average $CO_{2eq}$-intensities acquired by the methodology presented in [10], to analyze the average intensities in a selection of bidding zones in NordPool. The method was extended to consider 36 bidding zones, and the input data were generalized to allow the possibility of acquiring data for multiple years. This work utilizes the average intensities for NO2 during the year 2017. The RTP used for the analysis are also for the year 2017 and NO2, acquired from NordPool [37].

### 3.2. Scenario generation

The control system together with the SDP algorithm allows the possibility for multiple input data to be uncertain in the period of operation. To limit the range of uncertainty, the work here considers uncertainty within weather effects, more specifically the outdoor temperature and solar irradiation. Information such as electricity price, $CO_{2eq}$-intensity, EV departure/arrival time, and electric-specific demand is considered deterministic for the year. Multiple scenarios in electricity price and $CO_{2eq}$-intensity would affect the EFFCs as they show the weighted future cost. For EV departure/arrival, different scenarios would influence the timing of charging. However, as found in [18], the EV has long periods where it can charge between traveling, and thus could more easily load-shift to more convenient time steps. Varying electric-specific demand scenarios would influence the total demand and need for compensation, and could lead to more need to peak-shave with the BESS in hours with higher $CO_{2eq}$-intensity.

In total, three scenarios per week have been generated. The three scenarios are based on a normal distribution of the weather effects, with the mean and standard deviation as the discrete scenarios. With a normal distribution, the probability distribution is at $\rho_\mu = 68.2\%, \rho_\sigma = 15.9\%$ for the three scenarios. The probability distribution for the future scenario nodes is the same regardless of the current operating scenario.

Data for the weather effects have been obtained from Renewables.ninja [38]. This website offers country-level data on an hourly time resolution for the period of 1980–2019 using the MERRA-2 tool [39], in which a population-weighted factor for the data was chosen for Norway. The historical data were then used to create hourly normal distributions on both outdoor temperature and solar irradiation, to generate three discrete scenarios per week, consisting of the mean and the standard deviation in both directions.

### 3.3. Model cases

The scope of this work is to investigate the operational strategy for a ZEB with a goal of achieving net zero emission. To achieve zero emission, a cost-optimal strategy regarding $CO_{2eq}$-inventory over the course of the year must be generated. Through generated EFCCs with the SDP framework, we find the cost-optimal strategy on emission compensation for each decision week. To obtain an accurate description of the EFCC, the state variables are made up of 400 discrete points, with step sizes of 1 $kgCO_{2eq}$ in the boundary −200 to 200 $kgCO_{2eq}$. With three scenarios and a total of 52 weeks, the total number of combinations to analyze amounts to 62,400 per case. In addition, we seek to analyze how the penalty cost for leftover emission plays a role in the operational strategy. The penalty cost will put an upper limit on the cost increase for emission compensation, and affect the end inventory at the end of the year. Therefore, the analysis will investigate the SDP framework for multiple penalty cost values. The penalty costs considered are between 0 and 10 $\frac{EUR}{kgCO_{2eq}}$. In comparison, the highest cost for $CO_{2eq}$-quotas in 2019 was at 0.029 $\frac{EUR}{kgCO_{2eq}}$ [40]. Putting a penalty cost up to 10 $\frac{EUR}{kgCO_{2eq}}$, will result in operation where net zero emission is the most crucial goal and electricity prices play a smaller role. Another work has explored a price interval for external compensation of $CO_{2eq}$ between 0 to 2 $\frac{EUR}{kgCO_{2eq}}$ [8].

The impact of the penalty costs will be investigated in a simulation phase, where the economic performance over a year is analyzed week by week sequentially. We investigate the yearly performance 1000 times, each year with different scenario combinations. The initial start inventory is at 0 for each year.

In addition to the Norwegian case, we will compare the performance of this model and framework for the Danish bidding zone DK1. The comparison will provide a sensitivity analysis on how the strategy is influenced by location and temporal changes. For the Danish case, we have the same range of penalty costs, and a step size of 10 $kgCO_{2eq}$ between −1000 to 3000 $kgCO_{2eq}$. Input data for the weather are from the same source as for the Norwegian case, and the same regarding electricity and hourly $CO_{2eq}$-intensities, adjusted for the DK1 bidding zone.

## 4. Results & discussion

This section presents the results from the case study, and discusses the contributions and implications the results provide. As described in Section 2.5, the SDP framework generates expected future cost curves (EFCCs) for each stage during the course of a year. These curves represent the future costs for increased emission compensation, based on the $CO_{2eq}$-inventory. The future cost for compensation is influenced by the penalty cost at the end of the year, setting the threshold for how costly a marginal compensation increase should be. Either the compensation is performed through shifting load consumption, or it is dealt with at the end of the year as a penalty. Therefore, the penalty cost is crucial to the operational strategy throughout the year.

The results of the operational strategy from the EFCCs are presented in Section 4.1. Furthermore, the economic performance alongside net $CO_{2eq}$-inventory is found in Section 4.2, while the operational performance is showcased in Section 4.3. Finally, the performance for the Danish case study in DK1 will be investigated in Section 4.4.

### 4.1. Generation of expected future cost curves

The higher the penalty cost at the end of the year, the more the EFCC reflects the value of emission compensation throughout the year. Therefore, the future presents an opportunity to co-optimize operational cost and emission compensation. To illustrate the behavior of the curves over the whole year, and make them comparable, the EFCCs will be presented as marginal EFCCs (MEFCCs) in this section. The MEFCCs represent the marginal future cost of higher emission inventory, which is also the future cost saving if emission compensation is used to decrease the inventory marginally. Fig. 2 shows the MEFCCs for week 0 (which is the start of the year), for different penalty costs.

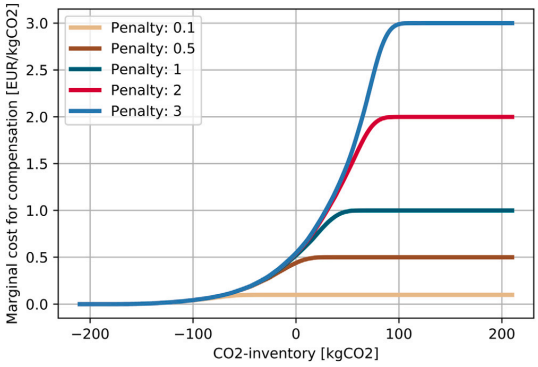


**Fig. 2.** MEFCCs for different penalty costs at week 0.

The MEFCCs in Fig. 2 capture how the future cost is affected by the change in $CO_{2eq}$-inventory, and that the inventory highly affects the marginal cost for emission compensation. On the far left of the figure, the marginal cost for inventory is 0. This 0 marginal cost is tied to the $CO_{2eq}$-inventory being at a satisfying level, where no future compensation that would increase cost of operation is needed to reach net zero emission. However, as the inventory increases, the net zero emission goal cannot be met without changing the operational strategy to include emission compensation during the year.

For a non-zero marginal value on the MEFCCs, the future cost portrays the expected future cost for the marginal $CO_{2eq}$-inventory increase. Some time in the future, there is a potential opportunity to increase compensation to decrease the inventory. This compensation opportunity and the corresponding cost are presented as this marginal cost, which we compare to the increased cost of increasing compensation at the current decision stage we are in. The optimization model finds the cost-optimal decision: Wait for the future, or adjust the operational plan now to increase compensation. For an increasing inventory, the marginal future cost increases, due to the increased emission compensation that is needed in the future for reaching net zero emission. Based on the current inventory, the MEFCC shows the highest marginal cost increase that should be considered for the decision stage.

The increase of marginal cost for the MEFCCs is tied to the penalty cost, which puts a limit on how much the marginal compensation increase should cost. As seen with the different penalty costs in Fig. 2, the future marginal cost flattens out at the penalty cost with increasing $CO_{2eq}$-inventory. This flat part represents the cost limit for compensation. If the marginal cost is equivalent to the penalty cost, increased compensation would reduce the penalty cost paid at the end. However, if the operational cost increase for decreasing the inventory is higher than the cost increase from the EFCCs, it is cost-wise better to pay the penalty at the end. Operating in the inventory level with a constant marginal cost indicates that the net zero emission goal will not be met, and that any further cost-optimal compensation increase only decreases the final penalty cost. Thus, the penalty cost influences our threshold for reaching zero emission. Note that the different MEFCCs start at the same point on the left side of the $x$-axis, but as the inventory increases, each one breaks off and flattens. The higher the penalty cost, the more cost-optimal opportunities exist, to cover the higher end cost. However, as the framework includes uncertainty, each MEFCC is a weighted future cost based on the weighted emission compensation in the future. The role of uncertainty is why the curves break off from the shared

path and slowly ascend towards the penalty cost; the weighted marginal cost is a combination of scenarios with different costs for compensation potential. Some scenarios would have cost-efficient compensation, and some scenarios find the specific penalty cost more cost-efficient.

The future marginal costs in the MEFCC in Fig. 2 present a future compensation opportunity that has not yet occurred. The boundary between marginal penalty cost and 0 decreases as the year progresses, due to fewer upcoming opportunities. This change in boundary means the curves also represent the range of how much the $CO_{2eq}$-inventory can vary while still achieving net zero emission at the end. Since the start of the year is plotted in Fig. 2, the boundary range shows the initial inventories we can start the year at to achieve zero emission without paying the penalty at the end. For a penalty cost above 0.5 $\frac{\text{EUR}}{\text{kgCO}_{2eq}}$, an initial $CO_{2eq}$-inventory at 0 or less should reach near zero emission without any penalty, although this is subject to uncertainty. Because of the potential for some penalty costs achieving zero emission even with a positive initial inventory level, the curves show the potential of covering embodied emission during operation.

As the MEFCCs are generated for each week during the year, the curves will change behavior to reflect the future potential given the weeks considered. Not only will the possible opportunities for compensation decrease as the year progresses, but the $CO_{2eq}$-inventory boundary between marginal penalty cost and 0 will shift on the $x$-axis. An inventory at 0 $kgCO_{2eq}$ might be manageable at the beginning of the year for certain boundaries, but not necessarily possible without paying a penalty if we are in a later week. The seasonal variations for the MEFCCs are presented as heatmaps in Fig. 3 for four different penalty costs.

The heatmaps of the MEFCCs over the year capture the cost change in emission compensation, based on both the time of year and inventory. For a given curve, the change in where the marginal cost is between 0 and the penalty cost represents the seasonal variations. An increasing inventory during winter is expected from the figures due to high energy demand. The summer period expects high export to decrease the inventory again from, for example, high PV production. The seasonal variations of the inventory are present for all penalty costs. However, the penalty cost area is pushed up with increasing penalty cost, increasing the boundary where there exist future potential for compensation. With increasing penalty cost, more cost-optimal opportunities for compensation exists in the future, giving a broader range of acceptable inventory levels. If operating a ZEB to optimize cost while achieving zero emission, the MEFFCs show the range of acceptable inventory levels throughout the year to avoid paying the penalty cost.

### 4.2. Economic operational performance

The economic operational performance is investigated by computing a year sequentially week by week, which is performed 1000 times to account for uncertainty. The EFCCs are given as input to guide the model throughout the year to make cost-optimal decisions regarding emission compensation. Table 1 presents the yearly average total cost for the ZEB and the ending $CO_{2eq}$-inventory, for penalty costs between 0 and 10 $\frac{\text{EUR}}{\text{kgCO}_{2eq}}$.

The trend in Table 1 shows that an increasing penalty cost leads to increasing operating cost. Disregarding the penalty cost gives the lowest operating cost and highest ending $CO_{2eq}$-inventory, since only costs from grid interaction are prioritized. Increasing penalty cost leads to more focus on dealing with emission costs. The flexible assets change their consumption pattern to participate in emission inventory reduction through the indications from the EFCCs, increasing operational costs. In addition, the total cost when including the penalty cost also increases for increasing penalty costs. An increasing penalty cost taxes the ending inventory more, affecting total cost, and promoting reduction of inventory. The end inventory is decreasing for higher penalty cost, saturating towards 0 the higher the penalty cost. Starting at 0.5 $\frac{\text{EUR}}{\text{kgCO}_{2eq}}$, the penalty cost contributes to achieving an inventory close to 0, indicated by the decrease in penalty paid at the end of the year. This threshold indicates that the ZEB during operation on average is close to achieving net zero emission. The ending $CO_{2eq}$-inventory is plotted for the penalty costs as a boxplot in Fig. 4 to illustrate this behavior.

**Table 1**
Average total operating cost with/without the penalty cost, and average ending $CO_{2eq}$-inventory.

| Penalty cost [$\frac{\text{EUR}}{\text{kgCO}_{2eq}}$] | Operating cost [EUR] | Operating cost + Penalty [EUR] | Ending $CO_{2eq}$-inventory [$kgCO_{2eq}$] |
|---|---|---|---|
| 0 | 459.7 | 459.7 | 146.5 |
| 0.01 | 459.8 | 461.1 | 130.0 |
| 0.02931 | 460.2 | 463.4 | 108.5 |
| 0.05 | 460.8 | 465.4 | 92.1 |
| 0.1 | 462.7 | 469.4 | 66.5 |
| 0.2 | 466.6 | 474.6 | 40.1 |
| 0.5 | 477.2 | 480.2 | 6.0 |
| 0.75 | 479.7 | 480.9 | 1.7 |
| 1 | 480.5 | 481.2 | 0.71 |
| 2 | 481.3 | 481.5 | 0.090 |
| 3 | 481.5 | 481.6 | 0.029 |
| 10 | 481.7 | 481.8 | 0.0045 |

Fig. 4 shows the range of ending $CO_{2eq}$-inventory for the operation of a ZEB over a year, based on the penalty cost used. As the problem includes uncertainty, the end value is influenced by the scenarios realized, indicated by the spread of end inventory values for each case. For an increasing penalty cost, the inventory level decreases and slowly approaches net zero emission. From 1.0 $\frac{\text{EUR}}{\text{kgCO}_{2eq}}$, the expected range and both whiskers are close to zero emission. However, there are some few rare outliers present that affect the penalty at the end. The outliers decrease with increasing penalty, showing that higher penalty cost ensures more cases reaching net zero emission with operation throughout the year.

Looking at the spread of end $CO_{2eq}$-inventory in Fig. 4, it is first from a penalty cost of 0.5 $\frac{\text{EUR}}{\text{kgCO}_{2eq}}$ that the zero emission goal is achievable. The 0.5 $\frac{\text{EUR}}{\text{kgCO}_{2eq}}$ penalty cost has the lower whisker of the boxplot flattened around zero emission. This observation corresponds well with the details from Table 1, where the total cost increase started to flatten out at the same penalty cost. In addition, the same observation was made regarding the MEFCC for this penalty cost in Fig. 2. The figure showed that a start inventory at 0 could achieve zero emission for the 0.5 $\frac{\text{EUR}}{\text{kgCO}_{2eq}}$, since the marginal future cost was not equal to the penalty cost. However, as mentioned in Section 4.1, the uncertainty influences this interval, where some scenarios would have compensation opportunities, and some would result in a penalty paid at the end. This observation fits with how the boxplot for this penalty cost is represented in Fig. 4. For the favorable scenarios, the zero emission goal is within reach and the end inventory saturates at this level. However, the ill-favored scenario realizations lead to a range of inventory levels up to 25 $kgCO_{2eq}$.

Case $EL = 0$ in Fig. 4 ignores any consideration of electricity cost, only focusing on achieving zero emission during operation. This $EL = 0$ case shows that the ZEB is capable of achieving this goal if disregarding the cost of operation. When comparing to the cases with multi-objective focus, the output is similar to the highest penalty costs tested. For a penalty cost between 1–10 $\frac{\text{EUR}}{\text{kgCO}_{2eq}}$, the end inventory is close to zero emission while also accounting for ill-favored scenarios. From Table 1, the 10 $\frac{\text{EUR}}{\text{kgCO}_{2eq}}$ and 1 $\frac{\text{EUR}}{\text{kgCO}_{2eq}}$ penalty costs come at an operational cost increase of 4.8% and 4.5% compared to no penalty cost, respectively. The low cost increase difference between the two aforementioned penalty costs shows that the operational cost increase is not directly increasing in correspondence to the penalty cost. However, increasing penalty cost leads to fewer situations where one would risk a possible future scenario leading to an increased penalty at the end.

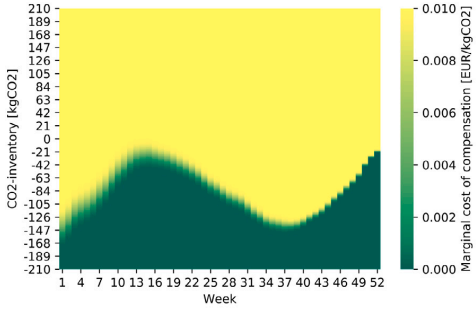


(a) Penalty cost at 0.01 $\frac{EUR}{kgCO_{2eq}}$

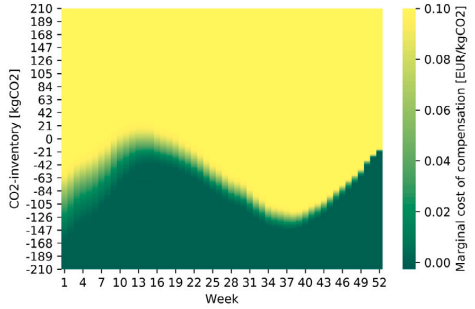


(b) Penalty cost at 0.1 $\frac{EUR}{kgCO_{2eq}}$

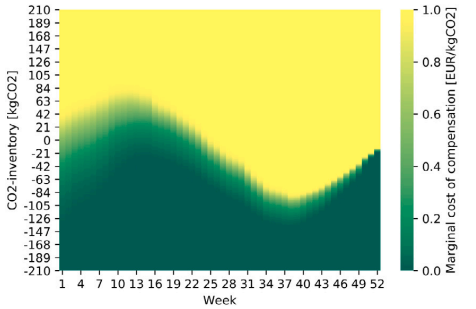


(c) Penalty cost at 1 $\frac{EUR}{kgCO_{2eq}}$

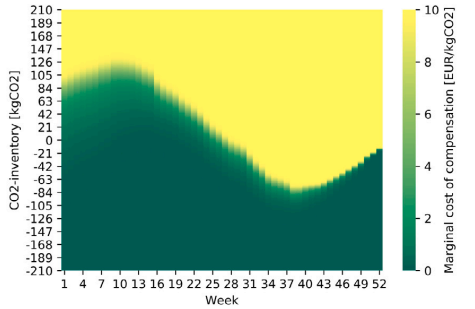


(d) Penalty cost at 10 $\frac{EUR}{kgCO_{2eq}}$

**Fig. 3.** Heatmap of the MEFCCs over a year with different penalty costs.

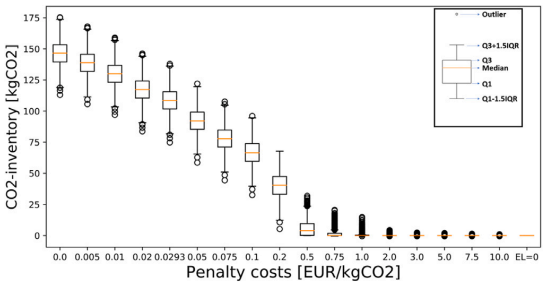


**Fig. 4.** Boxplot of the ending $CO_{2eq}$-inventory for the different penalty costs.

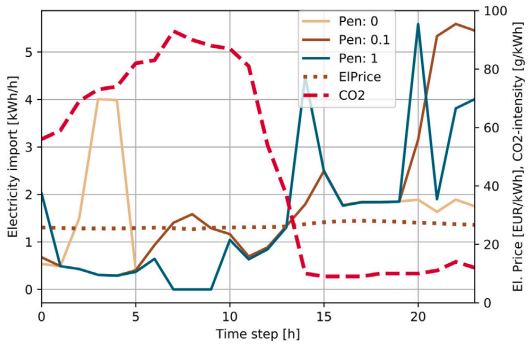


**Fig. 5.** The operational strategy during the first day for different penalty costs for a specific scenario. All cases have the same initial $CO_{2eq}$-inventory at start of operation.

### 4.3. Operation of the building

The operation of a ZEB will change based on the future implications given by the EFCC included as input. With an increasing penalty cost, the primary goal for the multi-objective optimization problem shifts to focus more on how to deal with the penalty cost at the end of the year. The EFCC changes the operational strategy regarding operational cost from grid interaction for the ZEB, shown in Fig. 5.

For the first day of the year 2017 in this analysis, as shown in Fig. 5, the grid interaction changes for a varying penalty cost. With a lower penalty cost, the operation focuses more on variation in electricity price, shifting electricity import more towards the night and afternoon where the electricity prices are normally lower. This strategy adjusts when the penalty cost increases, as the hourly $CO_{2eq}$-intensities have a different pattern than the electricity price for this day. With a higher intensity during the night and morning, the operational strategy for increasing penalty cost avoids high import of electricity for this period. In addition, there are periods where the import is lowered to 0 for the high penalty costs, which is to avoid high import of $CO_{2eq}$ emission. The decrease of import causes a rebound effect later during the day,

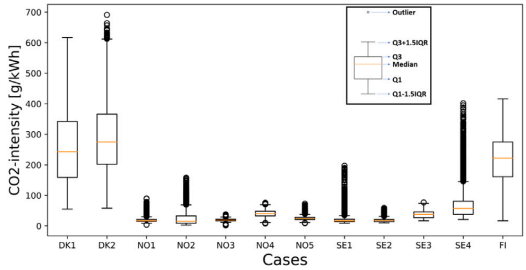


**Fig. 6.** Overview of hourly $CO_{2eq}$-intensities for the Nordic bidding zones in 2017.

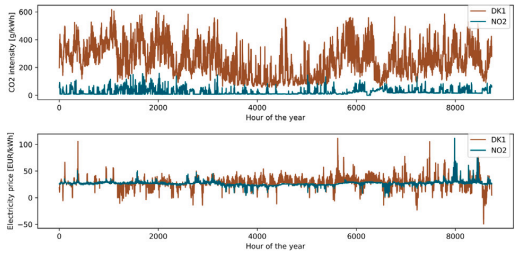


**Fig. 7.** Overview of hourly $CO_{2eq}$-intensities and electricity prices for DK1 and NO2 for the year 2017.

where the import increases with two high spikes during the evening for the 1 $\frac{\text{EUR}}{\text{kgCO}_{2eq}}$ penalty cost.

The operational strategy in Fig. 5 is during the first day of the year during winter. Periods of 0 import and high import spikes during the evening show an abnormal import strategy. This strategy indicates import during hours where there is increased risk of congestion in the grid. As discussed in [10], Norwegian bidding zones have tendencies where the electricity price and $CO_{2eq}$-intensity have opposite peaks during operation. The prices are low when the intensity is high and vice versa. This correlation is tied to the high amount of dispatchable hydropower sources available, which can store their water for production based on when the prices are highest, which then gives a high share of renewable energy when the electricity is needed the most. During hours with lower prices, the demand can be met with import from other bidding zones outside of Norway. NO2 is connected to both the Netherlands and Denmark, which when exporting to NO2 can give higher $CO_{2eq}$-intensity. Thus, this indicates that Norway with hydropower requires ZEBs to implement strategies that might go against a common strategy for the use of flexible assets, if hourly $CO_{2eq}$-intensities are to be used.

### 4.4. Comparison of emission compensation in DK1

Hourly average $CO_{2eq}$-intensity for bidding zones is tied together with the energy mix and interconnectors between each bidding zone. The energy mix is what not only comprises the $CO_{2eq}$-intensity on intensity levels, but also in the variation of intensity as some energy sources are intermittent and depend on the weather and other factors. The variations in the Nordic countries are shown in Fig. 6, where we see that both Norway and Sweden have the lowest intensity values. The intensity levels and variation in Norway are influenced by the high hydropower production [41]. For Denmark, the $CO_{2eq}$-intensity is higher and with more variation, due to a large amount of intermittent wind power and non-renewable energy sources [41]. Therefore, the value of operating a ZEB in DK1 and NO2 while considering emission compensation will have a different impact in each respective bidding zone. Not only will the variation in $CO_{2eq}$-intensity play an important role, but also how the variation is tied together with the electricity prices.

The Danish bidding zones experience more fluctuation in prices and $CO_{2eq}$-intensities than the Norwegian bidding zones for the year 2017, as shown in Fig. 7. NO2 shows lower variation and expected value of the $CO_{2eq}$-intensity over the year, from the high share of hydropower. DK1, with more intermittent wind power and interconnections to continental Europe, is more prone to both variation and higher intensity levels in its electricity mix. Denmark has a high proportion of wind power, but other energy sources with higher emission output are present, in addition to exchange with Germany and Norway. The variation in wind power output affects the average intensity during the year, and these variations would promote load shifting of a ZEB for emission compensation to a higher degree than the NO2 bidding zone can achieve.

The performance of the SDP framework for DK1 is presented in Fig. 8, where we include the MEFCC for different penalty costs at week 0, and a heatmap for the penalty cost of 0.1 $\frac{\text{EUR}}{\text{kgCO}_{2eq}}$. The main observation from both figures is the $CO_{2eq}$-inventory levels; a net zero emission goal for operation can be achieved without considering a penalty cost at all. The MEFCC has a 0 marginal cost at an initial inventory at 0 $\text{kgCO}_{2eq}$ in both figures, showing that there is sufficient compensation when only considering cost of operation to achieve the emission goal. In addition, the MEFCC curve shows that there is high potential to increase compensation further, where one could have an initial value at 2000 $\text{kgCO}_{2eq}$ with a penalty of 3 $\frac{\text{EUR}}{\text{kgCO}_{2eq}}$ and still be close to achieving zero emission. This high compensation potential is despite relatively lower $CO_{2eq}$-intensities during the summer period where there is high PV production compared to the rest of the year. The variation in $CO_{2eq}$-intensity promotes to a larger degree load shifting through flexible assets to increase compensation.

The economic performance for the different penalty costs ended on average with an inventory of −666 $\text{kgCO}_{2eq}$ regardless of the penalty cost, which illustrates the zero emission goal is achieved with normal operation without emission penalty. The ZEB used for this case study has sufficient PV production, together with flexible assets, to adjust import and export of electricity to cost-optimal time periods, without considering the emission inventory. Fig. 9 presents the correlation between $CO_{2eq}$-intensity and electricity price for NO2 and DK1 over week 7 in 2017. Week 7 was chosen as it had varying $CO_{2eq}$-intensity and electricity prices in DK1 during late winter, where negative prices occurred for some hours.

For DK1 in Fig. 9, the correlation with intensity and price fits an operational strategy trying to minimize cost of operation; the intensity in the grid is high with high prices, and the intensity decreases more when the price decreases. Due to the intermittent wind production, more wind and lower intensity pushes the price down, favoring more consumption in terms of cost savings and emission inventory. For NO2, this trend is not shown, rather, the opposite trend is occurring more frequently due to the dispatchable hydropower. Therefore, operation in NO2 would require more change of operational strategy when considering emission inventory than for DK1. In addition, an operational strategy with an increasing focus on emission compensation would require higher operational costs for NO2 than for DK1. The observation shows that a ZEB with a zero emission goal is influenced to a greater extent by both the location, type of renewable generation in the electricity mix, and the temporal $CO_{2eq}$-intensity. The Danish case shows that with higher variation of $CO_{2eq}$-intensity, and correlation between electricity prices and $CO_{2eq}$-intensity, a ZEB is more capable of achieving net zero emission. In addition, the ZEB will have more capacity to deal with embodied emissions during operation, compensating for other phases during the ZEB's lifetime.

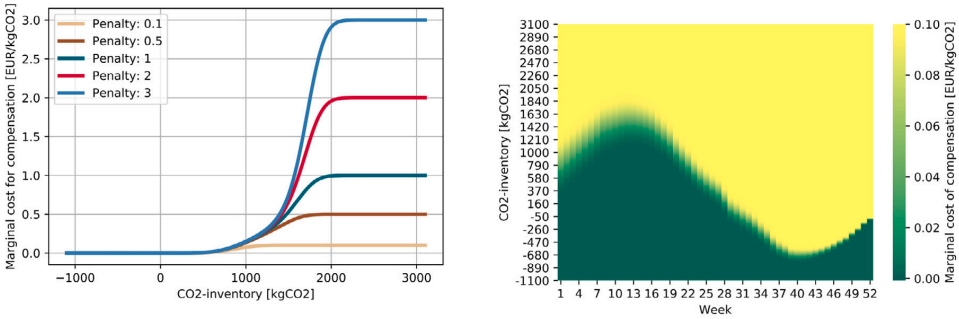


(a) MEFCCs for different penalty costs at week 0 for DK1.

(b) Penalty cost at 0.1 $\frac{EUR}{kgCO_{2eq}}$ for DK1.

**Fig. 8.** Results of the SDP framework for DK1.

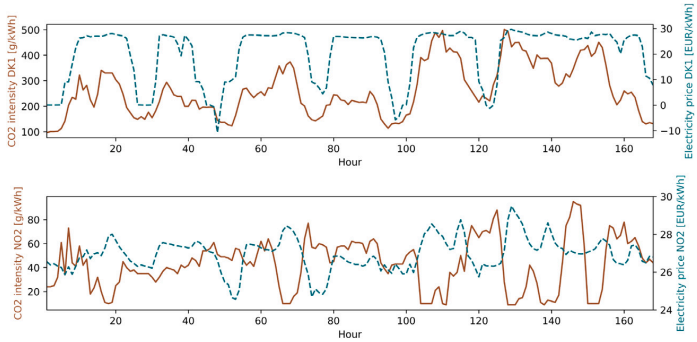


**Fig. 9.** Correlation between electricity prices and $CO_{2eq}$-intensities in NO2 and DK1 for week 7.

### 4.5. Limitations in this work

The work and results for the Danish and Norwegian cases have demonstrated the value of the optimization model and SDP-algorithm for building operation taking into account emission compensation. However, it is important to note the limitations of the presented approach, and what needs to be considered to implement this approach in practice.

Applications for automatic demand response with flexible assets are limited in real-world systems. Today, there exist pilot projects and local markets to promote end-user flexibility. However, they vary in different degrees depending on the regions and countries that the end-users are located in. In Norway, hourly electricity prices for end-users has been implemented through the roll-out of smart meters to residential and small business customers, while in France, flexibility markets for end-users are emerging and increasing in participation [42]. Enabling efficient market designs and price mechanisms for end-user flexibility is expected to increase the role of demand-side management on the end-user level in the future, which in turn can enable compensating $CO_{2eq}$-emissions from end-users.

Currently, real-time tracking $CO_{2eq}$-intensity and -inventory for end-users are not accounted completely during the power system operation. The power sector is primarily accounting for production-based emissions [11]. However, the consumer-based accounting methods, e.g., the proposed SDP-algorithm can assist end-users in tracking their emission impact over an operating year, based on both previous achievements and future compensation potential. This will particularly be relevant for Zero Emission Buildings and Neighborhoods, which has set clear long-term goals for the climate footprint: These users require operational tools to ensure that their day-to-day energy use is in line with the long-term goals.

## 5. Conclusion

Operating a zero emission building (ZEB) while accounting for both cost of operation and the hourly average grid $CO_{2eq}$-intensities over the course of a year requires the incorporation of a long-term strategy into the short-term operational decision-making process. Optimal operation of a ZEB requires accurate representation of both the $CO_{2eq}$-inventory to handle seasonal variations, and the cost-optimal time to use available flexible assets to increase emission compensation. We present a model that optimizes the operational strategy for emission compensation over a year, when trying to cost-optimally achieve zero emission for a ZEB during operation. Using a stochastic dynamic programming (SDP) framework, expected future cost curves (EFCCs) are generated, representing the future cost based on the current $CO_{2eq}$-inventory. The EFCC provides an overview of the marginal future value for increasing $CO_{2eq}$-compensation now versus later, throughout the year.

The proposed model was applied to a realistic Norwegian building located in the Norwegian bidding zone NO2 for the year 2017, to find the cost-optimal strategy for net zero emission. The operational strategy was tested for varying penalty costs at the end of the year. With an increasing penalty cost, the emission compensation increased, to counteract the penalty cost paid at the end. This is achieved by utilizing the available flexible assets in the ZEB to shift electricity import and export based on the variations in hourly average $CO_{2eq}$-intensity. A higher penalty cost made the flexible assets play a more

critical role, where they balanced the increased cost of operation to increase emission compensation against the future savings showed by the EFCCs. In addition, the temporal variation of the energy mix in different bidding zones impacts the operational strategy. DK1 showed a higher possibility of emission compensation, due to both higher variation in $CO_{2eq}$-intensity and better correlation between electricity prices and $CO_{2eq}$-intensity, compared to NO2.

When analyzing the economic performance over a year in NO2, the results showed that a penalty cost of 10 $\frac{\text{EUR}}{\text{kgCO}_{2eq}}$ met the net zero emission requirement at an expected total cost increase of 4.8% compared to not considering emission compensation. Without considering the emission compensation, the end $CO_{2eq}$-inventory was on average at 146.5 $\text{kgCO}_{2eq}$. Net zero emission was achievable from a penalty cost of 0.5 $\frac{\text{EUR}}{\text{kgCO}_{2eq}}$ and above. When increasing the penalty cost further, the average ending inventory reached closer to net zero emission and more cases reached zero emission, despite dealing with uncertainty during operation such as thermal demand and local production.

The operational strategy provided higher peaks of import with higher penalty costs, which could be at times when the electricity prices are high. With higher peaks at times with higher prices, this unnatural strategy could counteract congestion management, promoting further studies into how emission compensation can be performed from grid interaction. For instance, the introduction of marginal $CO_{2eq}$-intensities could be investigated. In addition, looking into embodied emissions for other phases during the lifetime of a ZEB would place more emphasis on the potential within the operational phase for compensation.

## CRediT authorship contribution statement

**Kasper Emil Thorvaldsen:** Conceptualization, Data curation, Formal analysis, Investigation, Methodology, Software, Writing – original draft, Writing – review & editing. **Magnus Korpås:** Conceptualization, Formal analysis, Investigation, Methodology, Supervision, Writing – original draft. **Karen Byskov Lindberg:** Data curation, Formal analysis, Investigation, Supervision, Writing – review & editing. **Hossein Farahmand:** Data curation, Formal analysis, Investigation, Methodology, Supervision, Writing – original draft, Writing – review & editing.

## Declaration of competing interest

The authors declare that they have no known competing financial interests or personal relationships that could have appeared to influence the work reported in this paper.

## Acknowledgments

This work was funded and supported by the Research Council of Norway (Grant Number: 257626/257660/E20) and several partners through FME ZEN, Norway and FME CINELDI, Norway. The authors gratefully acknowledge the financial support from the Research Council of Norway and all partners in CINELDI and ZEN. In addition , special thanks to John Clauss for providing and helping with re-creating his methodology to generate hourly $CO_{2eq}$-intensity values. Finally, thank you to Linn Emelie Schäffer at NTNU for your valuable discussions and help in reviewing the manuscript.

## References

[1] DIRECTIVE (EU) 2018/844 OF THE EUROPEAN PARLIAMENT AND OF THE COUNCIL of 30 May 2018 amending Directive 2010/31/EU on the energy performance of buildings and Directive 2012/27/EU on energy efficiency (Text with EEA relevance), Tech. rep., 2018.

[2] Directive 2010/31/EU of the European Parliament and of the Council of 19 May 2010 on the energy performance of buildings, Tech. rep., 2010.

[3] Lien K, Byskov Lindberg K. A Norwegian Zero Emission Building Definition, Tech. rep., URL http://www.laganbygg.se/UserFiles/Presentations/18._Session_5_T.Dokka.pdf, 2013.

[4] Selamawit F, Schlanbudch R, Sørnes K, Inman M, Andresen I. A norwegian ZEB definition guideline, Vol. January. 2016, p. 2017–24. http://dx.doi.org/10.13140/RG.2.2.26443.80162, URL.

[5] Marszal AJ, Heiselberg P, Bourrelle JS, Musall E, Voss K, Sartori I, Napolitano A. Zero energy building - a review of definitions and calculation methodologies. Energy Build 2011. http://dx.doi.org/10.1016/j.enbuild.2010.12.022.

[6] Fenner AE, Kibert CJ, Woo J, Morque S, Razkenari M, Hakim H, Lu X. The carbon footprint of buildings: A review of methodologies and applications. Renew Sustain Energy Rev 2018;94:1142–52. http://dx.doi.org/10.1016/J.RSER.2018.07.012, URL https://www.sciencedirect.com/science/article/pii/S1364032118305069.

[7] Lindberg KB, Doorman G, Fischer D, Korpås M, Ånestad A, Sartori I. Methodology for optimal energy system design of zero energy buildings using mixed-integer linear programming. Energy Build 2016;127:194–205. http://dx.doi.org/10.1016/j.enbuild.2016.05.039.

[8] Pinel D, Korpås M, B. Lindberg K. Impact of the CO2 factor of electricity and the external CO2 compensation price on zero emission neighborhoods' energy system design. Build Environ 2021;187:107418. http://dx.doi.org/10.1016/j.buildenv.2020.107418.

[9] Graabak I, Bakken BH, Feilberg N. Zero emission building and conversion factors between electricity consumption and emissions of greenhouse gases in a long term perspective. Environ Clim Technol 2014;13(1):12–9. http://dx.doi.org/10.2478/rtuect-2014-0002.

[10] Clauß J, Stinner S, Solli C, Lindberg K, Byskov, Madsen H, Georges L. General rights evaluation method for the hourly average CO2eq. intensity of the electricity mix and its application to the demand response of residential heating. 2019, http://dx.doi.org/10.3390/en12071345, Downloaded from Orbit.Dtu.Dk on.

[11] Tranberg B, Corradi O, Lajoie B, Gibon T, Staffell I, Andresen GB. Real-time carbon accounting method for the European electricity markets. Energy Strateg Rev 2019;26:100367. http://dx.doi.org/10.1016/j.esr.2019.100367.

[12] Norge S. Norsk Standard NS 3720:2018. Tech. rep., 2018.

[13] Helseth A, Fodstad M, Askeland M, Mo B, Nilsen OB, Pérez-Díaz JI, Chazarra M, Guisández I. Assessing hydropower operational profitability considering energy and reserve markets. IET Renew Power Gener 2017;11(13):1640–7. http://dx.doi.org/10.1049/iet-rpg.2017.0407.

[14] Fodstad M, Henden AL, Helseth A. Hydropower scheduling in day-ahead and balancing markets. In: International conference on the european energy market, EEM, Vol. 2015-August. IEEE Computer Society; 2015, http://dx.doi.org/10.1109/EEM.2015.7216726.

[15] Mo B, Fosso OB, Flatabø N, Haugstad A. Short-term and medium-term generation scheduling in the norwegian hydro system under a competitive power market. Tech. rep., 2002, URL https://www.researchgate.net/publication/306446062.

[16] Pinel D. Clustering methods assessment for investment in zero emission neighborhoods' energy system. Int J Electr Power Energy Syst 2020;121:106088. http://dx.doi.org/10.1016/j.ijepes.2020.106088.

[17] Emil Thorvaldsen K, Bjarghov S, Farahmand H. Representing long-term impact of residential building energy management using stochastic dynamic programming. In: 2020 international conference on probabilistic methods applied to power systems (PMAPS). IEEE; 2020, p. 1–7. http://dx.doi.org/10.1109/PMAPS47429.2020.9183623, URL https://ieeexplore.ieee.org/document/9183623/.

[18] Thorvaldsen KE, Korpås M, Farahmand H. Long-term value of flexibility from flexible assets in building operation. 2021, URL http://arxiv.org/abs/2105.11952.

[19] Botterud A, Holen AT, Catrinu M, Wolfgang O. Integrated energy distribution system planning: A multi-criteria approach optimal utilization of hydro power view project integrated energy distribution system planning: A multi-criteria approach. In: 15th power systems computation conference. Liege, Belgium; 2005, URL https://www.researchgate.net/publication/228340210.

[20] Liu ZJ, Sun DP, Lin CX, Zhao XQ, Yang Y. Multi-objective optimization of the operating conditions in a cutting process based on low carbon emission costs. J Cleaner Prod 2016;124:266–75. http://dx.doi.org/10.1016/j.jclepro.2016.02.087.

[21] Bellman R. A Markovian decision process -. 1957.

[22] Gudivada VN, Rao D, Raghavan VV. Big data driven natural language processing research and applications. In: Handbook of statistics, Vol. 33. Elsevier; 2015, p. 203–38. http://dx.doi.org/10.1016/B978-0-444-63492-4.00009-5.

[23] Beale EML, Forrest JJH. Global optimization using special ordered sets. Tech. rep., North-Holland Publishing Company; 1976, p. 52–69, URL https://link.springer.com/content/pdf/10.1007%2FBF01580653.pdf.

[24] Sonderegger RCRC. Dynamic models of house heating based on equivalent thermal parameters. PhDT 1978.

[25] Bacher P, Madsen H. Identifying suitable models for the heat dynamics of buildings. Energy Build 2011;43(7):1511–22. http://dx.doi.org/10.1016/j.enbuild.2011.02.005.

[26] Valentini M, Raducu A, Sera D, Teodorescu R. PV Inverter test setup for european efficiency, static and dynamic MPPT efficiency evaluation. In: 11th international conference on optimization of electrical and electronic equipment, OPTIM 2008. 2008, p. 433–8. http://dx.doi.org/10.1109/OPTIM.2008.4602445.

[27] SINTEF Energy Research KMB project 190780/S60, ElDeK, Electricity Demand Knowledge, URL https://www.sintef.no/en/projects/eldek-electricity-demand-knowledge/.

[28] ZEB Living Lab - https://www.zeb.no, URL https://www.zeb.no/index.php/en/pilot-projects/158-living-lab-trondheim.
[29] Vogler-Finck PJC, Clauß J, Georges L, Sartori I, Wisniewski R. Inverse Model Identification of the Thermal Dynamics of a Norwegian Zero Emission House. Springer, Cham; 2019, p. 533–43. http://dx.doi.org/10.1007/978-3-030-00662-4{_}44.
[30] Finocchiaro L, Goia F, Grynning S, Gustavsen A. The ZEB Living Lab: a multi-purpose experimental facility, Tech. rep., 2014.
[31] Berge M, Mathisen HM. Perceived and measured indoor climate conditions in high-performance residential buildings. Energy Build 2016;127:1057–73. http://dx.doi.org/10.1016/j.enbuild.2016.06.061.
[32] sonnenBatterie - https://sonnengroup.com, URL https://sonnengroup.com.
[33] Jafari M, Korpås M, Botterud A. Power system decarbonization: Impacts of energy storage duration and interannual renewables variability. Renew Energy 2020;156:1171–85. http://dx.doi.org/10.1016/j.renene.2020.04.144.
[34] Lakshmanan V, Bjarghov S, Olivella-Rosell P, Lloret-Gallego P, Munné-Collado I, Korpås M. Value of flexibility according to the perspective of distribution system operators — a case study with a real-life example for a Norwegian scenario, 2021.
[35] Sadeghianpourhamami N, Refa N, Strobbe M, Develder C. Quantitive analysis of electric vehicle flexibility: A data-driven approach. Int J Electr Power Energy Syst 2018;95:451–62. http://dx.doi.org/10.1016/j.ijepes.2017.09.007.
[36] Ringerikskraft - https://www.ringerikskraft.no/, URL https://www.ringerikskraft.no/.
[37] Nord Pool - https://www.nordpoolgroup.com, URL https://www.nordpoolgroup.com/.
[38] Renewables.ninja, URL https://www.renewables.ninja/.
[39] MERRA-2, URL https://gmao.gsfc.nasa.gov/reanalysis/MERRA-2/.
[40] CO2 European Emission Allowances PRICE Today — CO2 European Emission Allowances Spot Price Chart — Live Price of CO2 European Emission Allowances per Ounce — Markets Insider, URL https://markets.businessinsider.com/commodities/co2-european-emission-allowances.
[41] ORGANISATIONAL AND REGIONAL TABLES OECD Total, Tech. rep., URL www.iea.org/reports/covid-19-impact-on-electricity, 2021.
[42] Glover L, Villa M, Murley L, Coelho Ja, Adey-Johnson R, Pinto-Bello A. EU Market monitor for demand side flexibility. Tech. rep., 2021, URL www.delta-ee.com.

# Paper IV

The paper **"Long-term strategy framework for residential building operation with seasonal storage and capacity-based grid tariffs"** is currently under review with **Elsevier** in **Applied Energy**. The pre-print version is reprinted here.



This paper is awaiting publication and is not included in NTNU Open

ISBN 978-82-326-6267-8 (printed ver.)
ISBN 978-82-326-5885-5 (electronic ver.)
ISSN 1503-8181 (printed ver.)
ISSN 2703-8084 (online ver.)



NTNU
Norwegian University of
Science and Technology